NAVAL POSTGRADUATE SCHOOL
Monterey, California

SABOT HIGH SPEED INTERCEPTOR
AE 4273 AIRCRAFT DESIGN

September 1992

by

Dave Dober
Waleed Al-Hashel
Bob Baldocchi
Tim Berg
Harry Dunbrack
Curt Lindsay
Aaron McAtee
Dan Sergent

Project Advisor: Prof. Conrad Newberry

SABOT HIGH SPEED INTERCEPTOR

WAVERIDER INCORPORATED

Dave Dober	Project Engineer
Waleed Al-Hashel	Aerodynamics/Systems
Bob Baldocchi	Propulsion/Carrier Suit
Tim Berg	Structures/Weights
Harry Dunbrack	Stability/Control
Curt Lindsay	Structures/Materials
Aaron McAtee	Propulsion/Production
Dan Sergent	Aero/Performance
Prof. Conrad Newberry	Project Advisor

TABLE OF CONTENTS

I. Introduction

A. Background.....1

B. Design Team Organization.....2

C. Design Goals.....4

D. Alternatives Considered.....4

E. Mach Number Optimization.....6

F. Constraint Analysis.....7

II. Configuration and Weight

A. Background.....9

B. Carrier Suitability.....13

C. Final Design Results.....15

III. Aerodynamics

A. Airfoil and Wing Selection.....21

B. Drag Calculations.....24

C. V-N Diagram.....24

D. Lift Calculations.....31

E. Trade Studies.....31

IV. Propulsion System

A. Design Goals.....37

B. RFP Requirements.....37

C. Trade Studies.....37

D. Design Results.....38

V. Stability and Control

A. Introduction.....52

B. Static Stability.....52

C. Dynamic Stability.....56

D. Stability Augmentation.....65
E. Flying Qualities.....65
VI. Structures
A. Design Goals.....76
B. Requirements.....76
C. Material Selection.....76
D. Thermal Selection.....77
E. Wing Box Design.....82
F. Fuselage.....82
G. Landing Gear.....84
VII. Performance
A. Takeoff and Landing.....85
B. Specific Excess Power.....85
C. Climb.....88
D. Flight Envelope.....88
VIII. Aircraft Systems
A. Electrical System.....90
B. Hydraulics.....90
C. Fuel System.....92
D. Survivability.....94
E. Cockpit Design.....96
F. Maintainability.....104
G. Supportability.....106
IX. Production Facilities
X. Cost/Quality
A. Cost Estimating Relationships.....109
B. Quality.....111

XI. Summary

A. RFP Comparison.....113

B. Conclusions.....113

Appendix A

List of References

I. INTRODUCTION

A. BACKGROUND

Today's carrier based deck launched intercept (DLI) mission is a vital one that is aimed at protecting the carrier battle group and to deter potential adversaries. The assets deployed on our carrier decks are able to complete this mission but with very limited range. The waverider concept has great potential to increase the range of this carrier based mission. As a result, a Request for Proposals (RFP) was developed which contains design requirements for an aircraft that can complete this mission through the utilization of waverider technology. The following design requirements were listed in the RFP:

- Carrier based interceptor
- Utilization of waverider technology
- Single pilot
- Minimum radius of 700 nautical miles
- Dash Mach number below Mach 5
- Payload of 4 future missiles carried internally or conformably
- Operable from Nimitz class and subsequent carriers
- Mission cycle time of: 1 hour (minimum)
  1 hour 30 minutes (desired)
- 180 degree sustained turn of: 2g (minimum)
  4g (desired)
- Maximum takeoff weight of 85,000 lbs.
- Carrier approach speed:
  - longitudinal acceleration of at least 5 ft/sec^2 on a standard day at 0 flight path angle will be available within 2.5 seconds after initiation of throttle movement to military thrust position while in a stable approach at $V_{PA, MIN}$

- Catapult takeoff:
  - horizontal acceleration of at least .065g at the end of the catapult stroke and at the catapult end speed
  - rotation of aircraft not to exceed 0.9 $C_{L,MAX}$
  - maximum sink rate of aircraft cg not to exceed 5 feet
  - effect of engine thrust on catapult end speed not to exceed 5 knots
- Minimum wave-off rate of climb of 500 ft/min, with one engine inoperative at $V_{PA,\ MIN}$ at design carrier landing weight in the landing configuration

The deck launched intercept, as defined in the RFP, is shown in Figure 1.1. The mission profile consists of: takeoff and acceleration to Mach 0.3 at sea level, maximum power acceleration from Mach 0.3 to best rate of climb speed at sea level, maximum A/B climb to optimum cruise altitude, cruise out at design Mach number at optimum cruise altitude, 4g sustained turn at design Mach and altitude at maximum power for 180 degrees or 2g sustained turn at design Mach and altitude at maximum power for 180 degrees if 4g is not achievable, descend to optimum cruise altitude, cruise back at optimum altitude and Mach number, descend to sea level, fuel allowance equal 20 minutes loiter at sea level at speeds for maximum endurance plus 5% of initial total fuel.

B. DESIGN TEAM ORGANIZATION

A design team was formed which consisted of 8 members. Each member was assigned a primary area of responsibility in which he is the group expert. Several secondary responsibilities were assigned to each member to ensure that each member completed work in each of the major aerospace design subject areas. Figure 1.2 depicts each members primary area of responsibility.

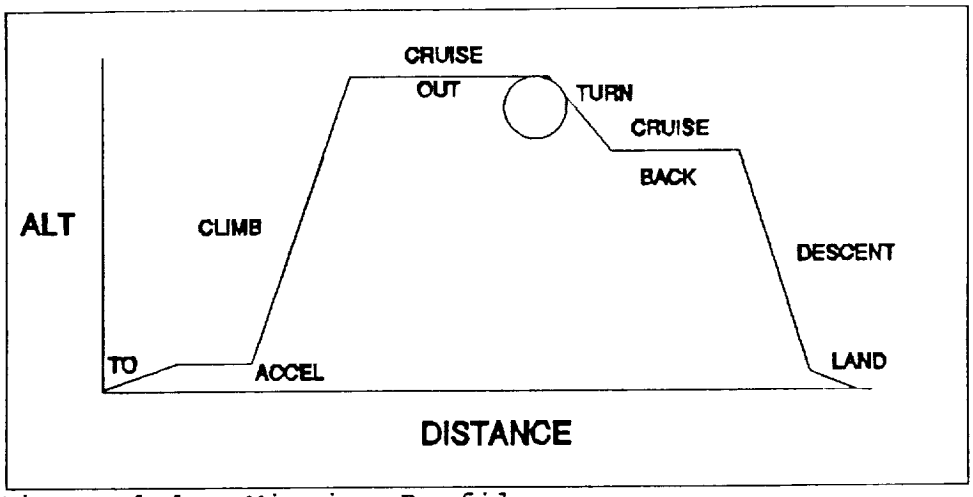

Figure 1.1: Mission Profile

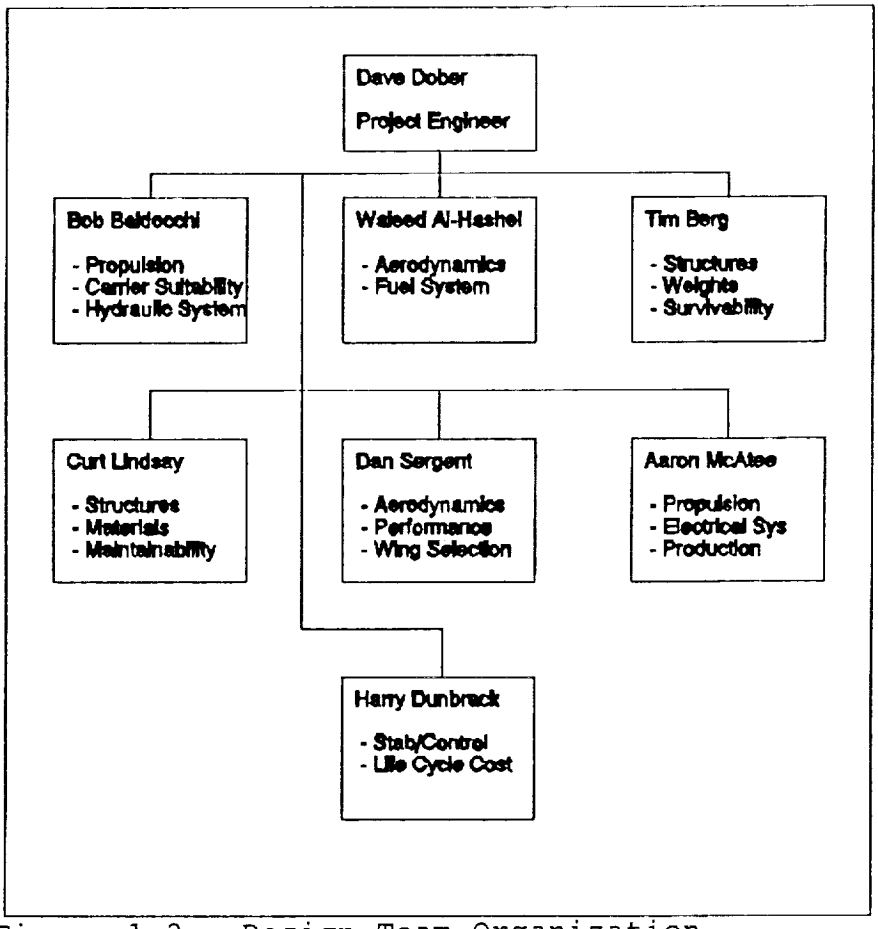

Figure 1.2: Design Team Organization

C. DESIGN GOALS

The basic philosophy utilized in the design of our waverider configured aircraft, nicknamed the Sabot, was to simply meet the requirements that were delineated in the RFP. There is no incentive to exceed the RFP requirements. While meeting the RFP requirements is the main goal of the design an important secondary goal was to keep the design as simple as possible. We wanted a design that was both geometrically and systematically simple. The only exception to this goal was the incorporation of multi-sensor integration (MSI) into the cockpit displays. MSI is an extremely complicated system that is used to relieve some of the pilot work load in single piloted aircraft by displaying all available information from the onboard sensors more efficiently than conventional systems. Another extremely important factor is cost. Our design utilizes Titanium for the aerodynamic heating problem associated with supersonic flight and composite materials to keep the gross weight within limits. Both materials are expensive and drive up the cost. The effect of using expensive materials was offset by using systems that are very similar to systems that are in use today. In effect, no new systems technology was required to be developed.

D. ALTERNATIVES CONSIDERED

When the RFP was first issued no one within our design group had extensive knowledge about waverider technology. Consequently, much individual research was completed to familiarize ourselves with waverider technology. Much of the information concerning

aerodynamic heating, propulsion and controls came from reports that were written on the North American XB-70 VALKYRIE and the Lockheed SR-71 Blackbird. Information about the flow field came from several NASA reports from the mid 60's and from missile aerodynamics publications.

The flow field around a waverider forces some of the geometric parameters of the waverider body to be fixed. For example, if the free stream Mach number and the semi-vertex angle of the cone generating the conical shock wave are known, then the leading edge wing sweep of the waverider vehicle will be known since the leading edge must capture the shock. Geometric constraints from shipboard compatibility requirements and from aircraft systems integration also helped fix some of the required geometry. We considered 3 different waverider configurations. One configuration is the caret waverider. This geometric shape results from a 2 dimensional wedge-shock solution to a flow field that has a known free stream Mach number. Two other configurations were considered that were generated from a conical shock solution to a flow field of known free stream Mach number. One of the requirements of our design is a required amount of fuselage volume that would carry all the aircraft systems and the required fuel to complete the mission. Our intention was to design an aircraft that would takeoff and land conventionally from an aircraft carrier. This self imposed constraint limits our design to include either vectored thrust or a variable geometry wing. One of these two systems would need to be utilized in our design in order to attain the required subsonic

performance for landing conventionally. The volume requirement coupled with landing gear integration forced us to abandon the caret waverider configuration. The geometry of the caret waverider does not provide for much fuselage volume and landing gear integration would require extremely long struts. The two remaining conical waverider configurations were then considered. One of these waverider shapes results from a free stream surface that intersects a shock generating cone below the vertex. The other waverider shape results from intersecting a shock generating cone through the vertex of the cone. The latter configuration contains the simplest geometry and was chosen for our design based solely on that fact.

E. MACH NUMBER SELECTION

Several factors had to be considered prior to selecting a design Mach number. One of these factors was the minimum and desired cycle times that were delineated in the RFP. Another factor was material selection versus surface skin temperature due to aerodynamic heating which is a function of Mach number. The last factor considered was the static pressure rise through a conical shock wave as a function of Mach number. The waverider concept is based on restricting the shock wave to the lower portion of the aircraft in order to exploit the static pressure rise through the shock wave. A higher free stream Mach number will result in a greater static pressure rise through the shock wave. A greater static pressure rise will yield a higher L/D ratio which will increase the range of the aircraft. The required minimum

radius of 700 nautical miles coupled with the minimum and desired cycle times dictates a Mach number range of 2.09 to 3.66. With these factors in mind a Mach number of 3.0 was selected. This Mach number will yield a static pressure ratio across the shock of 10.33 as compared to 4.93 which corresponds to a Mach number of 2.09. This greater pressure rise will result in better utilization of the waverider concept. A Mach number of 3.0 will also satisfy the minimum cycle time requirement. Materials already exist that can easily withstand the aerodynamic heating problem at this Mach number. Materials selection is fully covered in the structures portion of this report.

F. CONSTRAINT ANALYSIS

The Constraint Diagram for the Sabot is included as Figure 1.3. The reference for the constraint analysis is Aircraft Engine Design, by Mattingly. The constraint diagram was used to establish the minimum thrust-to-weight at sea level takeoff (T_{sl}/W_{TO}) and wing loading at takeoff (W_{TO}/S) to satisfy RFP requirements. The variables input to the Sabot Constraint Analysis were: takeoff distance of 4000 feet at sea level standard day and maximum gross weight, landing distance of 3000 feet at 60% of maximum gross weight, advanced turbojet thrust lapse, cruise and turns at 50,000 feet altitude, and sustained turn performance at 85% of maximum gross weight. The design point chosen for the Sabot was T_{sl}/W_{TO} = 0.55 and W_{TO}/S = 105 (lb/ft^2). The constraints which dictated the design point were takeoff and high speed turn performance.

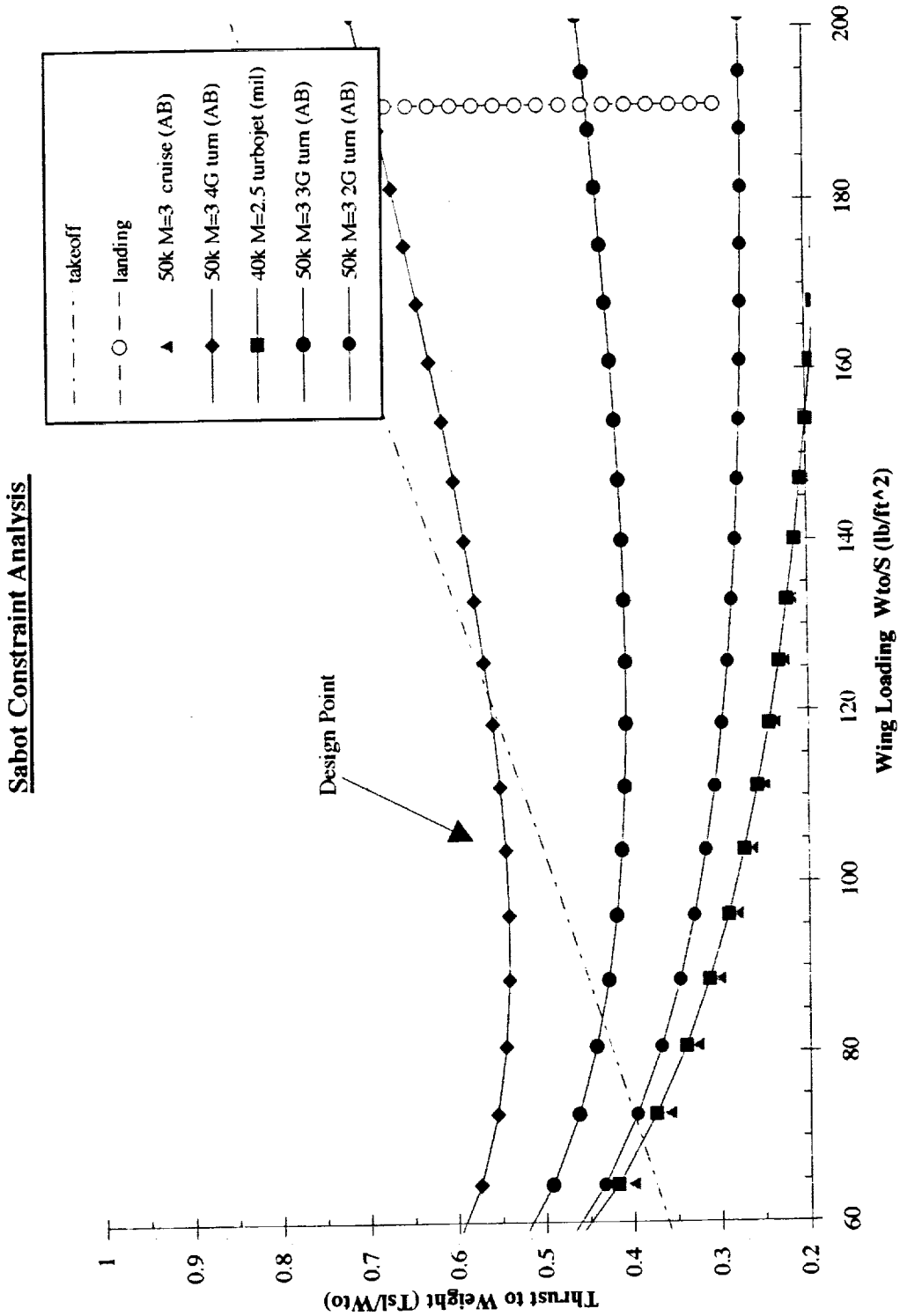

Figure 1.3: Constraint Diagram

II. CONFIGURATION AND WEIGHT

A. BACKGROUND

Long range high speed cruise dictated that the Sabot have large engines and fuel fraction. The fuselage sizing was primarily influenced by the required inlet capture area and fuel volume. A three view diagram is included as Figure 2.1. Sabot weight estimates were refined using a statistical group weights method developed from regression analysis of existing aircraft. The Sabot weight analysis utilized equations for USN carrier-based fighter aircraft from [Nicolai] and [Raymer]. Component weight equations were modified with fudge factors recommended to account for the use of composites in the structure and the integration of advanced technology systems into the design. Projected future capabilities were employed in the avionics, hydraulics, and survivability technologies. The aircraft component weights, center of gravity, moments of inertia, and volumes were computed with Microsoft Excel. Since many of the empirical weight equations were themselves dependent on takeoff weight, an iterative method was used to converge the solution. Weights are tabulated in the Summary Group Weight Statement (Table 2.1). From preliminary three view drawings, components were located relative to a datum defined as the nose of the aircraft. Using the method outlined in [Roskam], the moments of inertia were calculated in Table 2.1 and the center of gravity was calculated in Table 2.2. The C.G. varied from a forward location of 30.99 ft (23.86% mean aerodynamic chord) with the wings forward at maximum gross weight, to an aft location of

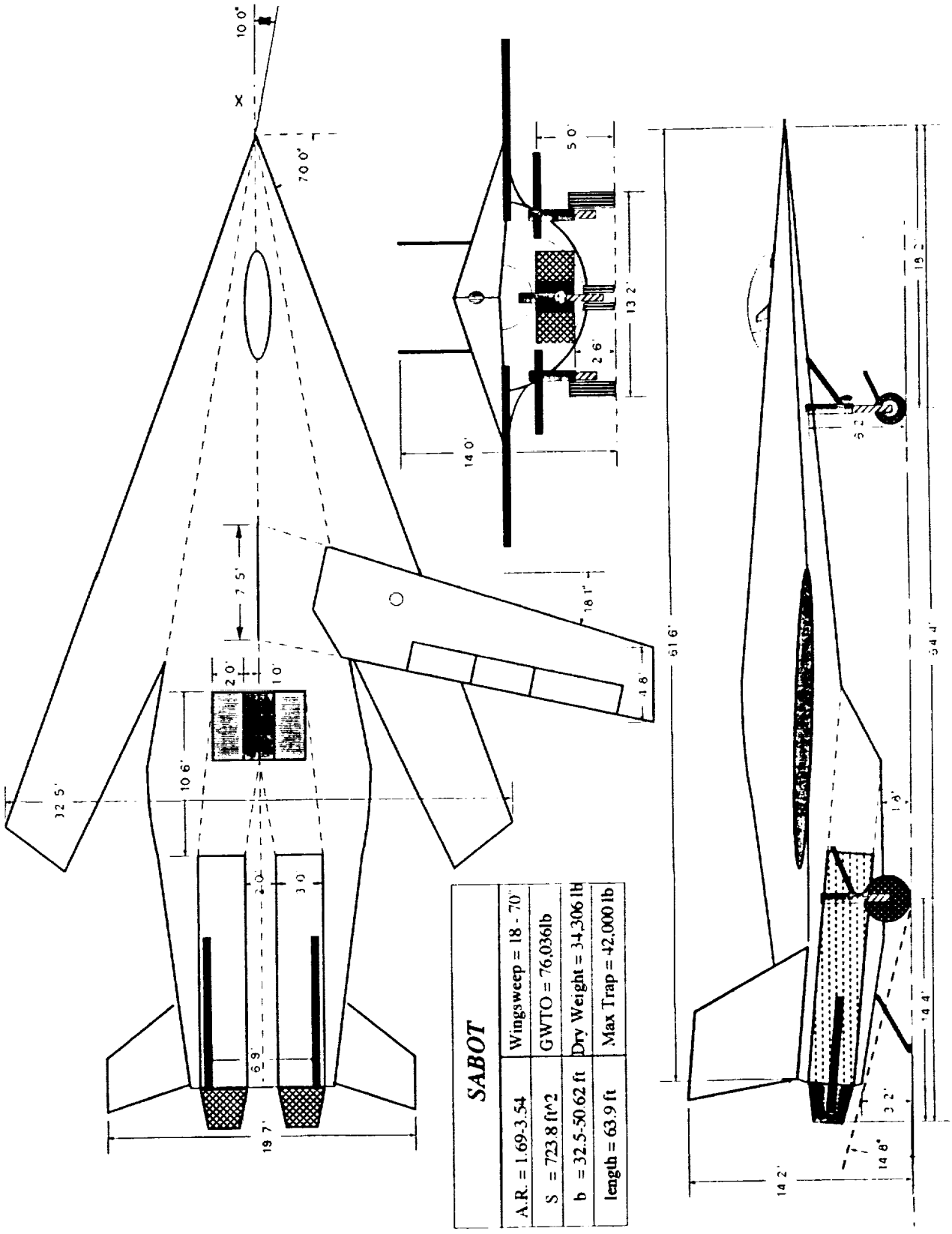

Figure 2.1: Three View Diagram

Group Weights and Moments Statement

		weight (lb)	*Centroid Location (ft* X	Y	Z	*Ixx* (slug-ft^2)
Structures Group						
	Wing	8,637.33	30	0	2	35.49
	Horizontal Tail	663.14	57	0	0	26.62
	Vertical Tail	338.87	55	0	-5	396.61
	Fuselage	8,898.11	29	0	-1	1,262.32
	Arresting Gear	608.29	55	0	3	65.66
	Catapult Gear	152.07	14	0	3	16.41
	Main Landing Gear	1,589.46	48	0	4	405.10
	Nose Gear	455.05	14	0	4	115.98
	Inlet/Ramps	834.05	37	0	1	936.53
Propulsion Group						
	Engines	6,000.00	50	0	2	68,073.68
	Engine Controls	48.79	40	0	-1	
	Starting System	264.38	37	0	1	704.43
	Fuel System	1,676.78	25	0	-2	8,020.30
Equipment Group						
	Hydraulics and Flight Controls	2,006.71	38	0	-2	613.55
	Electrical	572.74	20	0	0	22.99
	Avionics	1,039.35	10	0	-2	305.75
	Ejection seat	290.65	10	0	-2	88.87
	Air conditioning/ECS	230.58	25	0	-1	32.71
	Total Empty Weight =	**34,306.35**				
Useful Load Group						
	Pilot	230.00	10.00	0.00	-3.00	57.95
	Fuel	39,000.00				
	Ordnance	2,500.00	40.00	0.00	2.00	57.95
Takeoff Gross Weight						
	Flight Design Gross Weight =	**76,036.35**				

Table 2.1: Group Weights and Moments Statement

Center of Gravity

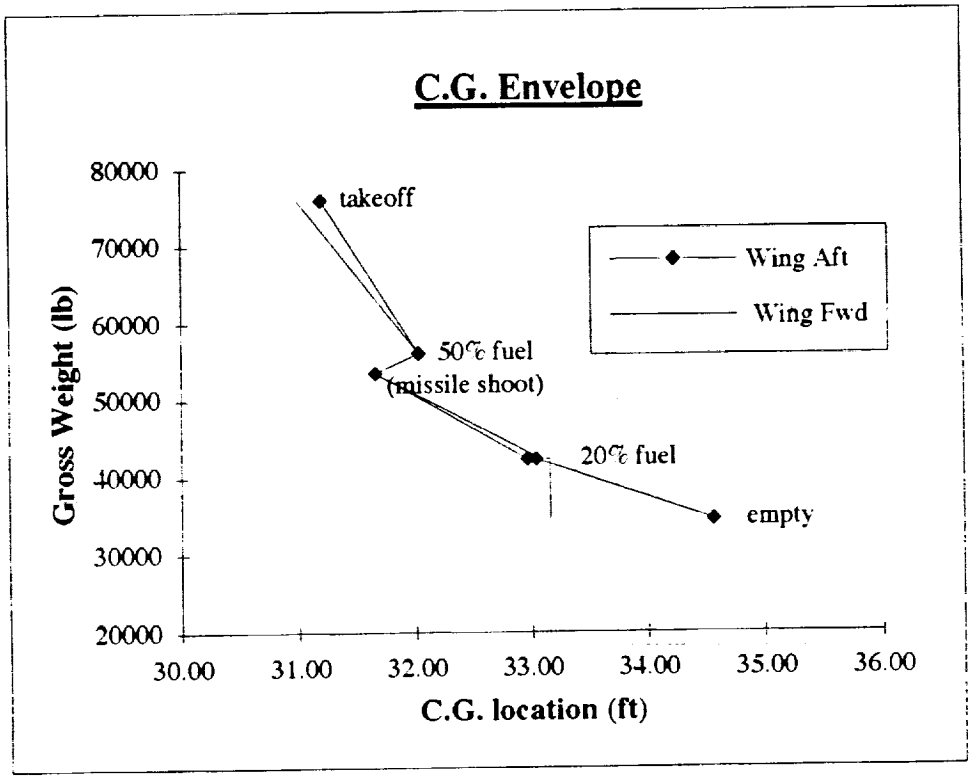

Figure 2.2: Center of Gravity

case	Gross Weight (lb)	Wings Forward ft	Wings Forward % mac	Wings Aft ft	Wings Aft % mac
Maximum Takeoff weight (gear down)	76036	30.99	23.86	31.20	53.46
50% fuel (19,500 lb) with 4 AIM-7	56036	32.03	40.51	32.03	67.41
50% fuel, no ordnance	53536	31.66	34.61	31.66	62.47
20% (7800 lb) fuel, gear up	42336	33.08	57.24	32.96	79.77
20% fuel, gear down	42336	33.16	58.53	33.04	80.84
empty weight	34536	33.16	58.53	34.56	83.53

Table 2.2: Center of Gravity Calculations

34.56 ft (83.53% mean aerodynamic chord) with the wings aft at dry weight. A plot of C.G. versus weight is included as Figure 2.2.

B. CARRIER SUITABILITY

The RFP demands on carrier suitability severely restricted the high speed performance benefits of the waverider design. Specifically, incorporation of existing technology to provide required pilot visibility and maximum engaging speed introduced complications which limited the design process.

Unlike current waverider programs, the Sabot was required to meet the cockpit visibility specifications set forth in MIL-STD-850B. This publication established a requirement for a minimum of 11 degrees down vision available from the pilots designed eye position. Due to volume constraints, the ejection seat was located 12 feet back from the nose of the aircraft. This required a canopy height of 2.5 feet. Additional research is necessary to determine the uncertainties introduced into the flow field by placing a canopy on the top of the vehicle.

Swing wing technology was incorporated to provide acceptable carrier approach speeds. Penalties associated with the performance and weight of this system further degraded the high speed design.

Carrier approach and landing speeds were predicated on forward visibility and maximum engaging speeds. To provide acceptable visibility, approach angle of attack was limited to 7 degrees AOA. The heavy line in Figure 2.3 represents the capacity limits of the MK-7 mod 3 arresting gear. Operations under no wind conditions are limited to full flap landings under 43,000 pounds. At that weight

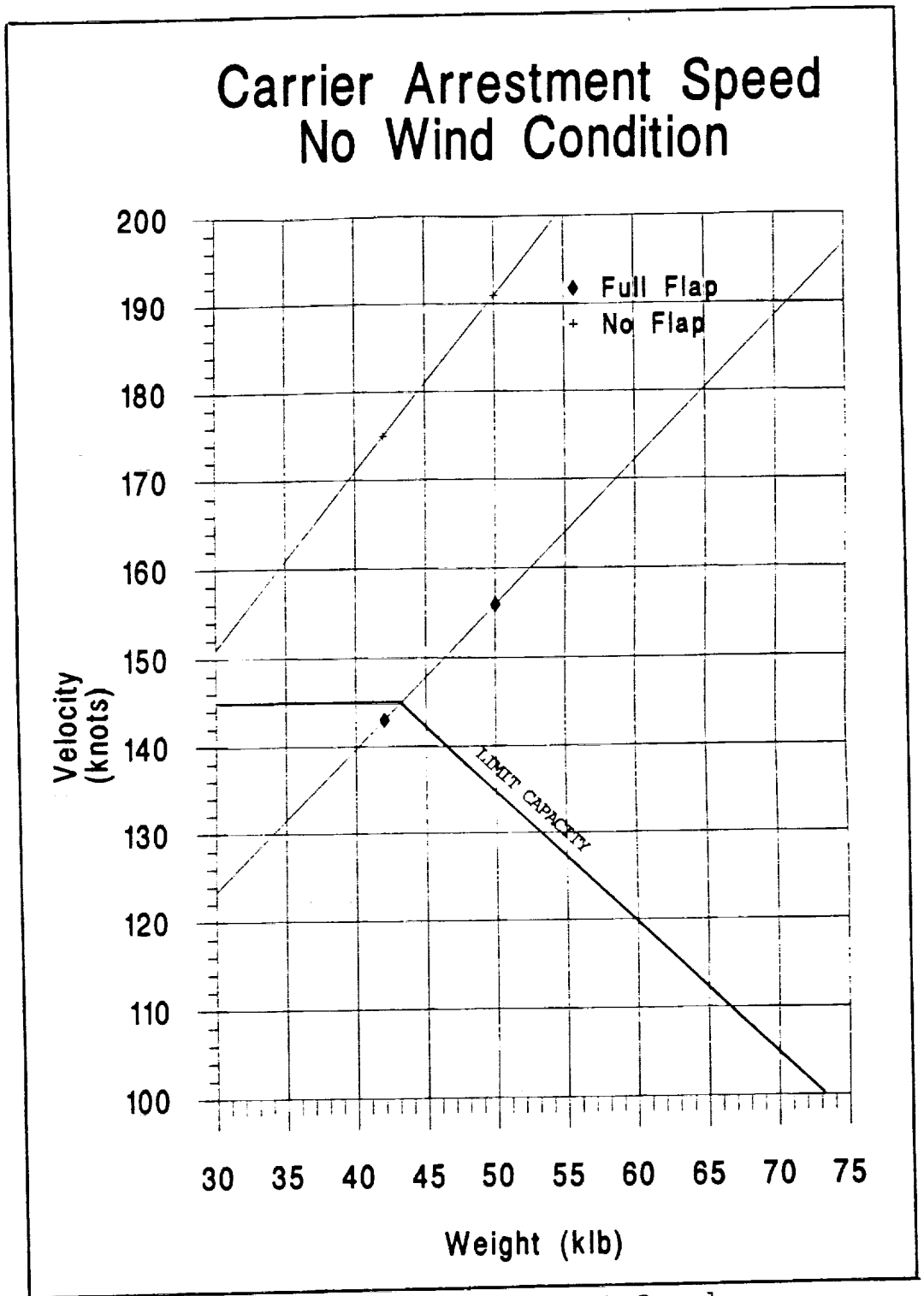

Figure 2.3: Approach and Arrestment Speed

no flap landings require 30 knots of wind over the deck. Barricade engagements risk damage to leading edge wing sections and require the canopy to be intact.

Deck handling characteristics are satisfactory and in compliance with MIL-STD-805A. In order to comply with the 130,000 pound limitation for dual aircraft elevator operation, the Sabots would be limited to partial fuel loads.

The deck launched interceptor mission is enhanced by an auxiliary power unit (APU) to provide independent starting operations and a modern cockpit design with multi-sensor integration which shortens alignment time and provides pertinent information to the pilot at an increased rate. Table 2.3 compares carrier suitability of the Sabot with the requirements set forth in the RFP.

C. FINAL DESIGN RESULTS

The Sabot design blends a low wave drag waverider configuration with acceptable low speed performance characteristics. The efficient transition from waverider to USN fighter requires area ruling the fuselage to minimize drag. The primary challenges to packaging were 736 cubic feet of fuel and 1125 cubic feet of engines and inlets. Cockpit visibility also was given high priority. Area Ruling and volume estimation techniques from [Raymer] and [Nelson] were used to improve the Sabot design. The cross sectional area of the Sabot is plotted along with an optimized Sears-Haack area distribution in Figure 2.4. Following the initial analysis, the fuselage shape was smoothed to

Category	Requirement	Sabot	Compliance
Max Gross Weight (lbs)	< 85000	76000	10.6% less
Max Wing Span (ft)	< 82	50.62	meets
Max Height (ft)	< 18.5	14.5	meets
Launch Bar to Tail Pipe Distance (ft)	< 45.83	45.44	meets
Max Landing Gear Width (ft)	< 22	13.2	meets
Max Launch WOD (knot) (over operational)	0	0	meets
Max Land WOD (knot)	0	0	meets
Min Longitudinal Accel After 2.5 sec (fps^2)	> 5	18.2	Exceeds by 72.5%
Min Approach Speed (knot)	> 1.1 Vpa	1.2 Vpa	Exceeds by 8.3%
Stability and Control	MIL-F-8785	N/A	meets
Time to Complete 50 ft Altitude Correction from Initial Flt Path	< 5 sec	4.5 sec	Exceeds by 10.0%
Min Horizontal Catapult Accel (g's)	> 0.065	.43	Exceeds by 63.5%
Max Rotation at Takeoff	< .9 Clmax	.88 Clmax	Exceeds by 2.2%
Single Engine Wave-Off Rate of Climb (fpm)	> 500	4320	Exceeds by 88.4%
Cockpit Visibility	MIL-STD-850B	N/A	meets
Min Tip Back Angle (deg)	15	15	meets

Table 2.3: Carrier Suitability

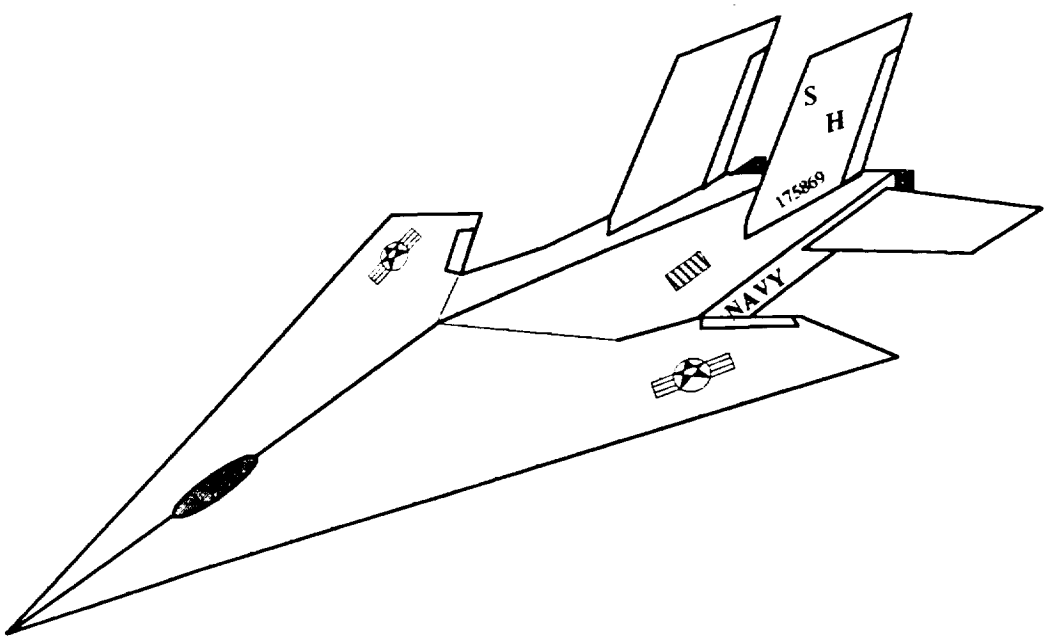

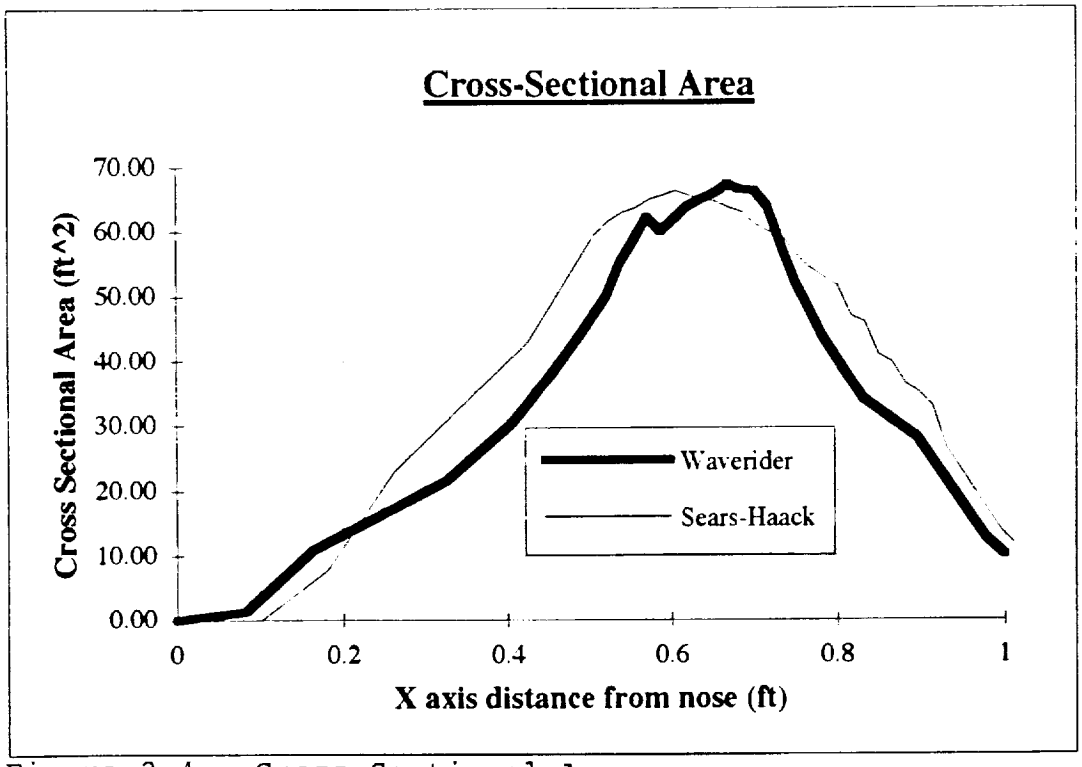

Figure 2.4: Cross-Sectional Area

approximate the Sears-Haack curve and minimize wave drag. Volume calculations were performed to estimate component volumes. A volumetric efficiency of 85% was used to account for expansion and piping to size the fuel tanks. The Sabot configuration volume is large enough to contain the proposed systems. A volume buildup summary is included as Table 2.4. Views of the Sabot's major component locations are included as Figure 2.5.

Volume Buildup

		weight (lb)	*estimated volume (ft^3)*
Structures Group			
	Wing	8,637.33	124.98
	Horizontal Tail	663.14	36.00
	Vertical Tail	338.87	27.69
	Fuselage	8,898.11	2,418.00
	Arresting Gear	608.29	2.00
	Catapult Gear	152.07	1.00
	Main Landing Gear	1,589.46	36.00
	Nose Gear	455.05	24.00
	Inlet Ramps	834.05	159.00
Propulsion Group			
	Engines	6,000.00	966.14
	Engine Controls	48.79	1.00
	Starting System	264.38	5.00
	Fuel System	1,676.78	865.70
Equipment Group			
	Hydraulics and Flight Controls	2,006.71	42.79
	Electrical	572.74	10.00
	Avionics	1,039.35	41.50
	Ejection seat	290.65	15.00
	Air conditioning ECS	230.58	15.00

Total Empty Weight = 34,306.35

Useful Load Group			
	Pilot	230.00	50.00
	Fuel	39,000.00	735.85
	Ordnance	2,500.00	82.50

Flight Design Gross Weight = 76,036.35

Volume Required = 2,317 (ft^3)

Volume Available = 2,543 (ft^3)

Aircraft Density (empty) = 24.20 (lb/ft^3)
Aircraft Density (full) = 53.63 (lb/ft^3)

(typical fighter density) = 30-45 (lb/ft^3)

(densities computed without propulsion stream tube)

Table 2.4: Volume Build-Up

Sabot Internal Layout

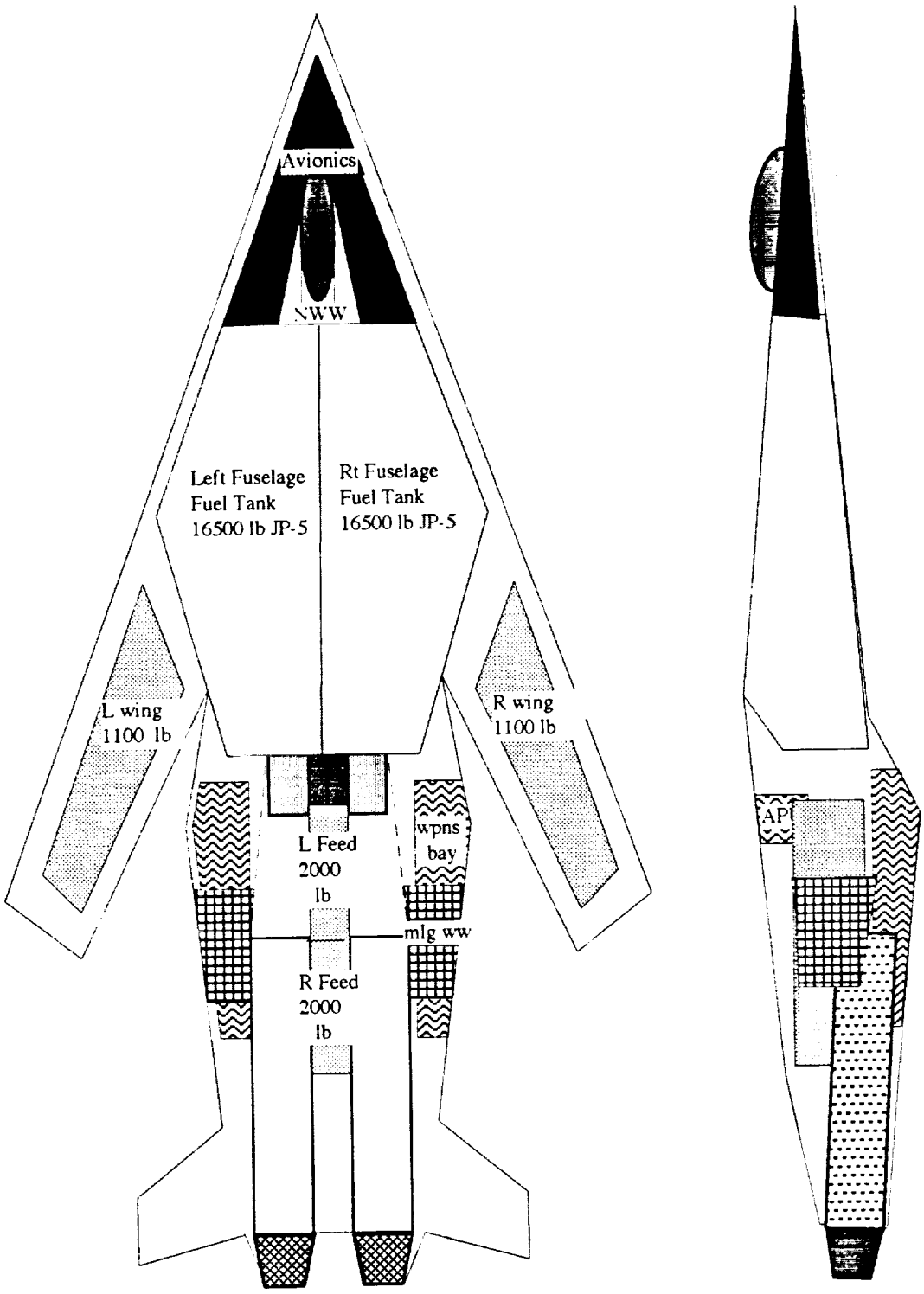

Figure 2.5: Major Component Location

III. AERODYNAMICS

A. AIRFOIL AND WING SELECTION

The following were used to determine the optimal airfoil section and wing that satisfied the design requirements:

The airfoil must operate in transonic and supersonic flow regimes which require minimum thickness, little camber, sharp leading and trailing edges and t/c_{max} located near midchord.

The airfoil must operate at slow speeds generating C_{Lmax} at or below 15 degrees AOA.

The wing must allow for placement of fuel and control surfaces.

The wing must support 76,036 lb maximum gross weight at takeoff.

The planform of the wing must conform with the waverider form of the forebody.

The result of the trade study showed that the NACA 63-206 provided the optimal airfoil section having good high speed characteristics and the best slow speed abilities (Fig 3.1). The wing is swept to provide the necessary lift at low speeds, while allowing it to be stowed inline with the forebody to continue the waverider effect at Mach 3. The leading edge utilizes a sharp radius "leading edge flap" to capture the shock while flying in a waverider configuration (Fig 3.2). An important consideration with the waverider is maintaining the proper attitude while the weight, and hence lift are decreasing throughout the flight due to fuel consumption. With multiple segmented leading edge flaps with sharp leading edges, the point the shock is released from the waverider can be controlled. This allows the lift to be reduced as the aircraft burns fuel, and maintain the optimal attitude.

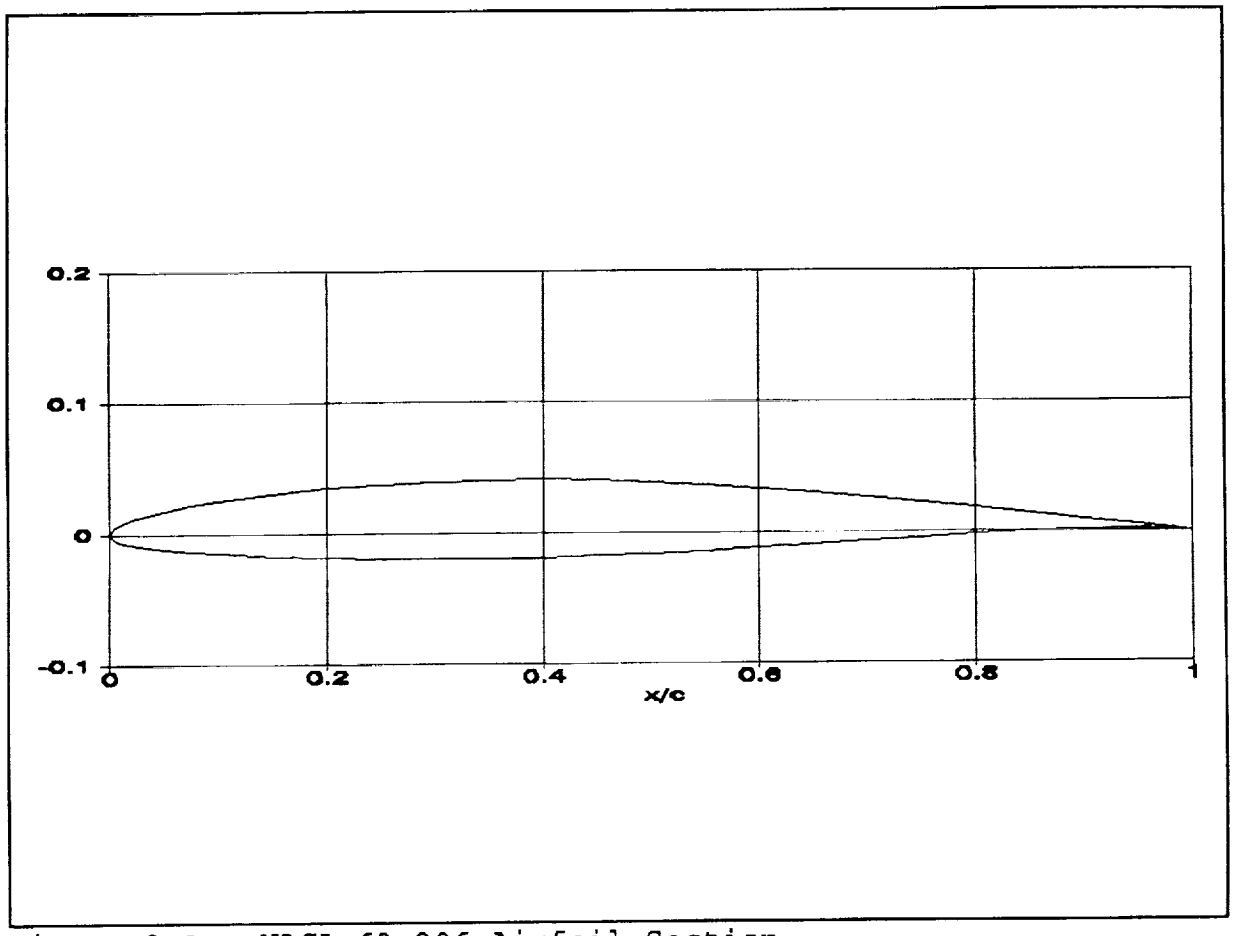

Figure 3.1: NACA 63-206 Airfoil Section

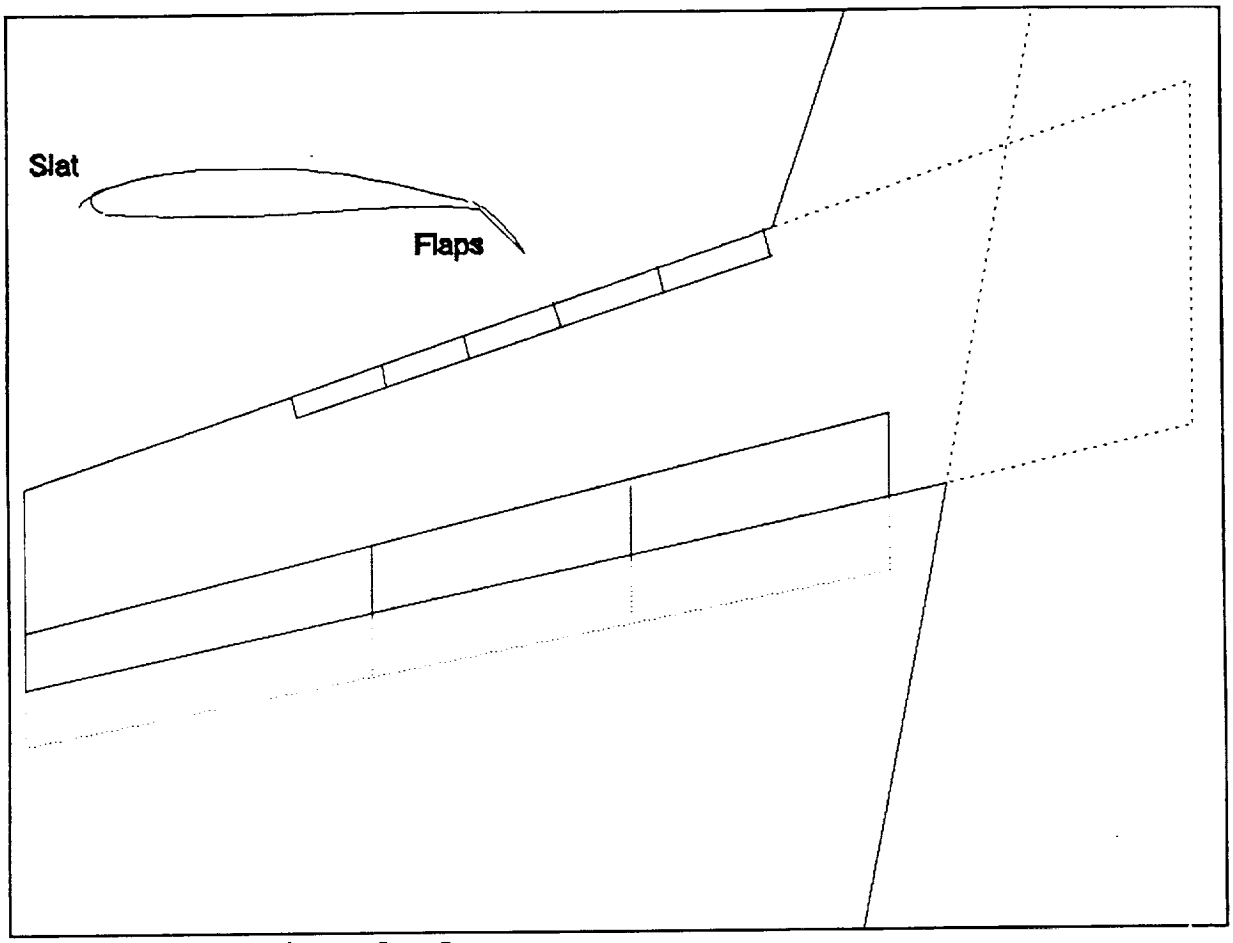

Figure 3.2: Wing Planform

B. DRAG CALCULATIONS

1. Zero Lift Drag Coefficient (CD_o)

CD_o was calculated for subsonic, transonic and supersonic speeds using USAF DATCOM. The results are given in Tables 3.1, 3.2 and 3.3 with the graph presented in Figure 3.3. Drag divergence mach # = 0.976. In subsonic region (M=0.2) CD_o is equal to 0.015; in transonic region the drag peaked at (M=1.10) and in supersonic region at (M=3.0) CD_o is equal to 0.013. The supersonic CD_o was too high initially due to a large aircraft base diameter which caused the body drag coefficient to be high. After trade-off studies were conducted the base diameter was reduced (by tapering the aircraft body) and the low supersonic CD_o was accomplished.

2. Drag Polars

Drag polars are presented in Table 3.4 and Figure 3.4 for various Mach numbers in accordance with Nicolai, chapter 11. The subsonic drag polar is comprised primarily of skin friction and parasite drag. On the other hand, transonic and supersonic drag is dominated by wave drag. The curves depict drag polars at M=0.2, 1.1 and 3.0.

C. V-N DIAGRAM

The V-N diagram was constructed using the guidelines established in the FAR part 25 and the standards set forth in the MIL-A-8861(ASL). Conditions were analyzed both at sea level and 50,000 ft. The gust load lines all fall within the operating envelope. The V-N diagrams are shown in Figures 3.5 and 3.6.

M	CD_{0W}	CD_{0HT}	CD_{0VT}	CD_{0B}	CD_0
0.1	0.007	0.001	0.059	0.068	0.015
0.2	0.006	0.001	0.076	0.063	0.015
0.3	0.006	0.001	0.086	0.060	0.015
0.4	0.006	$9.91E^{-4}$	0.093	0.058	0.015
0.5	0.006	$9.57E^{-4}$	0.099	0.057	0.015
0.6	0.005	$9.31E^{-4}$	0.103	0.055	0.015
0.7	0.005	$9.10E^{-4}$	0.107	0.055	0.015
0.8	0.005	$8.92E^{-4}$	0.111	0.054	0.015

Table 3.1: Subsonic CD_0 Buildup

M	CD_{0W}	CD_{0HT}	CD_{0VT}	CD_{0b}	CD_0
0.9	0.0055	0.0008	0.0002	0.0043	0.0108
0.95	0.0144	0.0033	0.0021	0.0044	0.0242
1.00	0.0232	0.0146	0.0034	0.0083	0.0495
1.05	0.0246	0.0148	0.0056	0.0099	0.0549
1.10	0.0249	0.0150	0.0065	0.0105	0.0569
1.20	0.0220	0.00079	0.00054	0.17	0.0330

Table 3.2: Transonic CD_0 Buildup

M	CD_{0w}	CD_{0HT}	CD_{0VT}	CD_{0b}	CD_0
1.5	0.014	$5.27E^{-4}$	$3.62E^{-4}$	0.146	0.023
2.0	0.009	$3.75E^{-4}$	$2.57E^{-4}$	0.137	0.018
2.5	0.007	$2.99E^{-4}$	$2.05E^{-4}$	0.121	0.015
3.0	0.006	$2.51E^{-4}$	$1.72E^{-4}$	0.110	0.013
3.5	0.005	$2.15E^{-4}$	$1.47E^{-4}$	0.102	0.011
4.0	0.004	$1.88E^{-4}$	$1.29E^{-4}$	0.097	0.010
4.5	0.004	$1.65E^{-4}$	$1.14E^{-4}$	0.089	0.009
5.0	0.003	$1.48E^{-4}$	$1.02E^{-4}$	0.085	0.009

Table 3.3: Supersonic CD_0 Buildup

CL	CD (M=0.5)	CD (M=1.10)	CD (M=3.0)
0	0.015	0.057	0.013
0.1	0.017	0.059	0.015
0.2	0.024	0.066	0.022
0.3	0.036	0.078	0.034
0.4	0.052	0.094	0.050
0.5	0.072	0.114	0.070
0.6	0.098	0.140	0.096
0.7	0.128	0.170	0.126
0.8	0.162	0.204	0.160

Table 3.4: Values of C_D for Different C_L

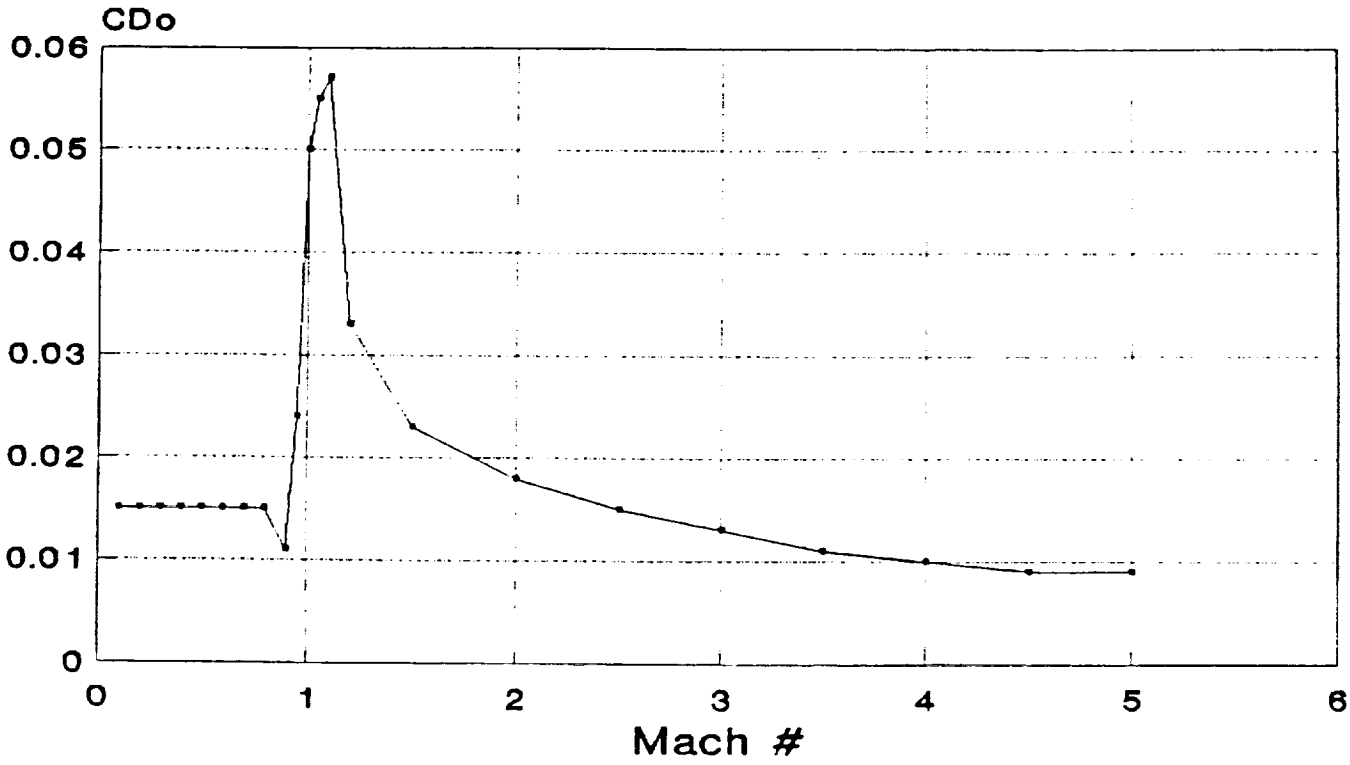

Figure 3.3: C_{Do} vs. Mach Number

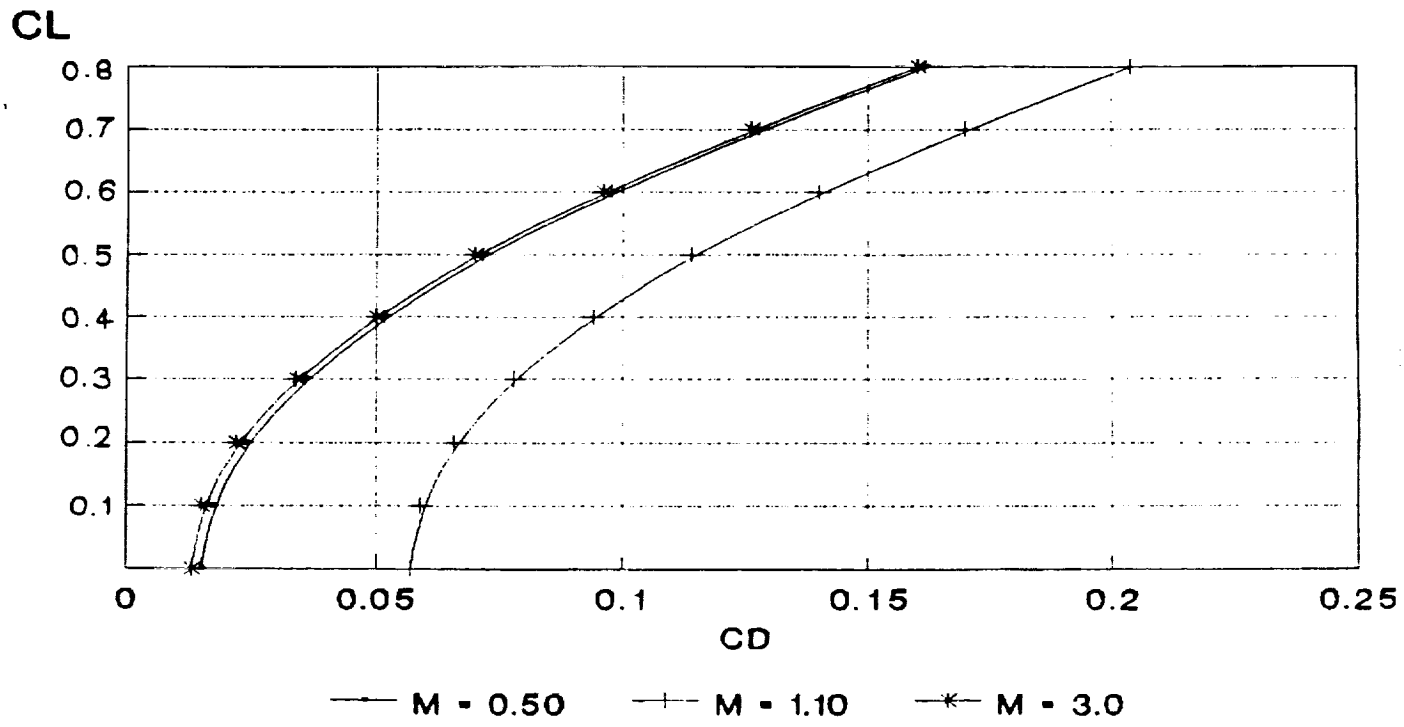

Figure 3.4: Drag Polars

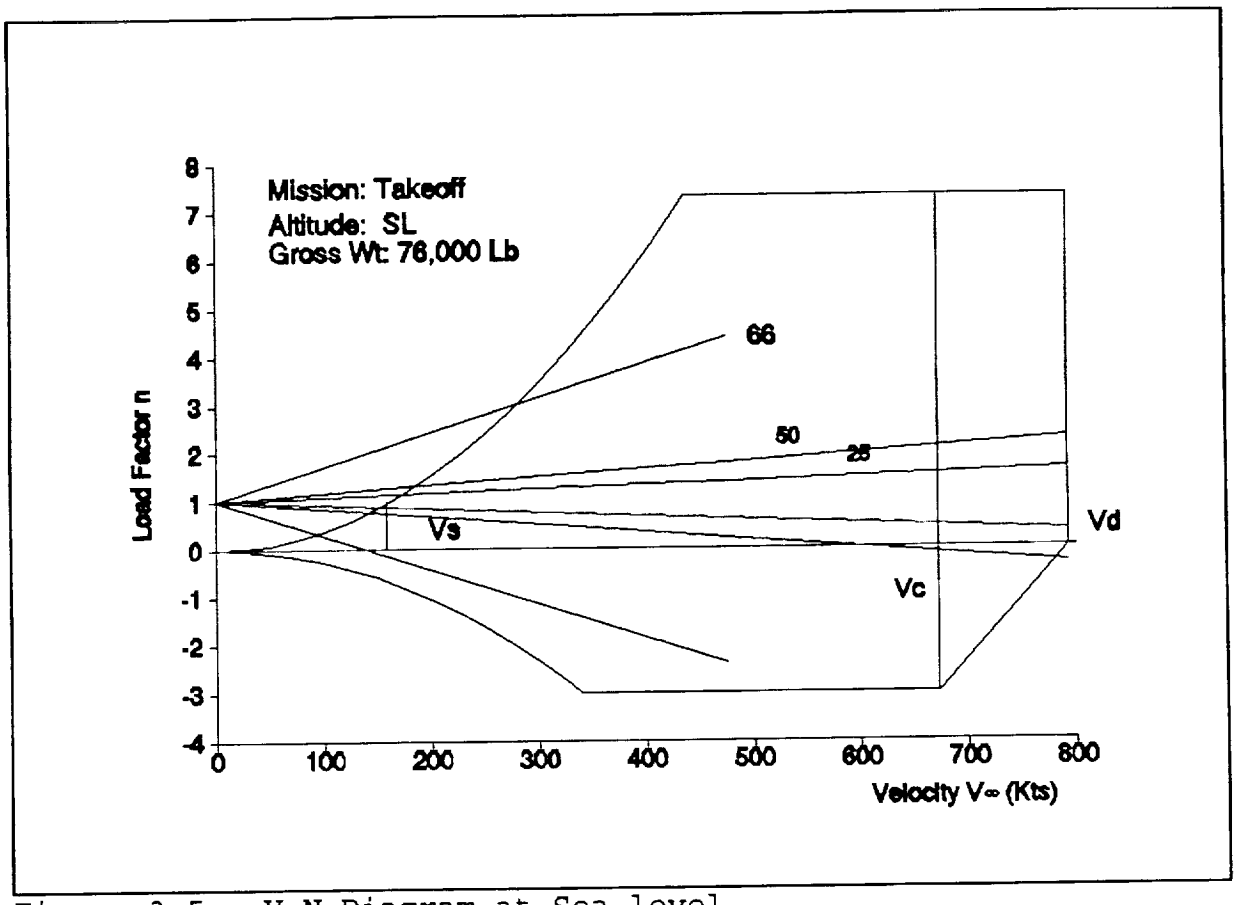

Figure 3.5: V-N Diagram at Sea level

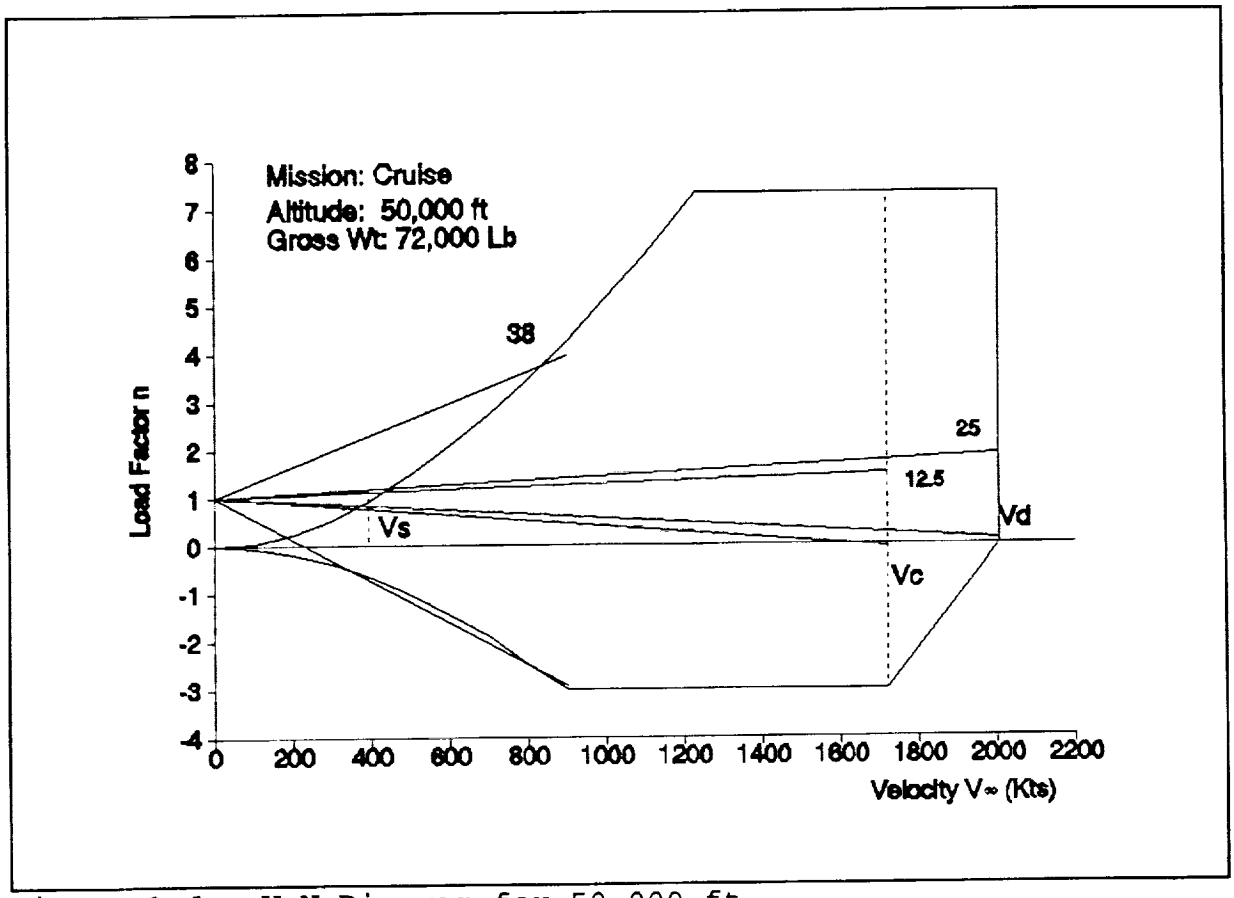

Figure 3.6: V-N Diagram for 50,000 ft

D. LIFT CALCULATIONS

1. Lift Curve Slope

The aerodynamics were analyzed using the Air Force Stability and Control DATCOM methods. At slow speeds the forebody was modeled as a leading edge strake, while at high speeds it was considered part of the wing. The wing was swept at Mach 0.8. The lift curve slope is shown for various Mach numbers in Figure 3.7. At Mach 0.2 Cl_α = 0.0661/deg and at Mach 3 Cl_α = 0.020/deg.

2. High Lift Devices

Lift is enhanced at low speeds by the addition of Fowler flaps along the trailing edge and by the leading edge strake effect of the forebody. Several high lift designs were considered including leading edge flaps, variable camber devices and slotted flaps. Leading edge flaps are being employed to hold the shock while flying at design Mach. Fowler flaps were chosen for their high lift benefits and simple design. Sizing was based on lift required and structural limitations. A 30° flap deflection was used for the lift calculations. This configuration provides a C_{Lmax} at an AOA of 10° of 1.4. The C_L vs α curve is shown in Figure 3.8.

E. TRADE STUDIES

1. Fuselage Geometry and Wing Leading Edge Sweep

The waverider effect is characterized by the generation of a shock wave that is restricted to the lower portion of the aircraft. The static pressure rise through the shock wave contributes to increased lift. With a design Mach number of 3.0, the selection of a specific semi-vertex angle for the shock generating cone will

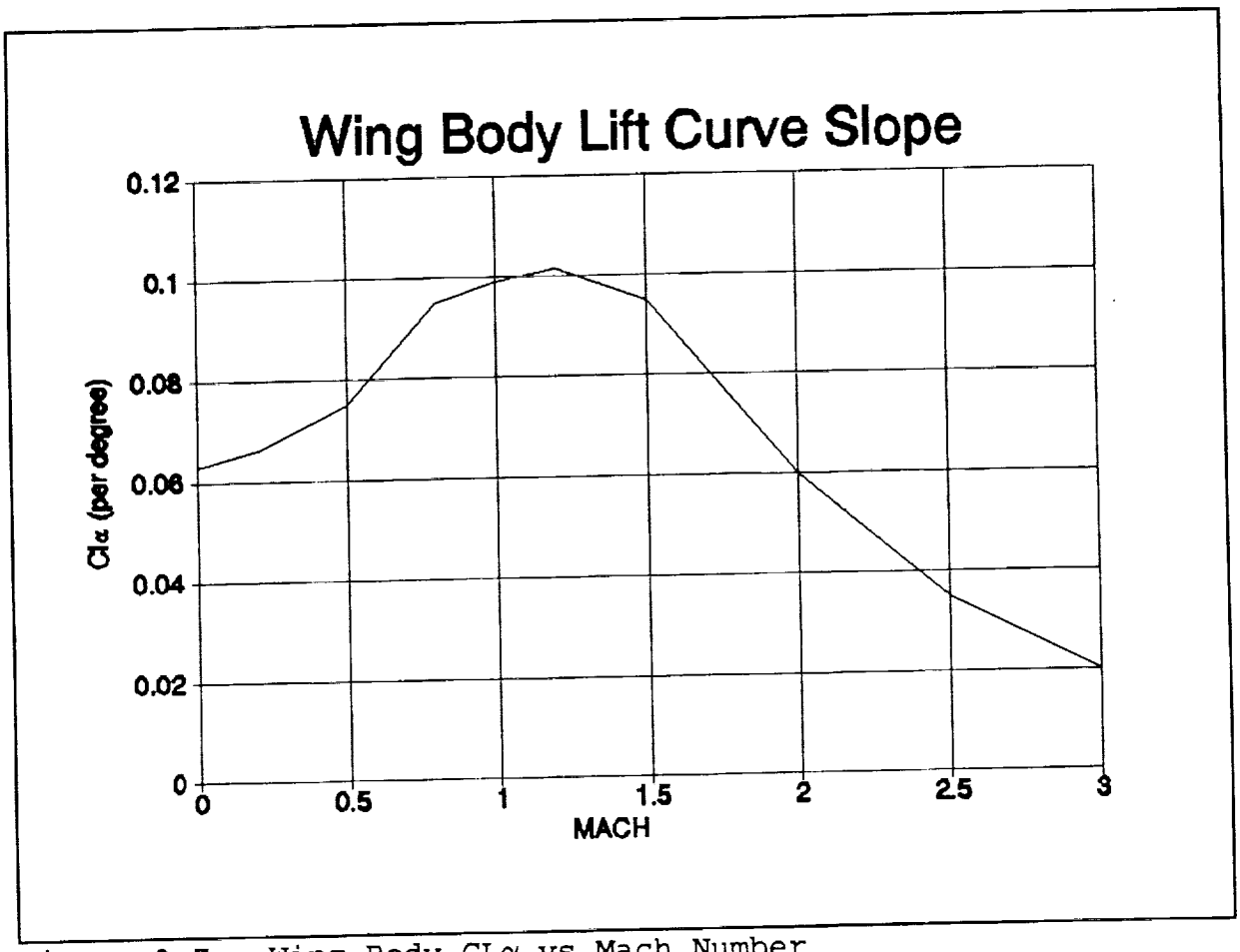

Figure 3.7: Wing Body CLα vs Mach Number

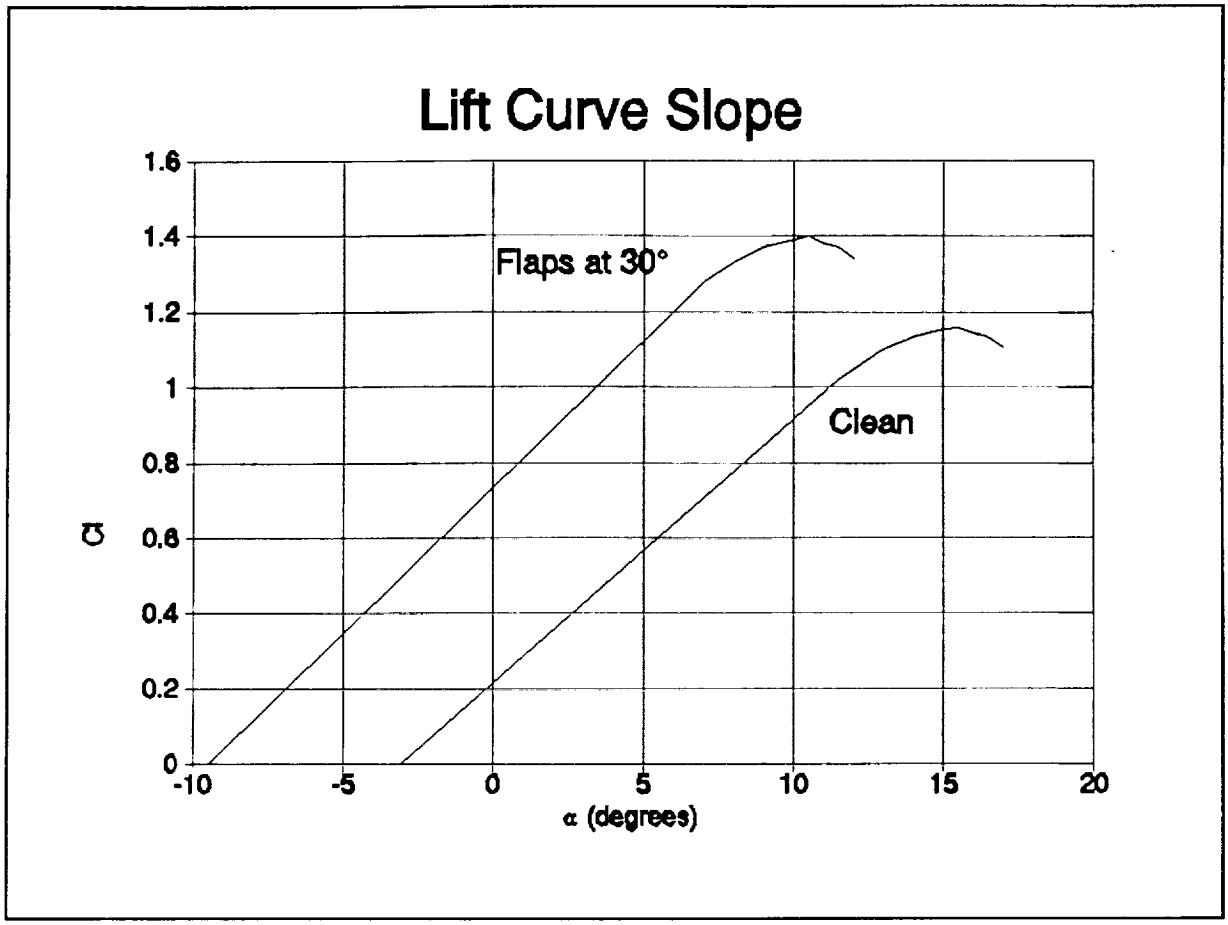

Figure 3.8: Lift Curve for clean and 30° Flap Configurations

specify the shock angle. This shock angle dictates the wing leading edge sweep since the wing must intercept the shock wave to restrict it to the lower portion of the aircraft. Table 3.5 illustrates the fact that the smaller the cone half angle is the higher the theoretical L/D. Table 3.5 comes from data in Newberry's Perspectives in Aerospace Design on page 662. We disregarded any cone half angle below 10 degrees because in order to fit a cockpit in the aircraft it would have to be placed extremely far back along the fuselage. This would force us to build a cockpit canopy that would rise far above the top surface of the aircraft to give the pilot the required visibility over the nose. Our design has a constraint to meet a minimum volume of 1546.9 ft^3. This is the required volume we need to be able to carry the required fuel, weapons, avionics and various aircraft systems. Another major constraint on the fuselage design was the maximum length restrictions due to shipboard compatibility for catapult takeoff. These two facts constitute a trade off. The last column in Table 3.6 shows the total aircraft length that would be able to contain the required volume for cone half angles from 10 to 15 degrees. These aircraft lengths do not include engine nozzles and do not include any taper in the latter half of the fuselage. Tapering the latter half is required in order to decrease the base drag. A very large majority of the lift at Mach 3 is generated from the waverider portion of the aircraft. The center of pressure of the waverider portion of the aircraft is relatively far forward compared to the overall length of the

Cone Angle (deg)	Shock Angle (deg)	Theoretical L/D_{MAX}
10	21.8	10.0
11	22.3	8.5
12	23.0	7.5
13	23.7	7.0
14	24.5	6.5
15	25.3	5.5

Table 3.5: Maximum L/D Ratios for Various Cone Semi-Vertex Angles

Cone Angle (deg)	Shock Angle (deg)	Pressure Diff. (lb/ft^2)	Wave Surface Area (ft^2)	Wave Length (ft)	Aircraft Length Area (ft)
10	21.8	129.24	491.33	35.05	52.37
11	22.3	150.62	421.59	32.06	49.90
12	23.0	173.23	366.56	29.39	47.98
13	23.7	197.03	322.29	27.10	46.37
14	24.5	220.49	287.99	25.14	44.96
15	25.3	246.56	257.54	23.34	43.89

Table 3.6: Comparison of Fuselage Geometries for Various Cone Semi-Vertex Angles

aircraft. The potential for controllability problems exists if the center of pressure is too far forward. The pressure difference column in Table 3.6 represents the amount of lift per ft^2 on the waverider optimized section of the aircraft. This column was calculated by assuming the surface pressure on the lower surface of the waverider portion of the aircraft, including the lower surface of the wings, was the same as the surface pressure on the shock generating cone. The waverider surface area column in Table 3.6 represents the amount of wing area that is needed for level sustained flight at Mach 3 at 50,000 ft. This assumes a gross weight of approximately 63,500 lb. after climb out and level off at Mach 3 and 50,000 ft. Our design point coupled with a takeoff gross weight of 76,000 lb. dictates a required wing area of 723.8 ft^2. In essence we have too much wing area for flight at Mach 3.

To summarize, a small cone half angle will generate a greater L/D and will utilize more of the wing area that is available. It will also require a longer fuselage that could lead to controllability problems. A larger cone half angle will yield a shorter fuselage which is better for controllability but will require only one half to one third of the wing area at Mach 3 to attain the required lift for level flight. With all these factors in mind we chose a 10 degree half angle. The overriding factor was the utilization of the wing area.

IV. PROPULSION SYSTEM

A. DESIGN GOALS

In order to meet the needs of the Navy well into the future, the engines on the Sabot have been designed from the start to be:

1. lightweight- using composites whenever possible
2. high performance- due to higher turbine inlet temperatures
3. maintainable- accessible and easily changeable parts
4. survivable-fail safe lubrication system

B. RFP REQUIREMENTS

1. Supercruise- ability to cruise at Mach 3 with a combat radius of 700 nautical miles.
2. Efficient fuel consumption- minimum mission time of 1 hour
3. 2g level turn- thrust available for constant altitude turn at 50000 feet.
4. Single engine performance- rate of climb of 500 fpm

C. TRADE STUDIES

The two major design criteria that were used to evaluate the various engine types were efficient fuel consumption at subsonic speeds to ensure a minimum mission time of 1 hour and the ability to maintain a constant cruise speed of Mach 3 with a combat radius of 700 nautical miles.

During the design process several basic engine types were evaluated to determine the engine best suited for these two mission phases. A parametric study of specific thrust and specific fuel

consumption versus bypass ratio was conducted at various altitude/Mach number combinations using the ONX/OFFX programs [Mattingly]. Ramjet performance was also evaluated to enable comparison of the three engine types (Figs 4.1 & 4.2).

After preliminary calculations were made it was determined that the best possible engine would be a combination of the various engines. Because of the added weight and complexity, the concept of a turbo-ramjet engine or a single ramjet coupled with dual turbofan engines was not considered to be worthwhile. The performance gain of each of these systems at Mach 3 flight is minimal. This narrowed the choices down to dual turbofan engines with afterburner, dual turbojet engines with afterburner, or variable cycle turbofan engines.

Although the variable cycle engine will weigh approximately ten percent more than a conventional engine, the total aircraft mission weight will be reduced because of the decrease in fuel consumption.

D. DESIGN RESULTS

1. Engine Design

The trade studies mentioned above show that the wide operating envelope required of a carrier based waverider interceptor aircraft necessitates designing and building a variable cycle engine. Therefore the engine of choice is a variable bypass turbofan engine with afterburner. Automatic engine controls vary the bypass ratio from 0.0 (turbojet) at high Mach numbers to 1.0 at subsonic speeds.

The maximum turbine inlet temperature is 3200 R with maximum

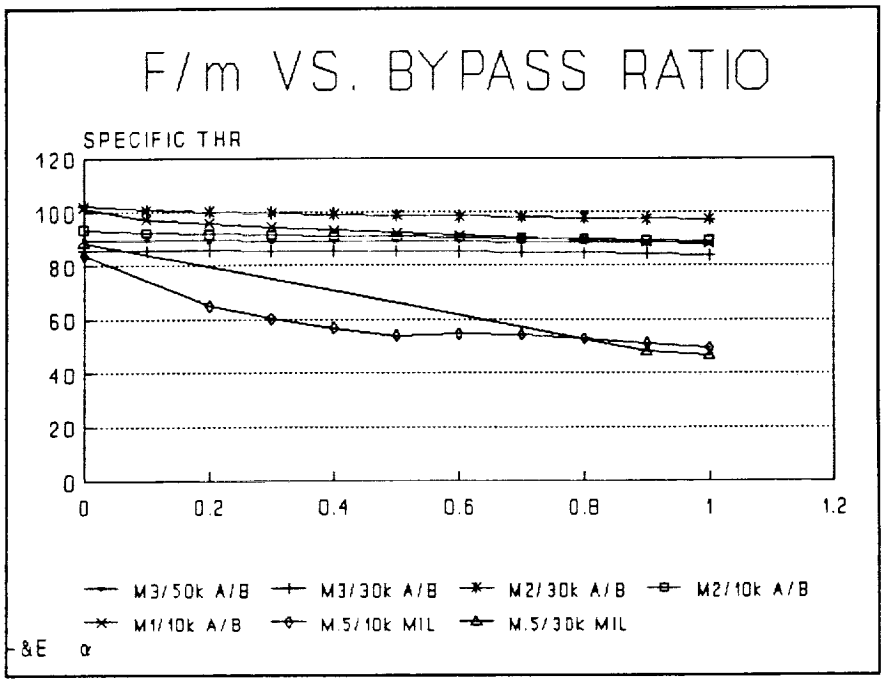

Figure 4.1: Specific Thrust vs. Bypass Ratio

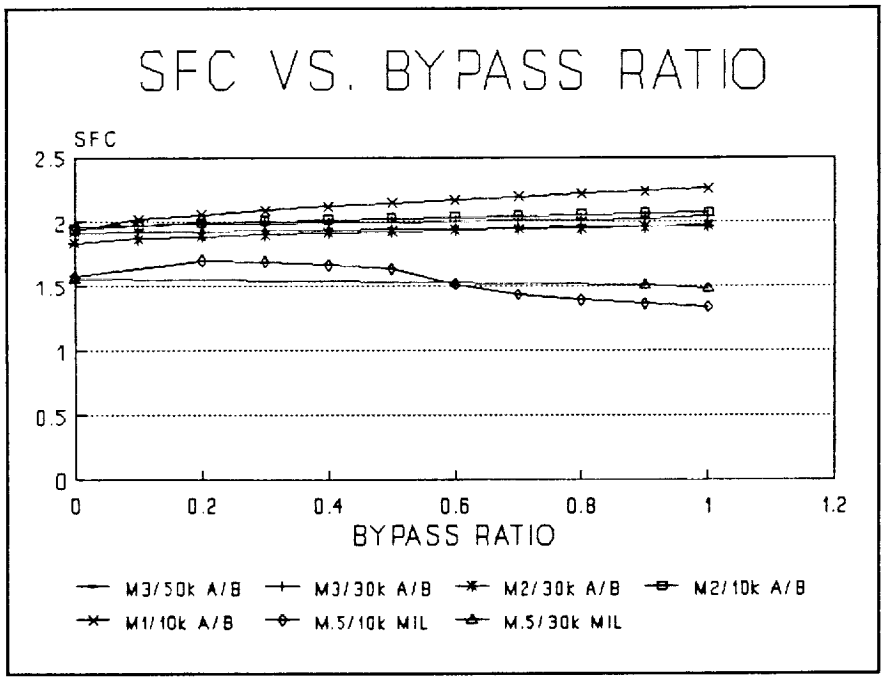

Figure 4.2: SFC vs. Bypass Ratio

afterburner temperature of 3700 R. This allows sufficient thrust without requiring significant bleed air for cooling, thus minimizing required engine inlet area. The fan has three stages with a compression ratio of 6.0 and is driven by a single stage turbine. The low pressure compressor is single stage with a compression ratio of 1.8. It is driven by a separate single stage turbine. The compression ratios were set by the design criteria of Mach 3 at 50000 feet. Any higher compression ratio would result in excessive engine case pressure.

After choosing the engine type, carpet plots of specific thrust and specific thrust fuel consumption were made with Mach number and bypass ratio being the variables (Figs 4.3 & 4.4). From these plots the optimum performance from the engine at all flight conditions can be assessed.

The installed thrust of the engine is plotted with and without the afterburner, as well as the required thrust for straight and level flight at various Mach numbers (Fig 4.5 through 4.7). As evidenced by Figure 4.5, it is possible to "supercruise" without afterburner at the design altitude of 50000 feet. This results in a significant fuel savings and is a direct result of waverider technology.

2. Nozzle Design

The nozzle is a two-dimensional, variable area, external expansion system with a rotating deflector to allow thrust vectoring. During normal cruise conditions, the rotating deflector is positioned outside of the engine casing to prevent airflow

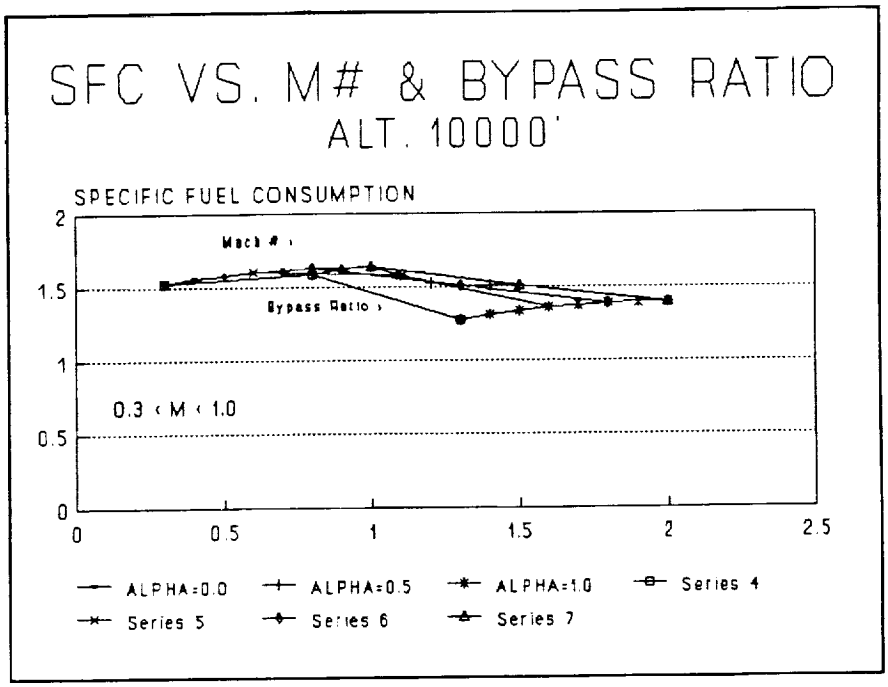

Figure 4.3: SFC Carpet Plot

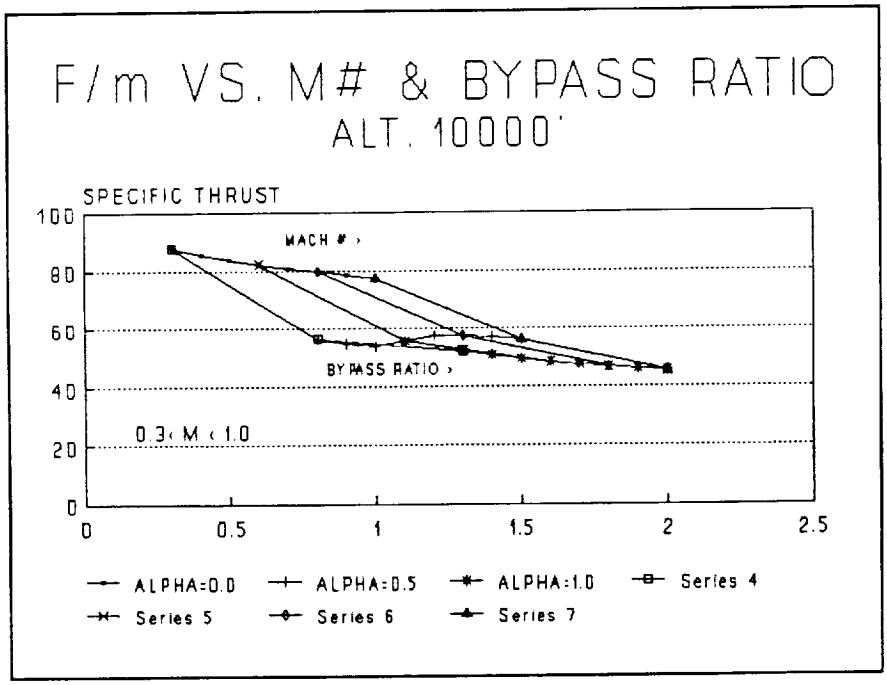

Figure 4.4: Specific Thrust Carpet Plot

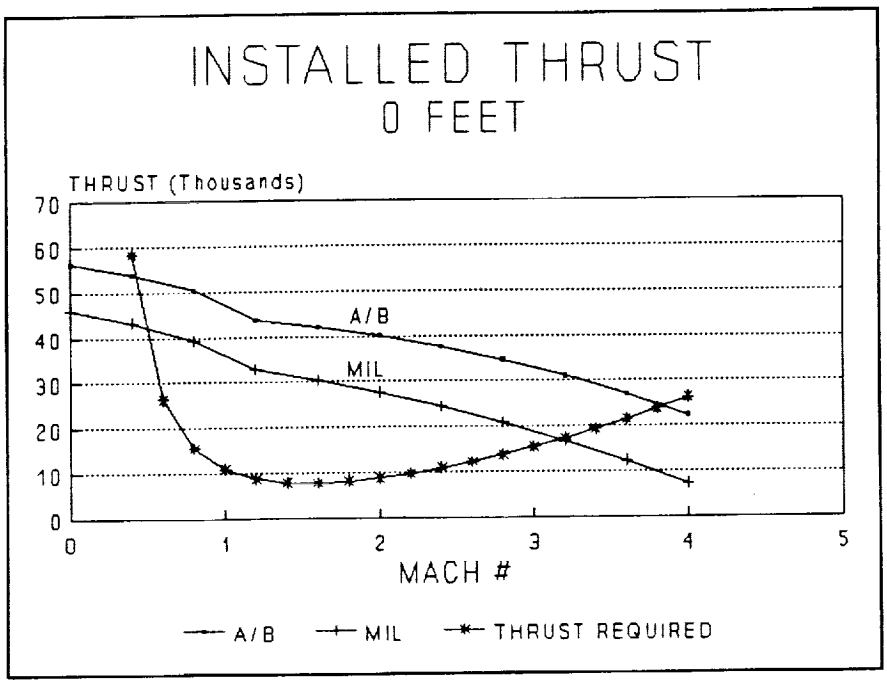

Figure 4.5: Installed Thrust

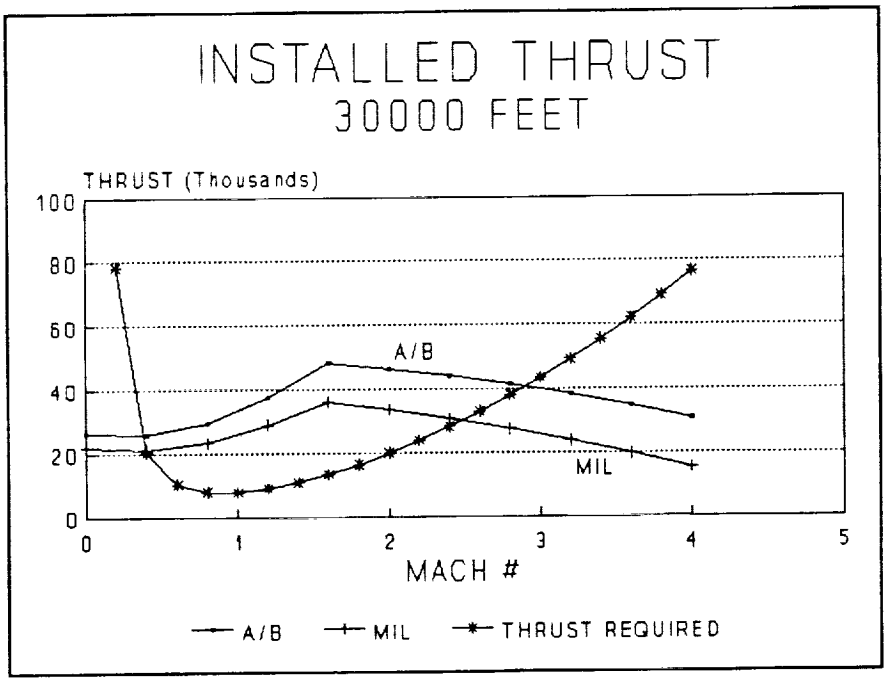

Figure 4.6: Installed Thrust

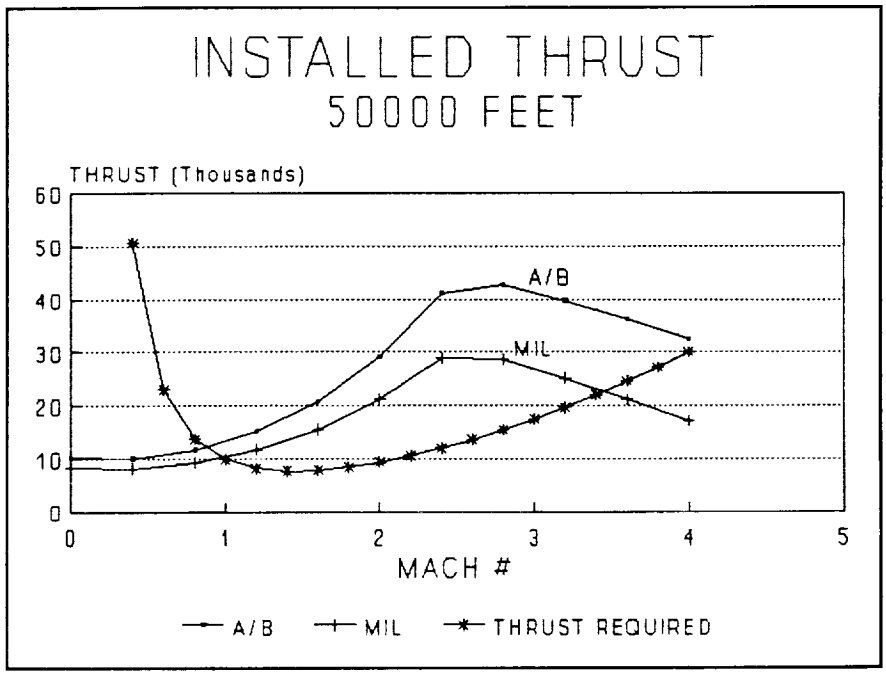

Figure 4.7: Installed Thrust

distortion. During maneuvers the deflector can be rotated down to deflect the exhaust stream a maximum of fifteen degrees, and therefore increase maneuverability.

3. Inlet Design

Inlet selection and design was driven by the wide range of flight parameters the Sabot would encounter. Ultimately engine mass flow rate requirements at takeoff and the difference in mass flow requirements between cruise and the 4g turn configuration at design altitude and Mach number, determined the size and geometry of the inlet.

Air approached the inlet at Mach 2.7 having decelerated through the attached bow shock. Total pressure losses through the bow shock were negligible due to its conical nature. This is in contrast to a caret waverider configuration where the total pressure losses through the bow shock would be much larger since the caret configuration is based on a two-dimensional tangent wedge shock solution. The inlet chosen to provide optimum mass flow throughout the flight envelope was a two-dimensional, external compression, three ramp variable geometry inlet.

Parametric studies were conducted to identify the optimum inlet geometry. Factors considered during selection are listed in Figure 4.8. Two-dimensional inlets were selected over axisymmetric inlets due to superior performance during prolonged periods of oblique flow and compatibility with the three variable geometry ramps required to sustain total pressure recovery.

MIL-E-5008B defines the military specification for total

Two-Dimensional	**Axisymmetric**
Turning Flight	Weight
Design Simplicity	Total Pressure Ratio
Inlet Flow Variation	Design Cruise Configuration
Boundary Layer Bleed	Current Technology
External Compression	**Mixed Compression**
Length/Weight	Ramp Geometry
Flow Turning Angle	Shock Instability
Total Pressure Ratio	Bleed Air Required
Cost	Cost

Figure 4.8 Inlet Type Considerations

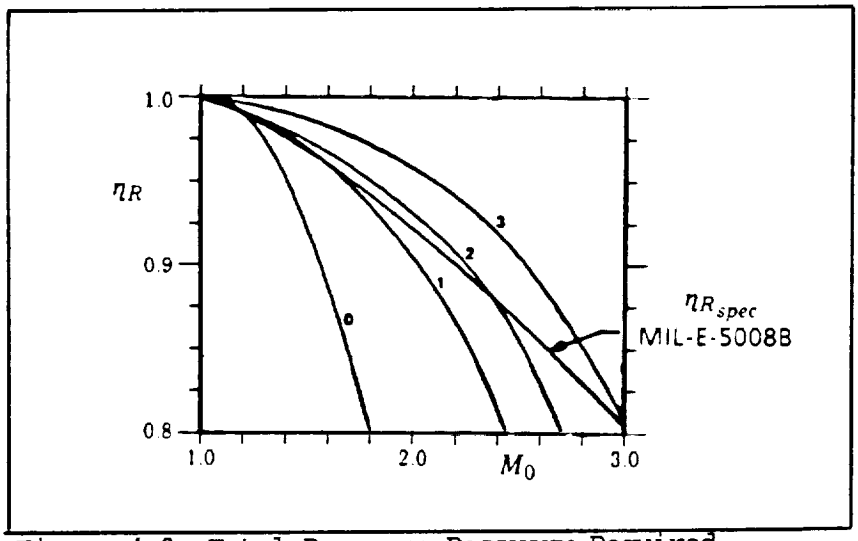

Figure 4.9 Total Pressure Recovery Required

pressure recovery of the supersonic inlet as

$$\eta_{r_{spec}} = 1 - 0.075 (M_0 - 1)^{1.35}.$$

Figure 4.9 was taken from the inlet section of Mattingly's Aircraft Engine Design book. A three oblique shock system is required to meet the military specification at Mach 2.7. Figure 4.10 is a side view of the inlet. Ramps are shown positioned for cruise condition at Mach 2.7. Ramp position, shock angles and Mach numbers throughout the ramp system were obtained from Hermann's Supersonic Inlet Diffusers and Introduction to Internal Aerodynamics. Figure 4.11, also from Hermann's book shows the ramp deflection angles which would be programmed for the control unit as the Sabot accelerated to design speed. To minimize control engineering only Mach number would be used as a variable input parameter to the control unit.

The external compression three ramp variable geometry system maintained a balance between an acceptable total pressure ratio and cowl drag at Mach 2.7. Figure 4.12 shows the turning angle of the external compression shock system that attains the total pressure recovery of MIL-E-5008B as a function of Mach number [Mattingly]. This large turning angle of approximately 35 degrees required a longer, heavier thus costlier subsonic diffuser to turn the flow back to the axial direction. This effort was offset by normal shock stabilization and manufacturing costs associated with the mixed compression inlet as discussed in the next several sections.

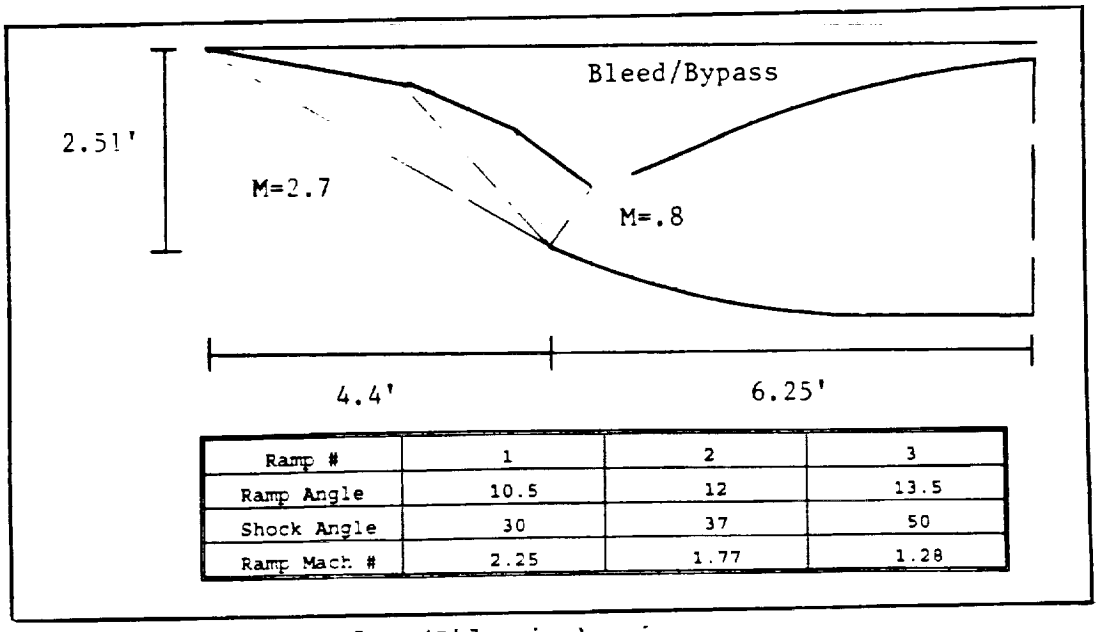

Ramp #	1	2	3
Ramp Angle	10.5	12	13.5
Shock Angle	30	37	50
Ramp Mach #	2.25	1.77	1.28

Figure 4.10 Sabot Inlet (Side view)

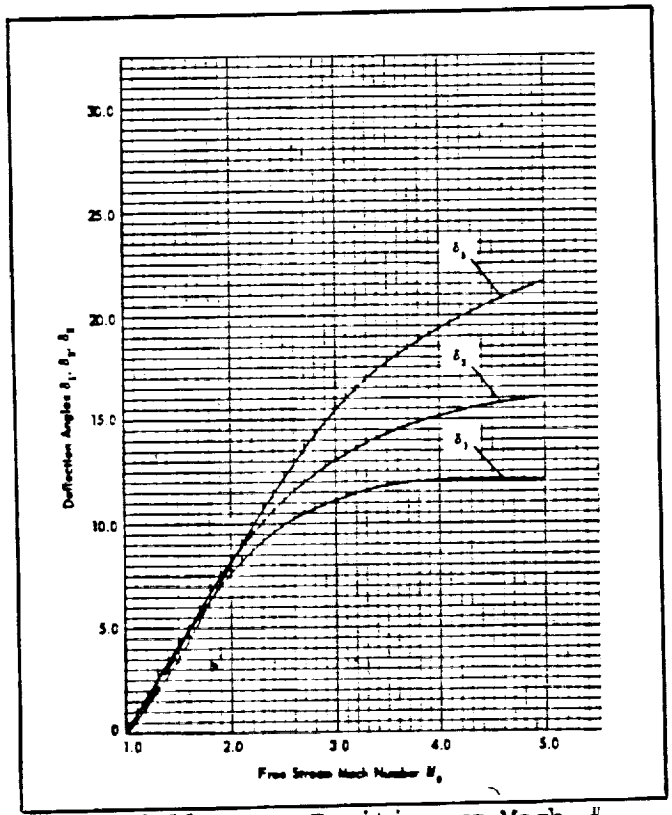

Figure 4.11 Ramp Position vs Mach #

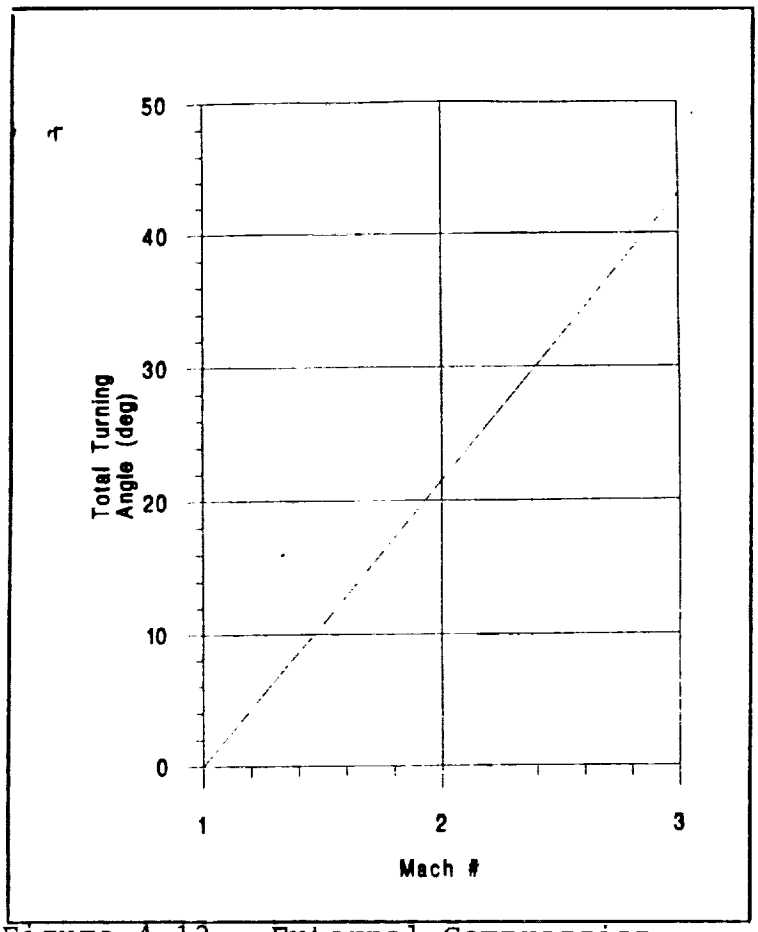

Figure 4.12: External Compression Turning Angle

Per Inlet	Takeoff	Mach 3 Cruise	Mach 3 4g Turn
Mass Flow Rate	261 lbm/s	190 lbm/s	235 lbm/s
Throat Area	3.71 sq ft	1.87 sq ft	2.31 sq ft
Capture Area	13.48 sq ft	5.02 sq ft	6.21 sq ft

Figure 4.13: Critical Engine/Inlet Requirements

Figure 4.13 summarizes mass flow rate, throat and capture area requirements for the three critical phases within the flight regime: takeoff, Mach 3 cruise and the 4g turn at Mach 3. At Mach 3 design conditions the size of the capture area was critical and was determined by the streamtube the intake would swallow. For takeoff the Mach number at the throat was critical and was limited to Mach 0.8 to prevent choking the throat area.

The RFP required a maximum range of 700 nautical miles. Since a large portion of the Sabot's flight would be spent at the Mach 3 cruise condition the inlets needed to be sized for this condition. The 4g turn required an additional mass flow rate of 45 lbm/s per engine. A larger capture area was required but would increase the additive drag during the cruise condition. Figure 4.14 contains a top down view of the inlet. In order to perform the 4g turn maneuver a sliding external door covered the inner one half foot of each inlet. During cruise the sliding door was closed providing the capture area required for a mass flow rate of 190 lbm/s per engine. For takeoff, subsonic flight and the 4g turn maneuver the sliding door was opened to expose the additional capture area required. Behind the doors an independently activated ramp system operated to provide the additional mass flow rate at the proper conditions. Metering doors which introduced this additional flow to the diffuser section would be controlled by the fuel control unit using mass flow rate and acceleration as input variables. Shock stabilization for a mixed compression inlet posed too costly a solution compared to the marginal performance of the external

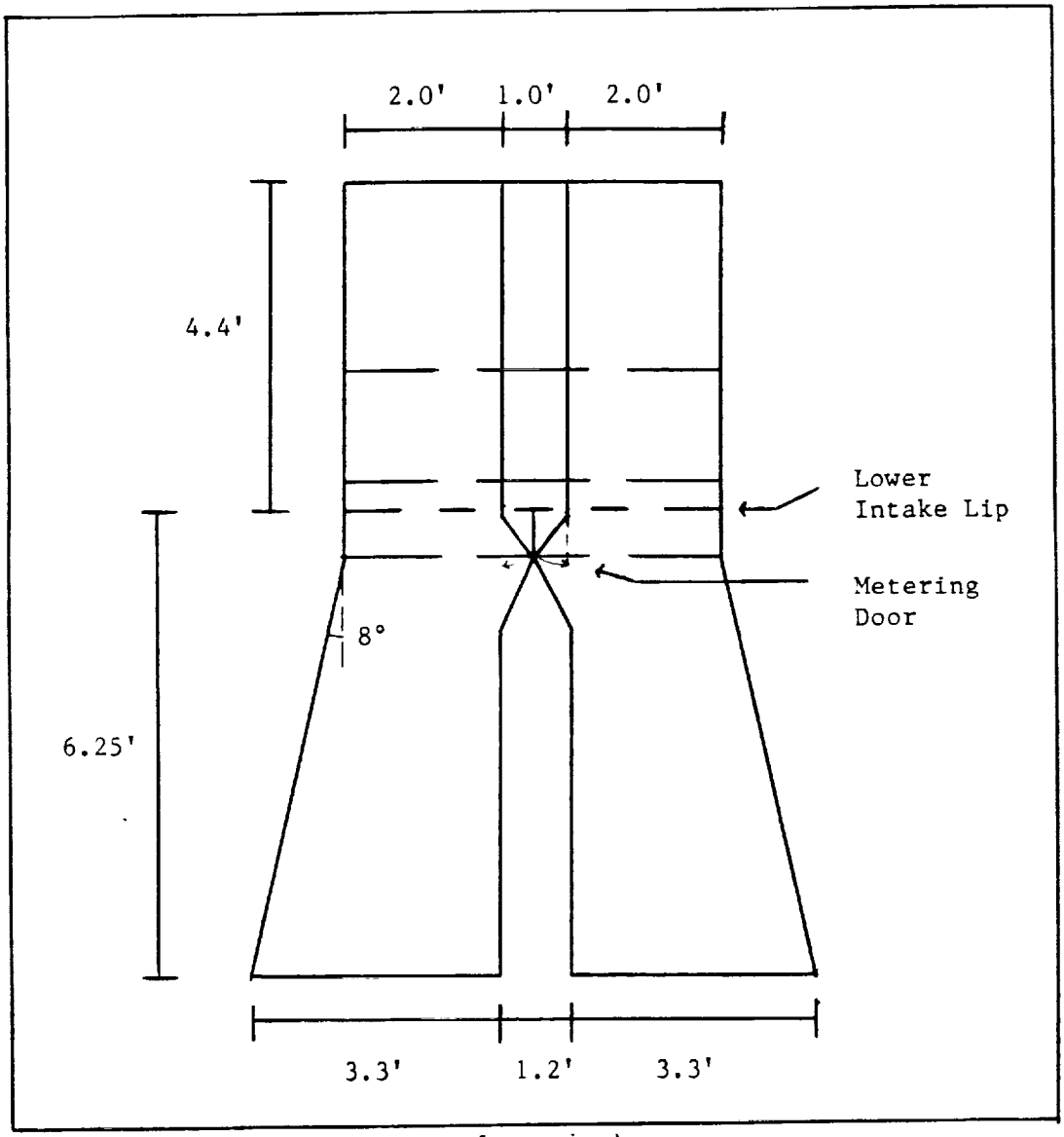

Figure 4.14 Sabot Inlet (Top down view)

compression inlet at Mach 3.

To minimize flow separation and total pressure losses, both slot and porous plate bleed methods were incorporated in the ramp and diffuser section. To further reduce inlet losses the lower inlet turning angle was restricted to 12 degrees and the diffuser half angle was limited to 8 degrees.

V. STABILITY AND CONTROL

A. INTRODUCTION

A comprehensive stability analysis was performed on the Sabot aircraft after the initial sizing was complete. The aircraft demonstrated excellent static and dynamic stability characteristics in all modes, although stability augmentation is recommended to achieve desired flying qualities and to compensate for the large range of center of gravity travel. Dynamic analysis was performed using full state space matrices and equations of motion when possible, and linearized approximations when necessary. All stability and control derivatives were obtained from the USAF Stability and Control DATCOM manuals. Aircraft flight control surfaces were sized to provide adequate response to control inputs and sufficient control throughout the entire flight envelope. Upon completion of the dynamic simulations, control law design was performed using state-variable feedback techniques resulting in a fully stable, stability-augmented aircraft. Flight conditions and aircraft geometries are described in Figure 5.1.

B. STATIC STABILITY

1. Longitudinal

The basic requirements for static stability include a positive zero lift pitching moment (C_{mo}) and a negative pitching moment with a change in angle of attack ($C_{m\alpha}$). The Sabot achieved these objectives (Fig. 5.2) and demonstrated positive stability in the take-off configuration as shown by the stable roots in the Root-Locus Plot (Fig. 5.3). The center of gravity in the landing

Flight Conditions	**Mach 0.2**	**Mach 3.0**
Altitude	Sea Level	50,000
Velocity	253.17 ft/sec	2903.83 ft/sec
Density (slugs/ft^3)	2.3769×10^{-3}	3.6391×10^{-4}
Geometry		
Wing M.A.C.	6.25 ft	15.56 ft
Wing Area	723.8 ft^2	723.8 ft^2
Wing Span	50.6 ft	34.97 ft
Weight	77544 lb_f	77544 lb_f
Aspect Ratio	3.54	1.69
I_{xx}	109626 slugs-ft^2	105870 slugs-ft^2
I_{yy}	206384 slugs-ft^2	220249 slugs-ft^2
I_{zz}	203378 slugs-ft^2	217090 slugs-ft^2
$x_{a.c.}$	29.59 ft	30.77 ft
$h_{a.c.}$	0.254	0.499
$x_{c.g.}$	31.37 ft	31.06 ft
$h_{c.g.}$	0.5385	0.5180
x_n	31.90 ft	36.52 ft
h_n	0.6238	0.8691
Static Margin	0.0853	0.3511

Figure 5.1: Flight Conditions and Geometries.

Longitudinal Derivatives	Mach 0.2	Mach 3.0
C_{m_α}	-0.3032	-0.6426
$C_{m_{\dot{\alpha}}}$	-1.3457	0.2134
C_{m_q}	-21.660	-0.2127
C_{m_o}	-0.0273	0.0098
C_{L_α}	3.730	1.830
$C_{L_{\dot{\alpha}}}$	-0.8379	0.0943
C_{L_q}	4.6684	-0.0244
C_{D_α}	0.0165	0.04812
$C_{m_{\delta e}}$	-1.01	-0.007
$C_{L_{\delta e}}$	0.36	0.68
$C_{D_{\delta e}}$	0	0

Figure 5.2: Longitudinal Derivatives.

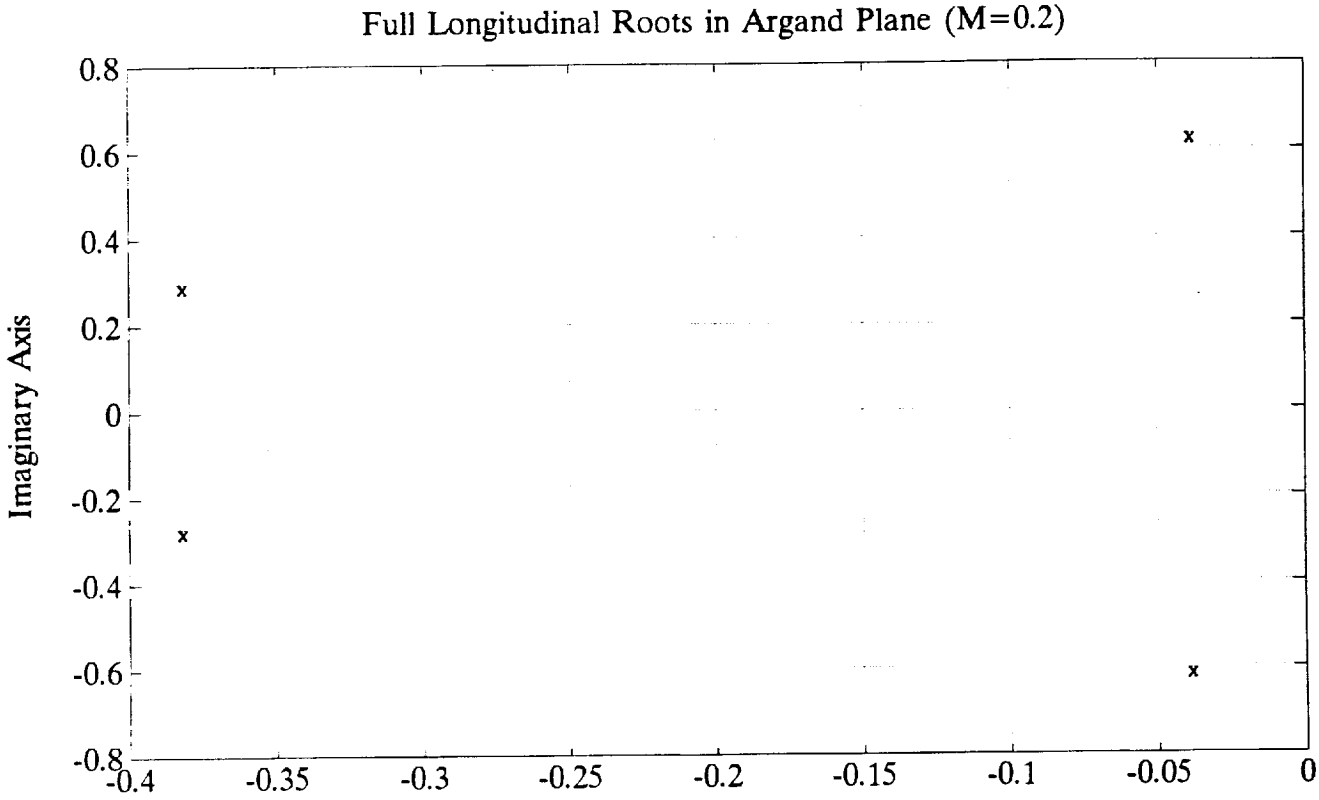

Figure 5.3

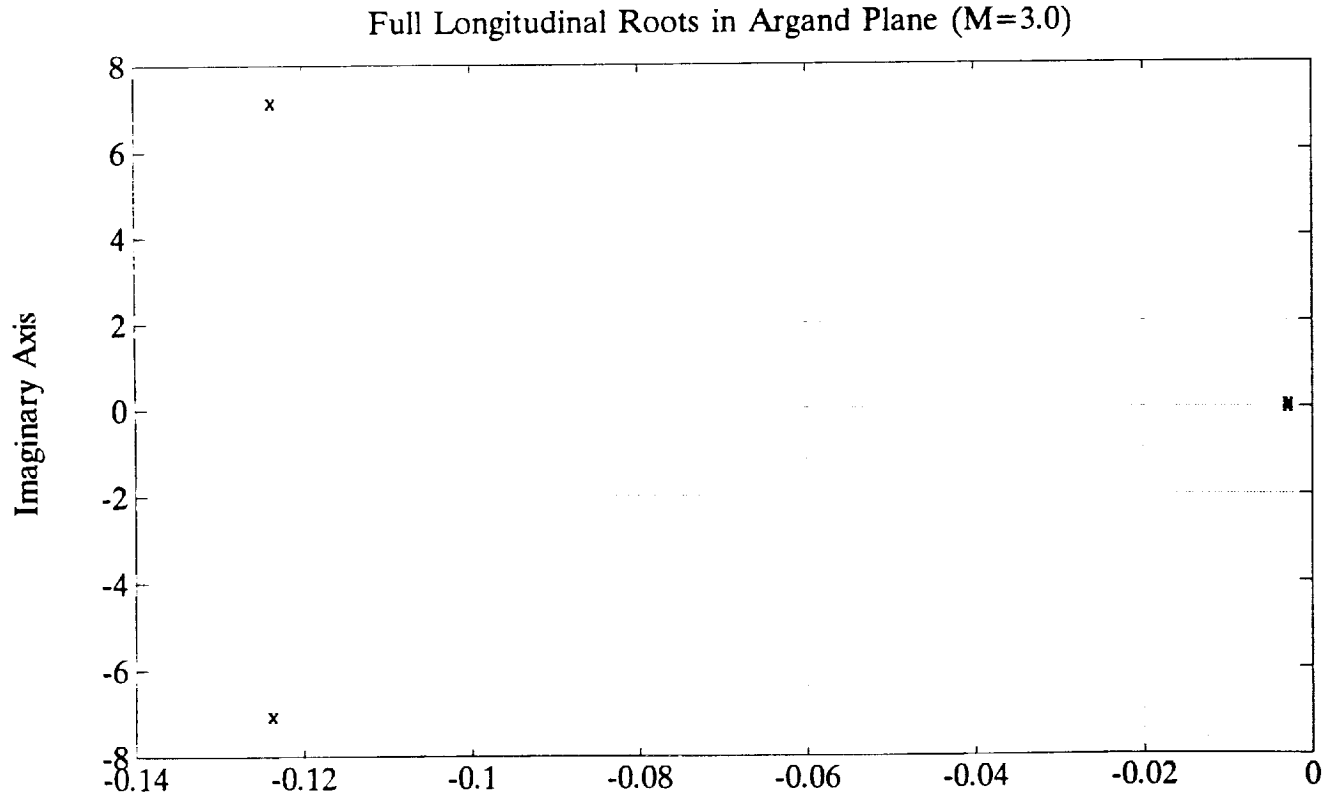

Figure 5.4

configuration however, moves aft five feet from the take-off configuration, resulting in a negative static margin. The Sabot also had stable roots in the cruise configuration (Fig. 5.4), although the proximity of the roots to the Imaginary Axis indicates the need for more detailed analysis.

2. Lateral Directional

The Sabot is stable both directionally and laterally at all flight speeds. The directional stability (C_{n_β}) was positive for most of the speed range and only slightly negative at Mach 3.0, while the roll stability (C_{l_β}) was negative for all speeds. The Sabot achieved its lateral and directional objectives (Fig. 5.5) and possesses stable roots (Fig. 5.6 & 5.7) in the Dutch Roll approximation for both Mach 0.2 and Mach 3.0.

C. DYNAMIC STABILITY

1. Longitudinal

A Dynamic stability analysis demonstrated the Sabot to be stable in both the phugoid mode and the short period mode (Fig. 5.8). Using a short-period approximation at M=0.2, the Angle of Attack Rate (α) and Pitch Rate (q) response to a unit elevator step function (Fig. 5.9) were found to be quite acceptable without the use of stability augmentation. The Sabot is also stable in both the phugoid and short period modes at Mach 3.0, although slightly underdamped (Fig. 5.10 & 5.11). To increase the short period damping, the $\{M_q+M_{\dot{\alpha}}\}$ stability derivative was increased [Nelson, p.138] and resulted in adequate damping and dynamic response (Fig. 5.12 & 5.13).

Lateral-Directional Derivatives	Mach 0.2	Mach 3.0
C_{l_β}	-0.6677	-0.0662
	-0.3573	-0.1311
C_{l_r}	0.5632	0.15
C_{n_β}	1.3201	-0.0751
C_{n_p}	-0.3467	-0.09
C_{n_r}	-1.4149	-0.65
C_{y_β}	-1.53	-1.22
$C_{l_{\delta a}}$	0.051	0.025
$C_{l_{\delta r}}$	0.05	0.008
$C_{n_{\delta a}}$	0.01	0.025
$C_{n_{\delta r}}$	-0.20	-0.04
$C_{y_{\delta r}}$	0.210	0.042

Figure 5.5: Lateral-Directional Derivatives.

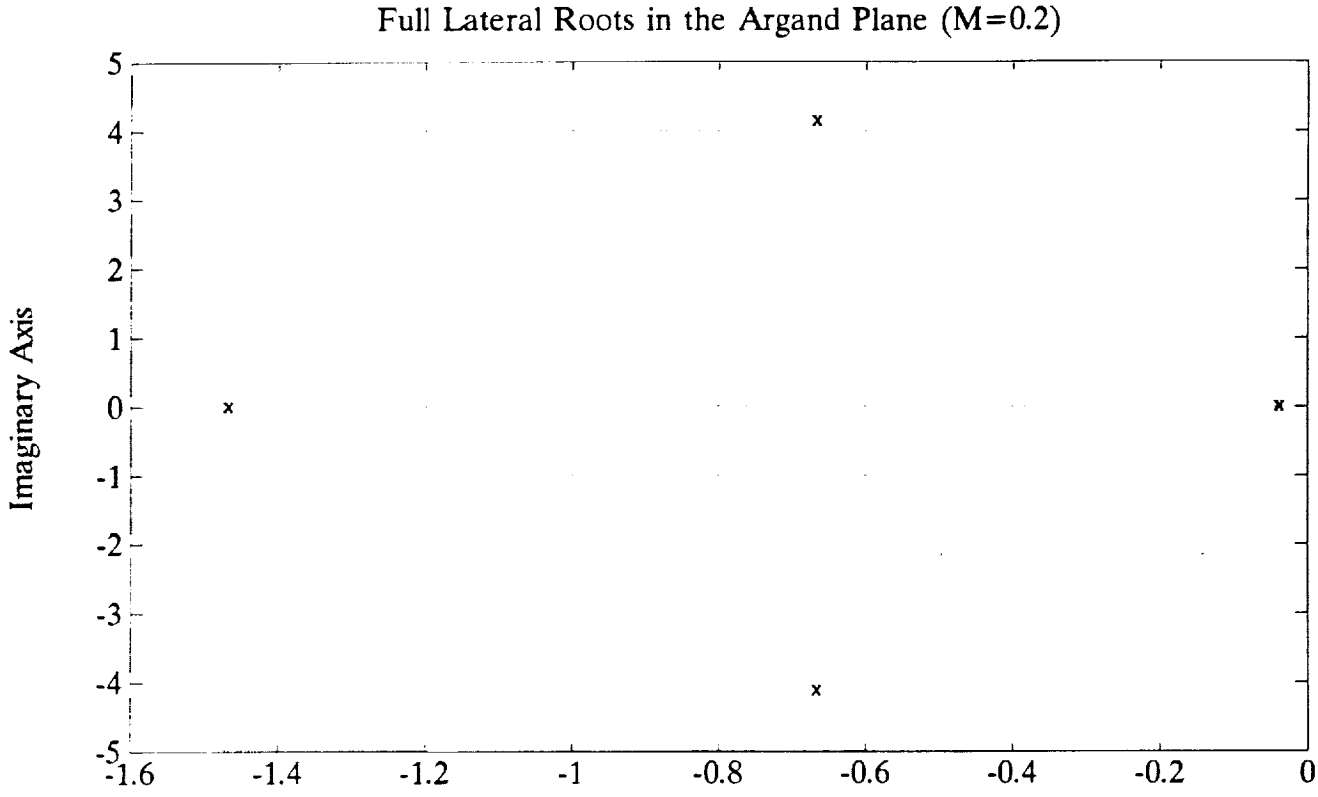

Figure 5.6

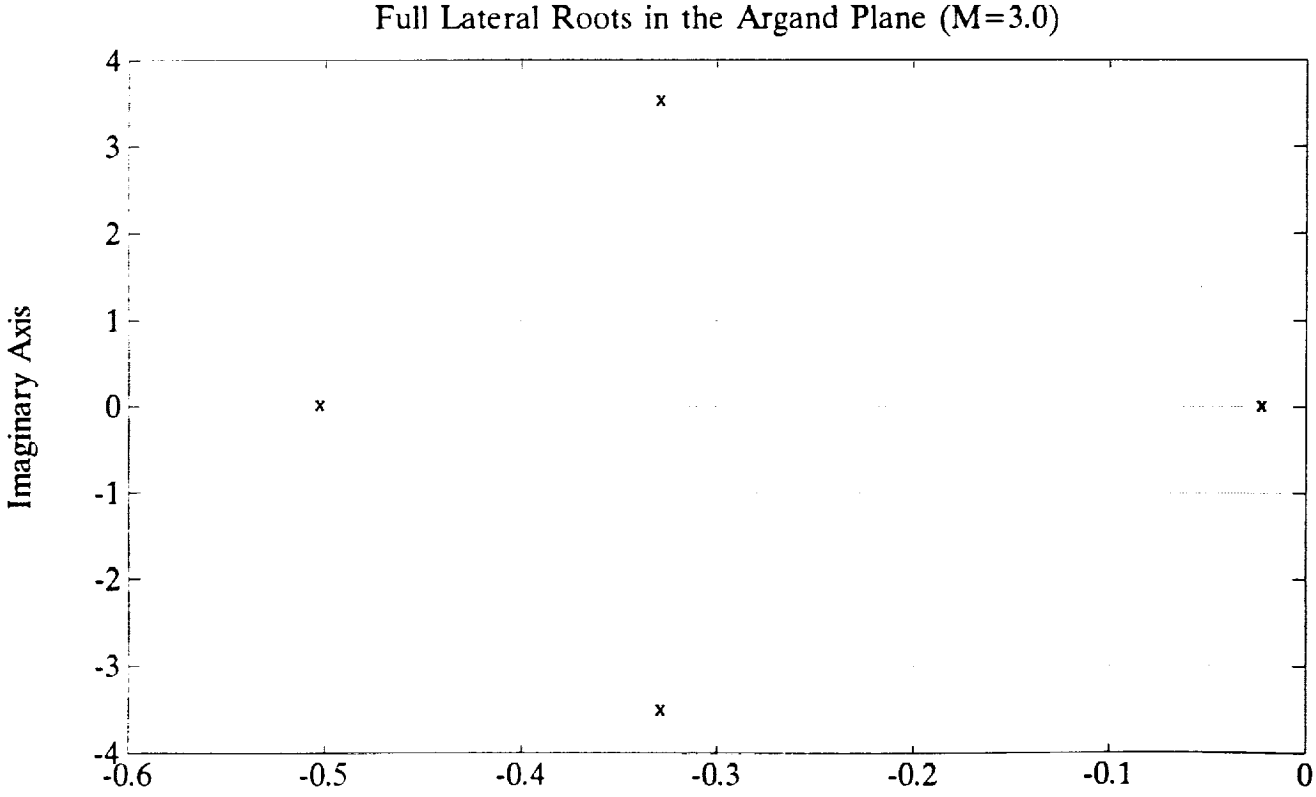

Figure 5.7

Short Period	Mach 0.2	Mach 3.0
ω_{sp}	0.4762 rad/sec	0.0359 rad/sec
ζ_{sp}	0.8018	0.0765
Phugoid		
ω_p	0.6204 rad/sec	7.1002 rad/sec
ζ_p	0.0621	0.0174

Figure 5.8: Longitudinal Dynamic Stability

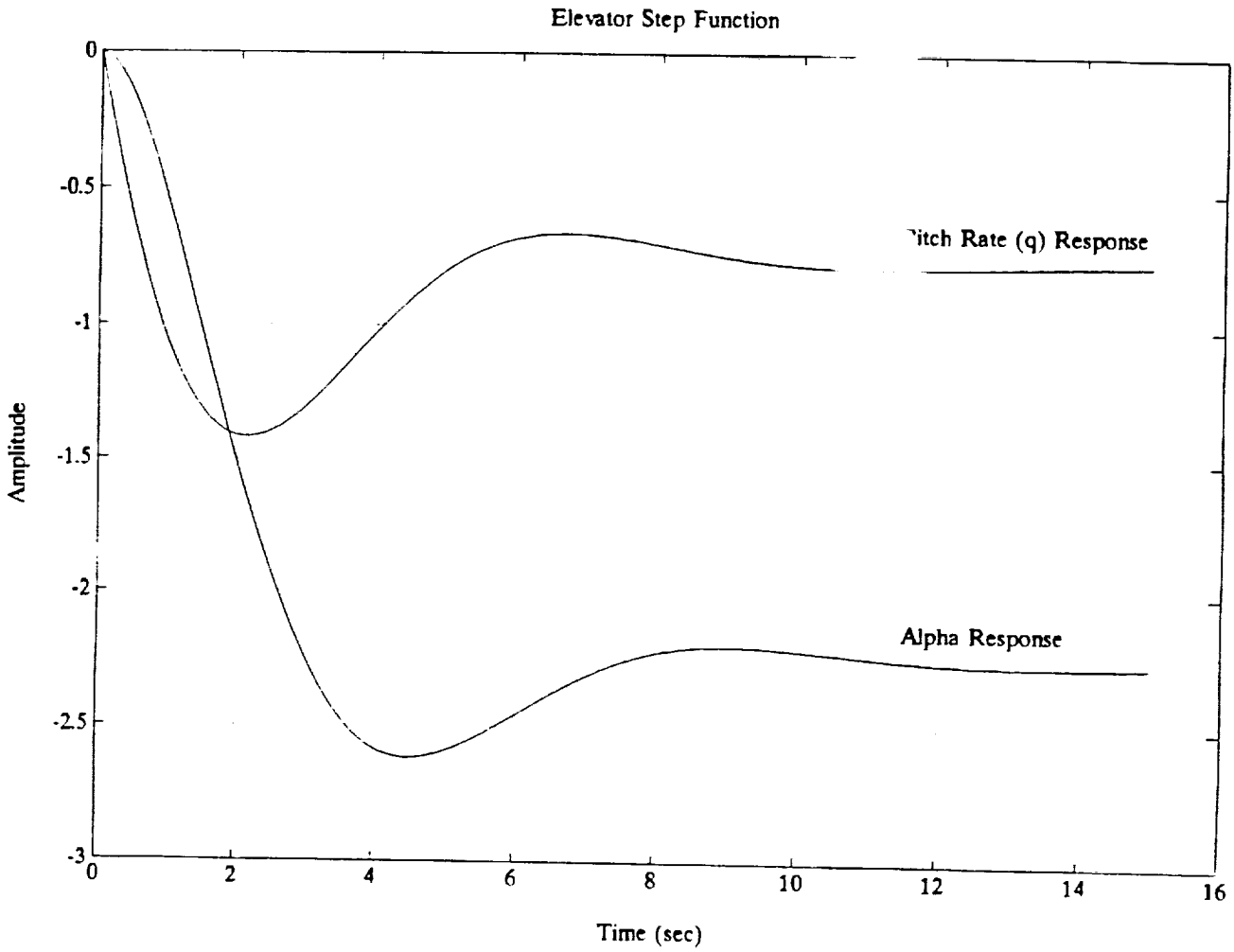

Figure 5.9: Unaugmented Elevator Step Function (M=0.2)

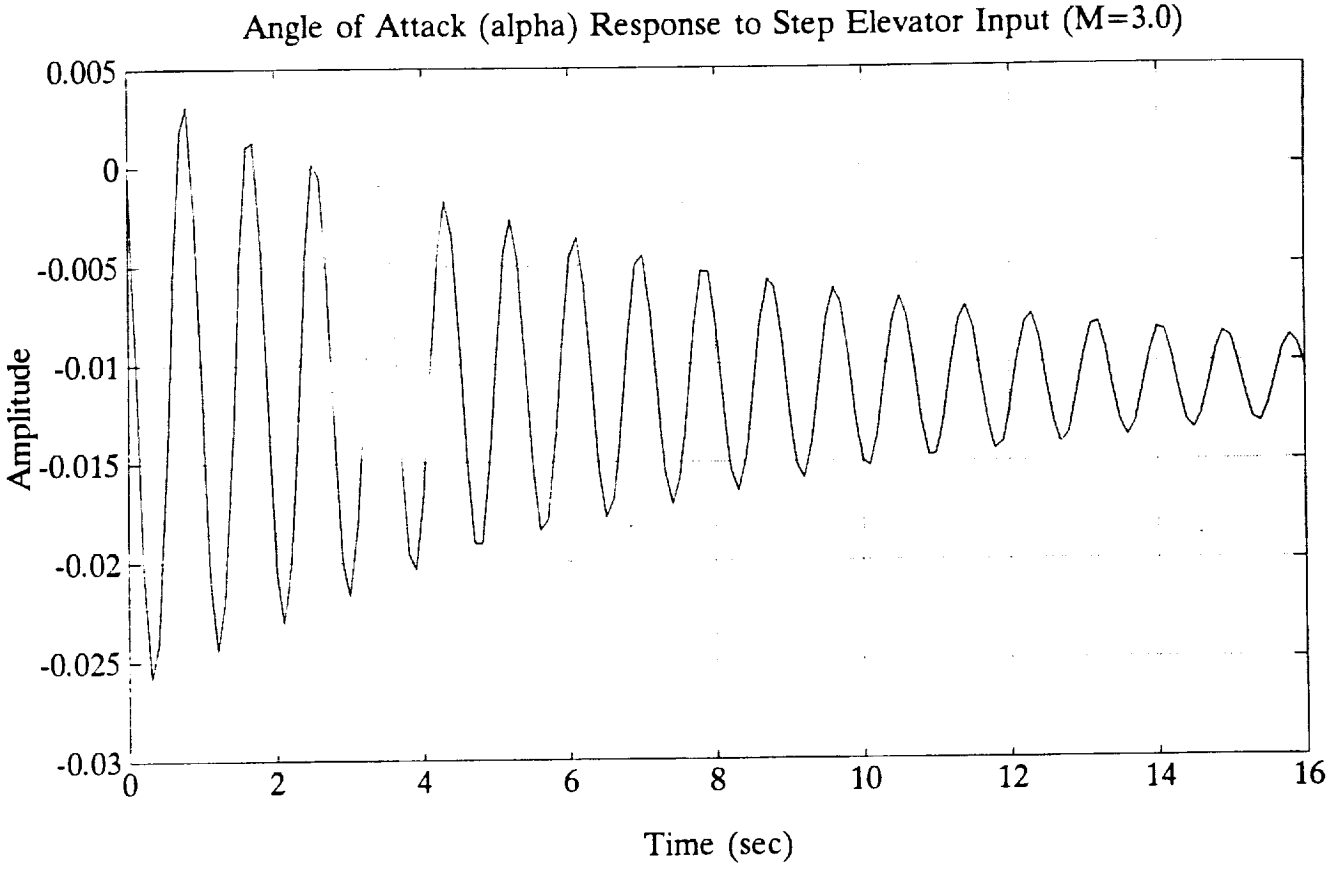

Figure 5.10: Unaugmented Elevator Step Function (M=3.0)

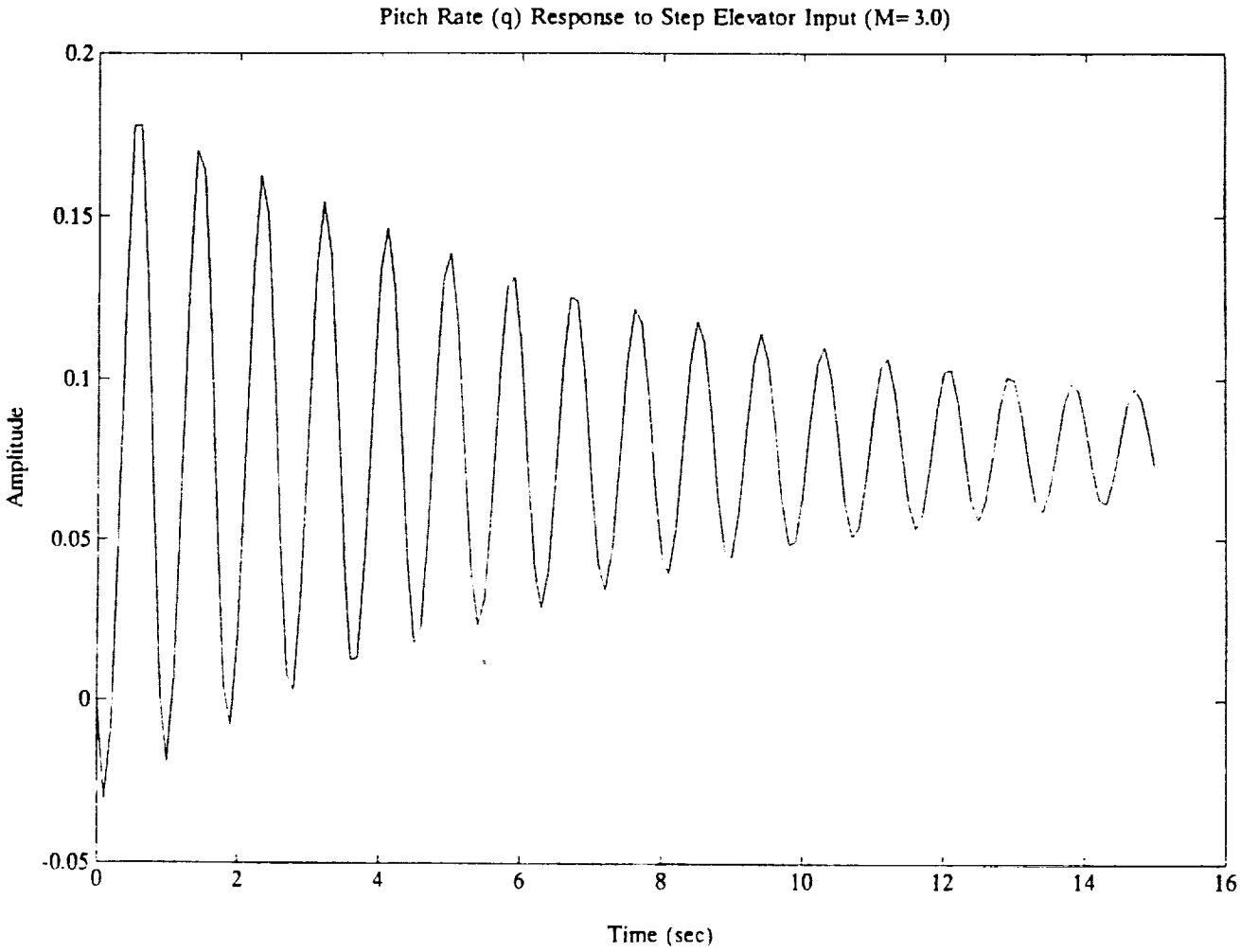

Figure 5.11: Unaugmented Elevator Step Function (M=3.0)

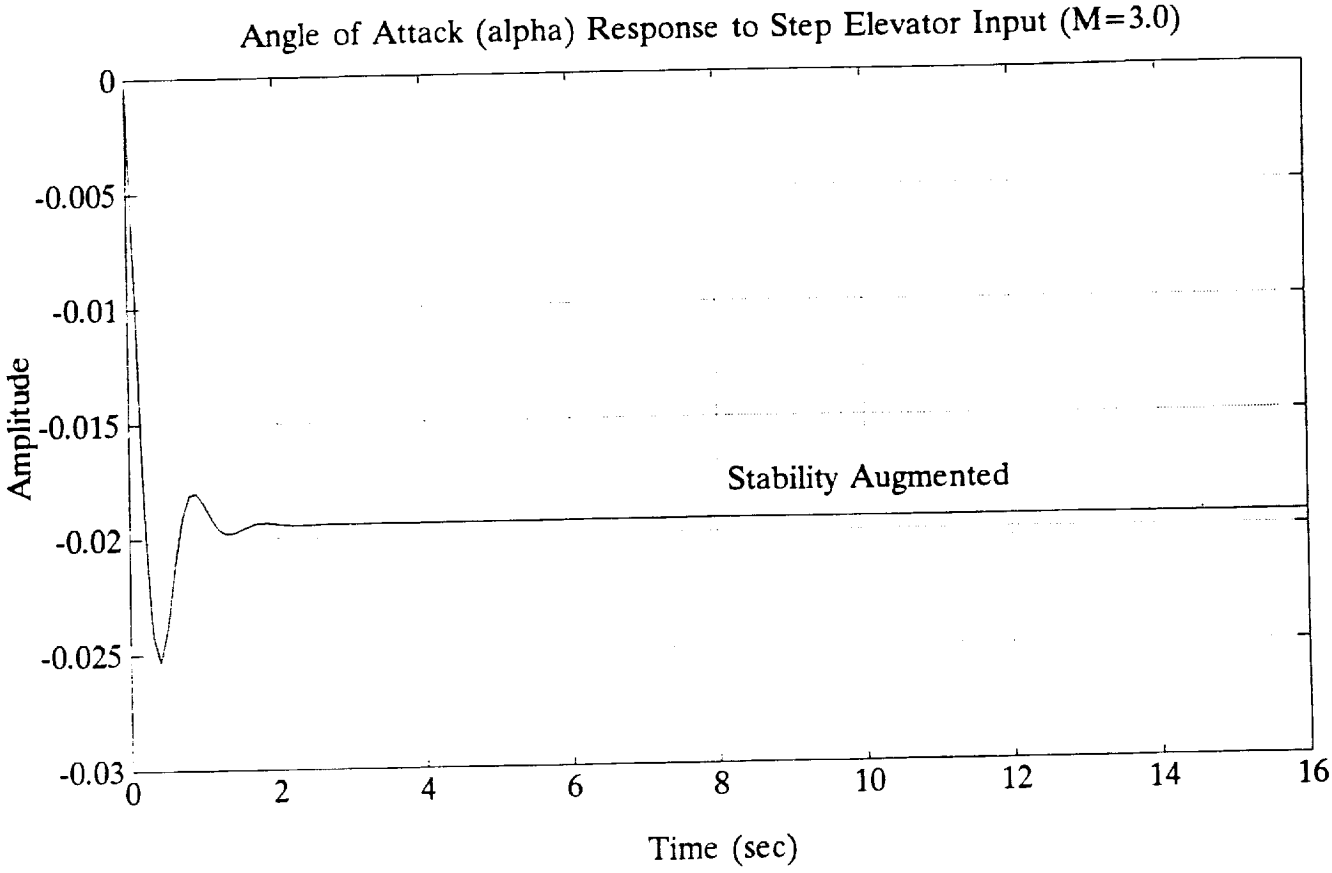

Figure 5.12: Augmented Elevator Step Function (M=3.0)

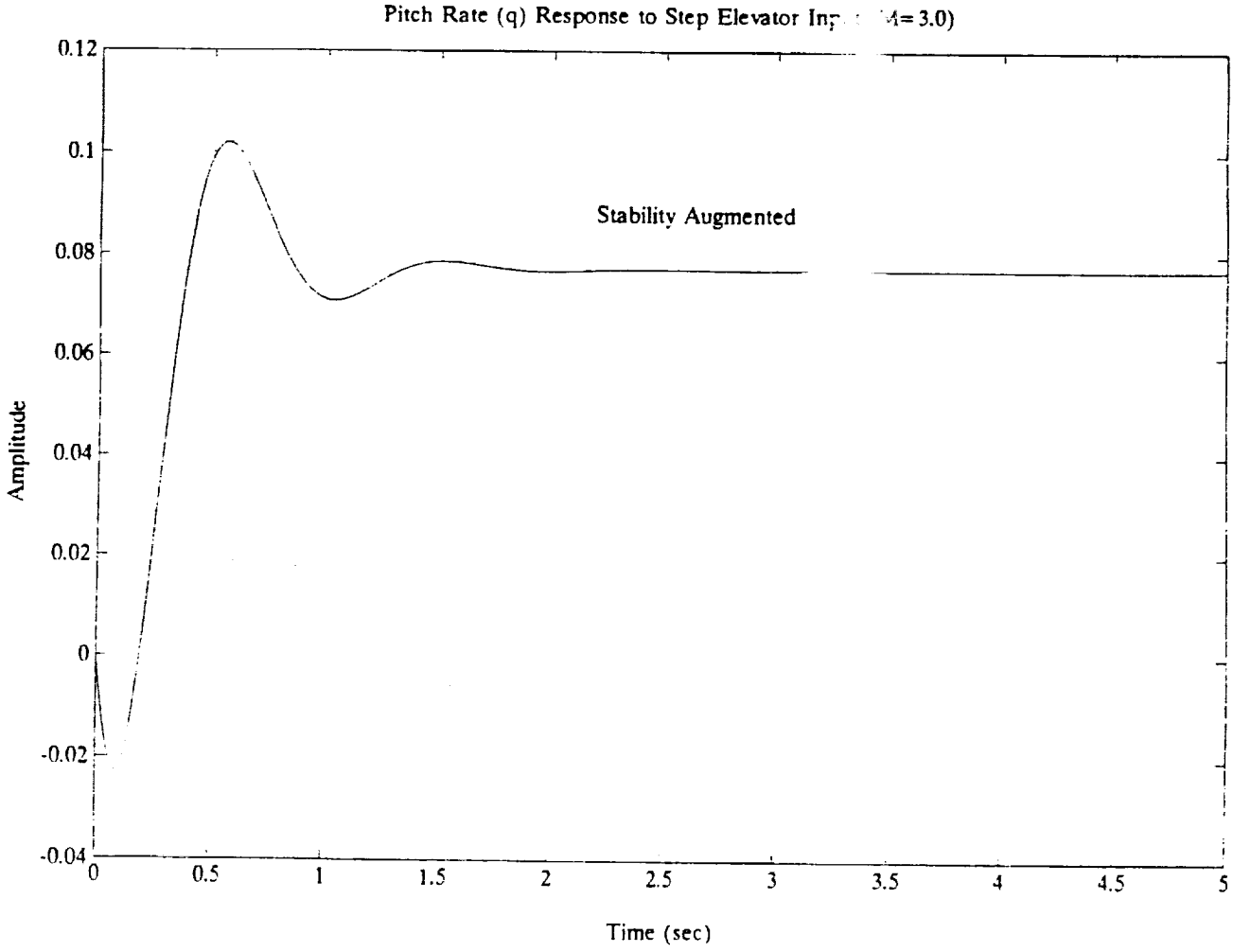

Figure 5.13: Augmented Elevator Step Function (M=3.0)

2. Lateral Directional

The Sabot proved to be dynamically stable in the lateral-directional mode (Fig. 5.14). It also exhibited excellent unaugmented Lateral-Directional response for both Mach 0.2 and Mach 3.0 (Fig. 5.15 & 5.16), although slightly underdamped for desired flying qualities. Incorporation of a yaw damper increases the damping to yield superior impulse response results (Fig. 5.17).

D. STABILITY AUGMENTATION

1. Control Law Design

The excellent stability characteristics of the Sabot minimize the amount of stability augmentation required. It is expected however, that achievement of waverider benefits will only be realized using sensitive control inputs. The waverider sensitivity, along with the large center of gravity travel, require the use of three-axis stability augmentation. For effective stability augmentation, it is assumed that all state variables are controllable and observable as necessary. The dynamic characteristics of the stability-augmented system are shown in Figure 5.18.

E. FLYING QUALITIES

The control design goal for the Sabot was to meet and exceed MIL-F-8785C requirements, for a Class IV aircraft in all flight phase categories with level 1 performance. With stability augmentation, all modes are stick fixed. Control forces are all controlled by the flight control system.

Dutch Roll Response	Mach 0.2	Mach 3.0
ω_{DR}	4.1841/sec	3.5364/sec
ζ_{DR}	0.1592	0.0929
T_{DR}	1.502 sec	1.7767 sec
Roll Response		
τ_{Roll}	0.6814 sec	1.9897
Spiral Response		
τ_{Spiral}	27.248 sec	45.045 sec

Figure 5.14: Lateral-Directional Dynamic Stability

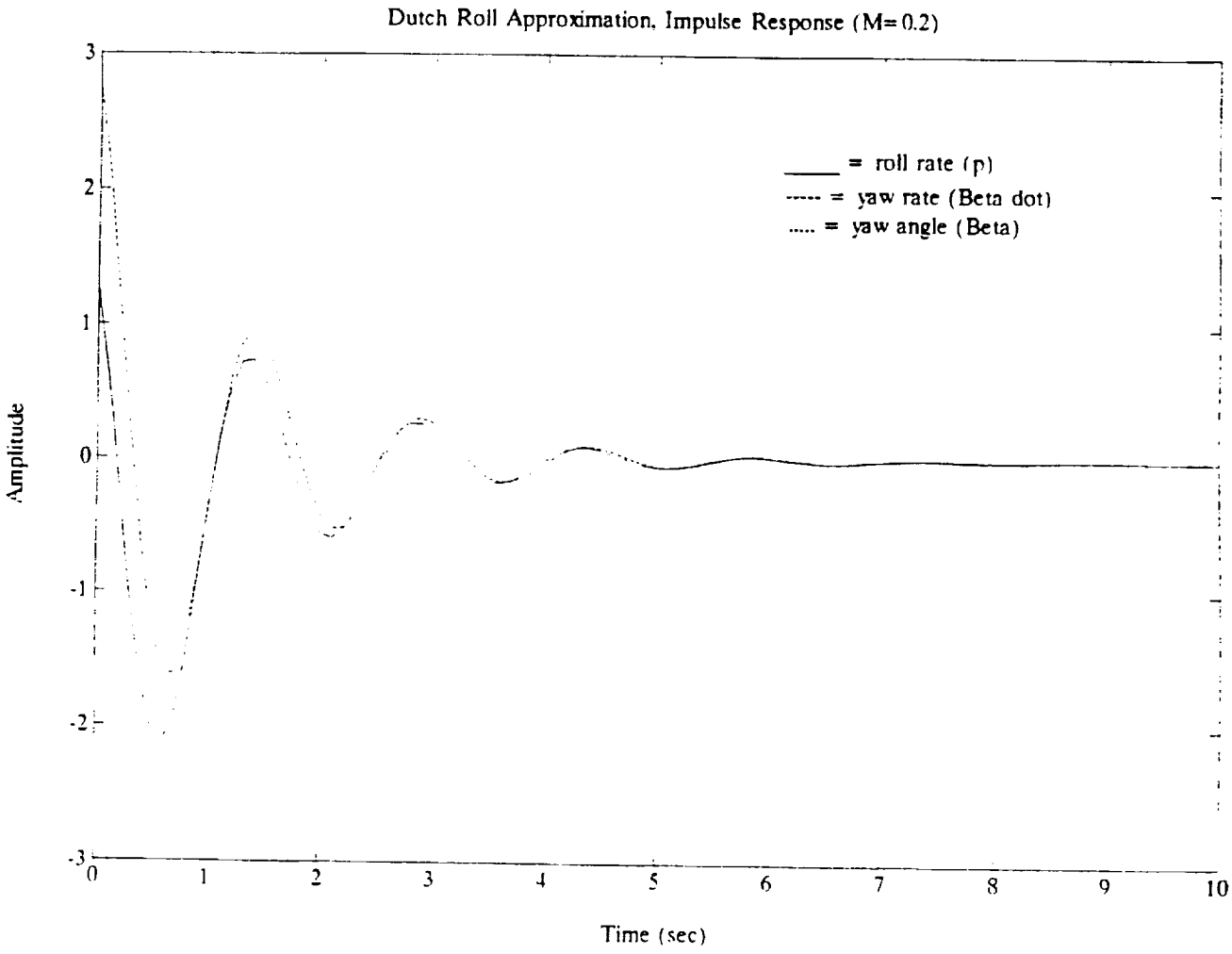

Figure 5.15: Dutch Roll Approximation (M=0.2)

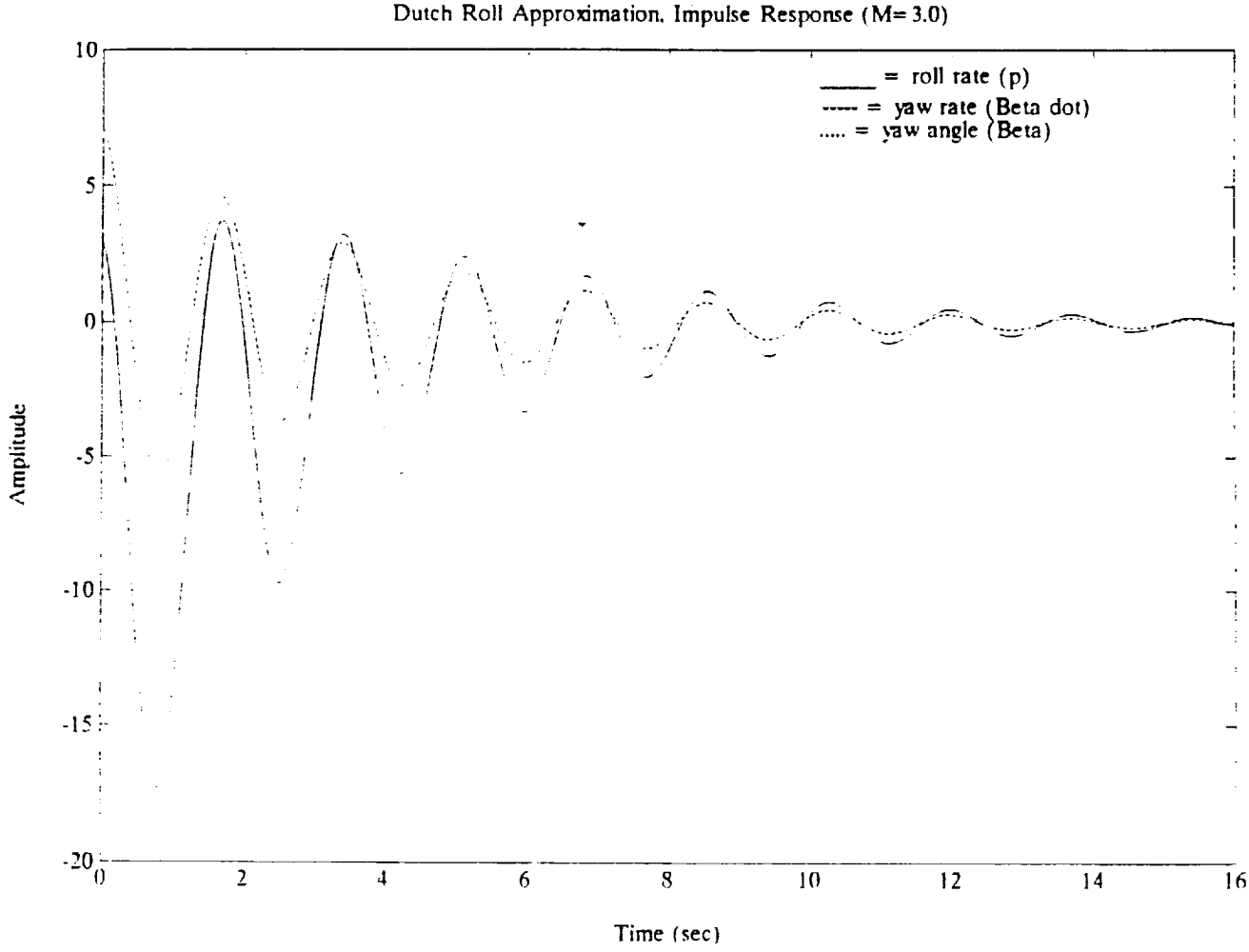

Figure 5.16: Dutch Roll Approximation (M=3.0)

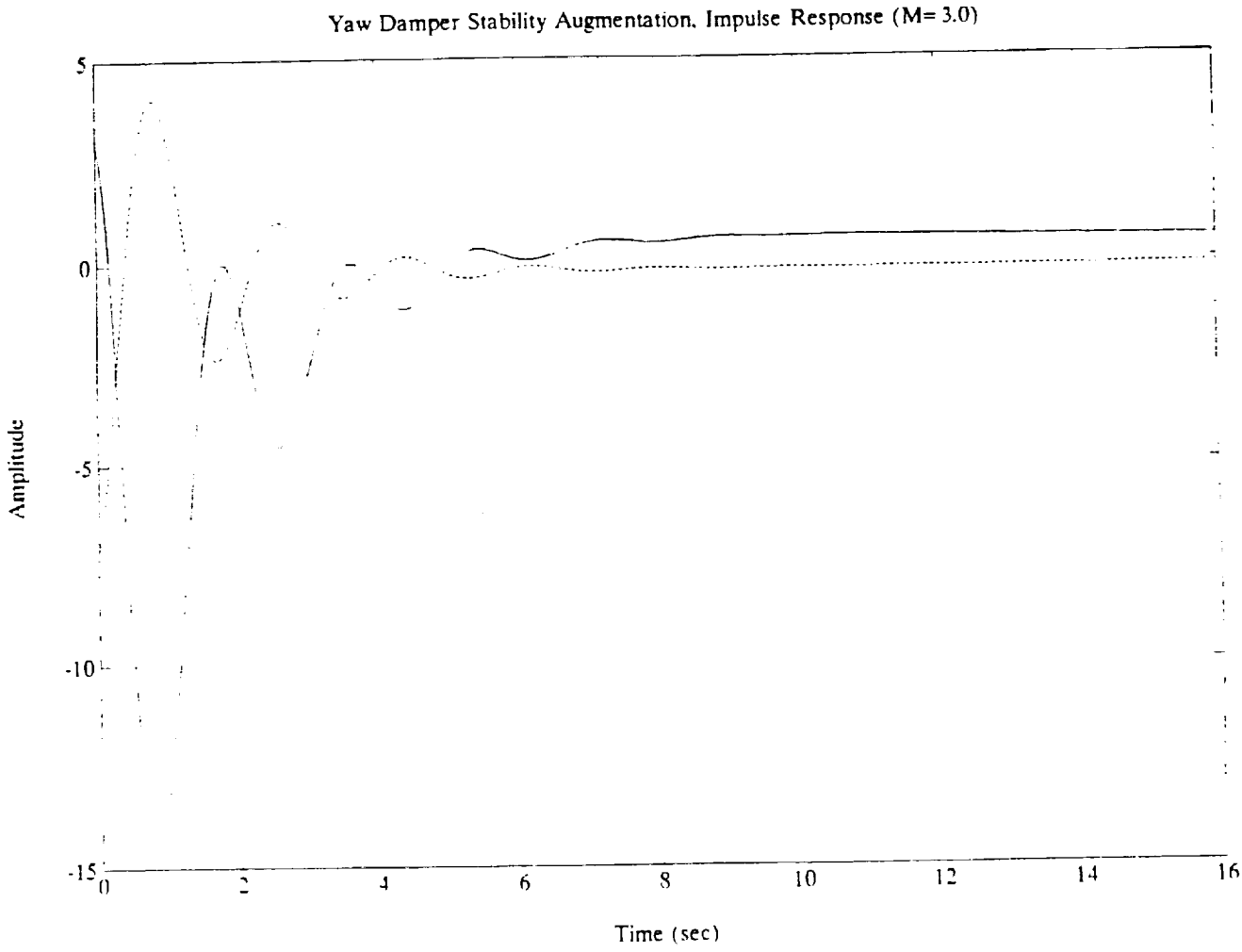

Figure 5.17: Yaw Damper Stability Augmentation (M=3.0)

Augmented Stability	
Longitudinal	**Elevator**
ω_h	7.2143/sec
ζ	0.4043
Lateral-Directional	**Yaw-Damper**
ω_{DR}	3.5347/sec
ζ_{DR}	0.1938
τ_{Roll}	2.0851 sec
τ_{Spiral}	21.1416 sec

Figure 5.18: Augmented Dynamic Stability

1. MIL-F-8785C

MIL-F-8785C Flying Quality requirements for a class IV aircraft, in all flight phase categories with level 1 performance, are compared with those of the Sabot (Fig. 5.19). As shown, the Sabot exceeded all requirements except for a small excursion in exceeding the maximum roll-mode time constant (τ_{roll}). A short-period frequency and acceleration sensitivity analysis was also performed on the Sabot, which met all requirements for level 1 performance in all flight phase categories (Figs. 5.20-5.22).

2. Cooper-Harper Ratings

While the Cooper-Harper rating system is somewhat subjective, it was estimated that the Sabot exhibits a Cooper-Harper pilot rating of 3. In this rating, the aircraft handling characteristics are acceptable and do not increase pilot work load but would benefit by slight improvements.

Flying Qualities	Sabot	MIL-F-8785C
Longitudinal-Short Period		
ω_{sp}	7.2143	n/a
ζ_{sp}	0.4043	$0.35<\zeta<1.3$
Longitudinal-Phugoid		
ω_p	0.6204	n/a
ζ_p	0.0621	> 0.04
Lateral-Dutch Roll		
ω_{DR}	3.5347	> 1.0
ζ_{DR}	0.1938	> 0.19
Lateral-Roll		
τ_{Roll}	2.0851	< 1.0
Lateral-Spiral		
τ_{Spiral}	21.142	> 20.0

Figure 5.19: Flying Quality Comparison

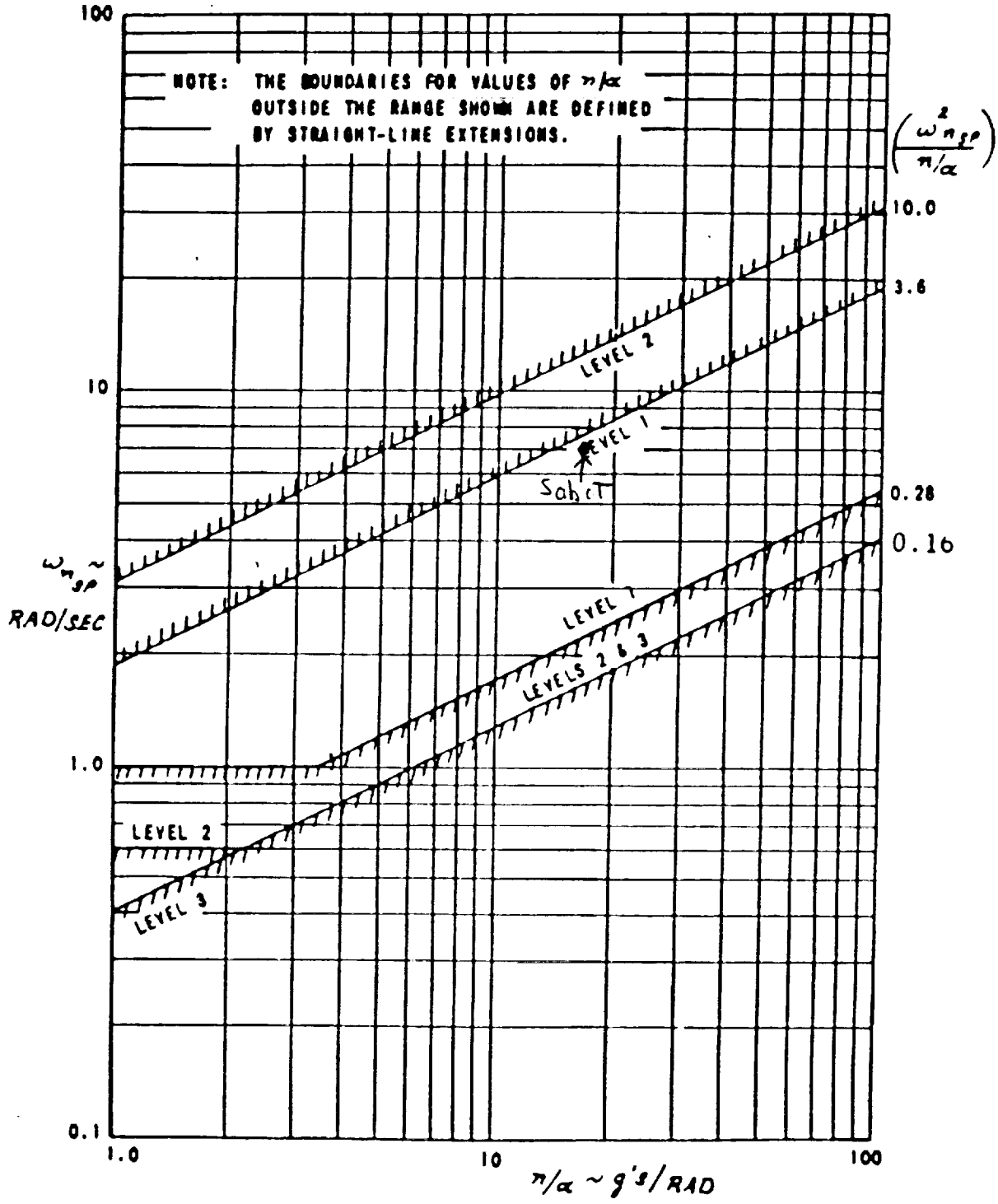

Figure 5.20: Short Period Frequency Rqmts.- Cat A

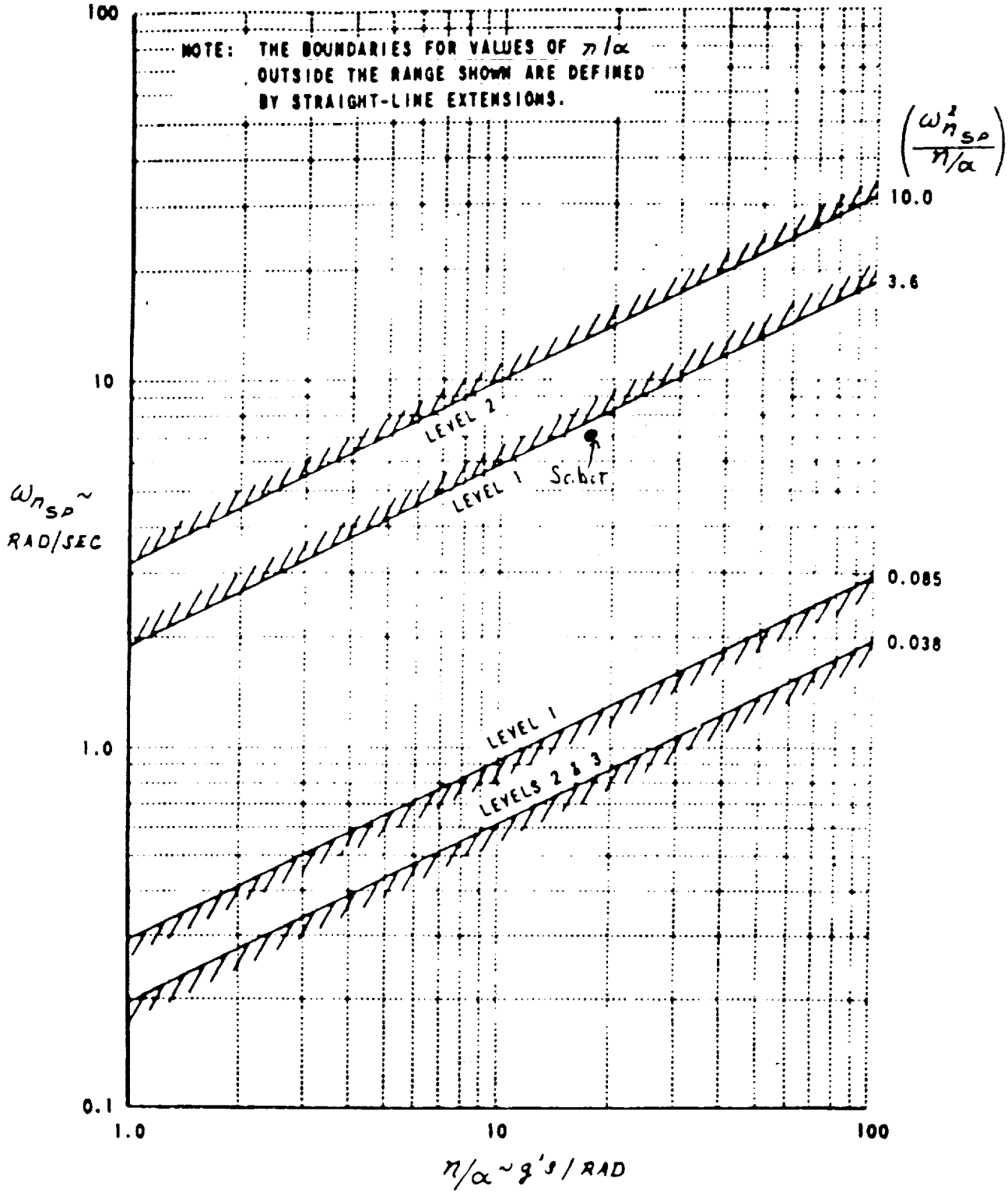

Figure 5.21: Short Period Frequency Rqmts.- Cat B

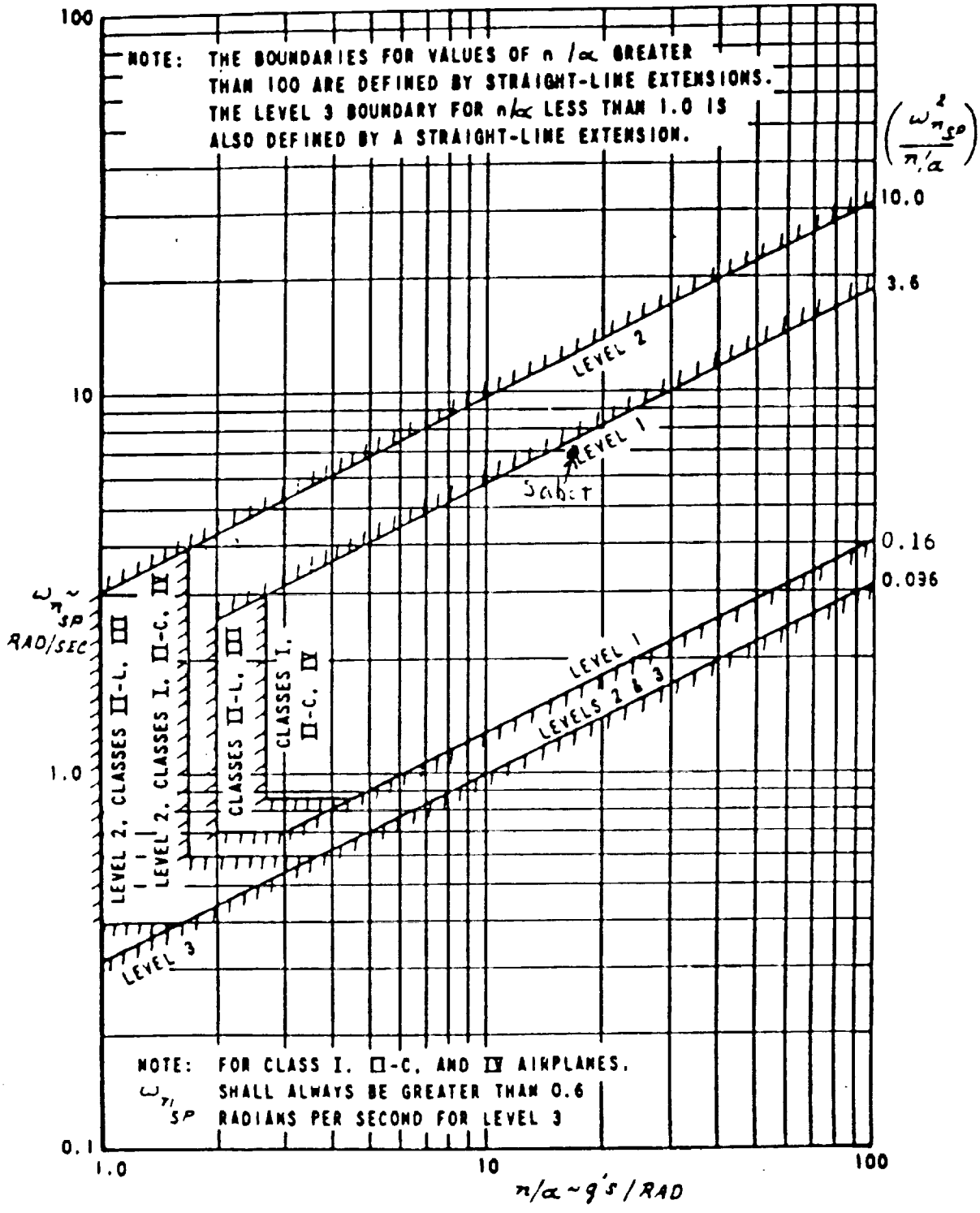

Figure 5.22: Short Period Frequency Rqmts.- Cat C

VI. STRUCTURES

A. DESIGN GOALS

Many parameters were considered when designing the aircraft structure. Most important were strength and weight, but cost, availability, heating characteristics, and corrosion resistance were also considered. In order to simplify the design, reduce cost and eliminate any technological development lag, techniques and materials were limited to those currently available.

B. REQUIREMENTS

This was driven by RFP requirements for carrier operations and a maximum gross weight of 85,000 pounds with a load factor 4g's. An extremely important requirement was to able to operate at a sustained Mach of at least 3.

Compliance with military specifications for structure was another requirement. Mil-Specs were used in the following areas: Mil-A-8860 for strength and rigidity, Mil-A-8870 for vibration and flutter and Mil-Std-2066 for carrier launch and arrestment forces. Some applicable military specifications were:

1. Maximum gross weight to be used for catapulting.
2. Flight design weight is maximum gross weight minus 40% of the internal fuel weight.
3. Ultimate load (safety factor) of 1.5 times the limit load.
4. Landing weight is empty weight, plus loiter fuel for 20 minutes, 5% of maximum internal, 10 minutes at normal thrust, plus armament.

C. MATERIAL SELECTION

A primary driving factor for this design was the thermal load at mach cruise. With skin temperatures around 600F selection was limited to steel alloys, titanium alloys, boron aluminum composite

and graphite polyamide composite. Steel was by far the cheapest, but its higher strength was offset by its increased weight. The next alternative was Titanium which offered a good trade-off between strength, weight and cost. Boron-Aluminum composite which has good strength and weight characteristics was judged to be too expensive compared to the alternatives. The final alternative, graphite polyamide composite, offered a fairly good balance of strength, weight and cost [Nicolai 19-8]. Estimates at the weight savings achieved by the use of the graphite polyamide over the titanium is about 14% [SCAR p 616].

D. THERMAL ANALYSIS

The aerodynamic heating of the waverider was done using the basic heat equations and two FORTRAN computer programs to solve for the skin and leading edge temperatures. The basic heat equation used was

$$m\ c_p\ dT/dt = q\ A - \text{sigma epsilon}\ A\ T^4$$

m	-	mass of the material
c_p	-	specific heat of the material
Dt/dt	-	time rate of change of temperature
q	-	heat transfer
sigma	-	Stefan-Boltzman constant
epsilon	-	emissivity
A	-	area
T	-	temperature

Two different formulas for q were used. The first was the convective heat transfer for the skin and the second was the stagnation heat transfer for the leading edge.

$$q_{skin} = h\ A\ (T_{aw} - T_{skin})$$

$$q_{le} = 20800/R^{0.5}\ (rho_{inf}/rho_{sl})^{0.5}\ (V_{inf}/26000)^{3.25}\ (1 - T_{skin}/T_{tinf})$$

h - local convective heat transfer coefficient
T_{aw} - adiabatic skin temperature
T_{skin} - skin temperature
R - radius of the leading edge in feet
rho_{inf} - density of air at altitude
rho_{sl} - density of air at sea level
V_{inf} - speed in feet per second
T_{tinf} - stagnation temperature at altitude

In order to simplify calculations, the geometry of a cone was assumed. Within the program itself, a mix of ideal gas and empirical formulas were used. Copies of the two programs, THERMAL and STAGTEMP, as well as an explanation of their logic can be found in Appendix A.

Using these programs, it was possible to effect several trade studies. Material selection was a primary concern. Using the SR-71 as base, it was expected that current materials would be more than adequate [SCAR]. Material selection had a minimal effect on heating, merely changing the rate of temperature change with a minimal change in the cruise temperature. Emissivity had a similar effect, so skin condition should not effect mission capabilities. Skin thickness affected the rate of temperature change and this was not readily apparent until skin thicknesses approached 0.25 inches.

By far the largest contributor to skin temperature was the flight profile. Figure 6.1 shows the temperature profile for varying skin thickness throughout the flight profile. A lower cruise altitude or higher cruise mach sent the temperatures into a realm where different materials or an active cooling system would have been required (Figure 6.2). A cruise Mach of 4 resulted in the skin temperature approaching 1500 degrees Rankine (Figure 6.3). Changes in cruise altitude were weak functions at Mach 3, but grew

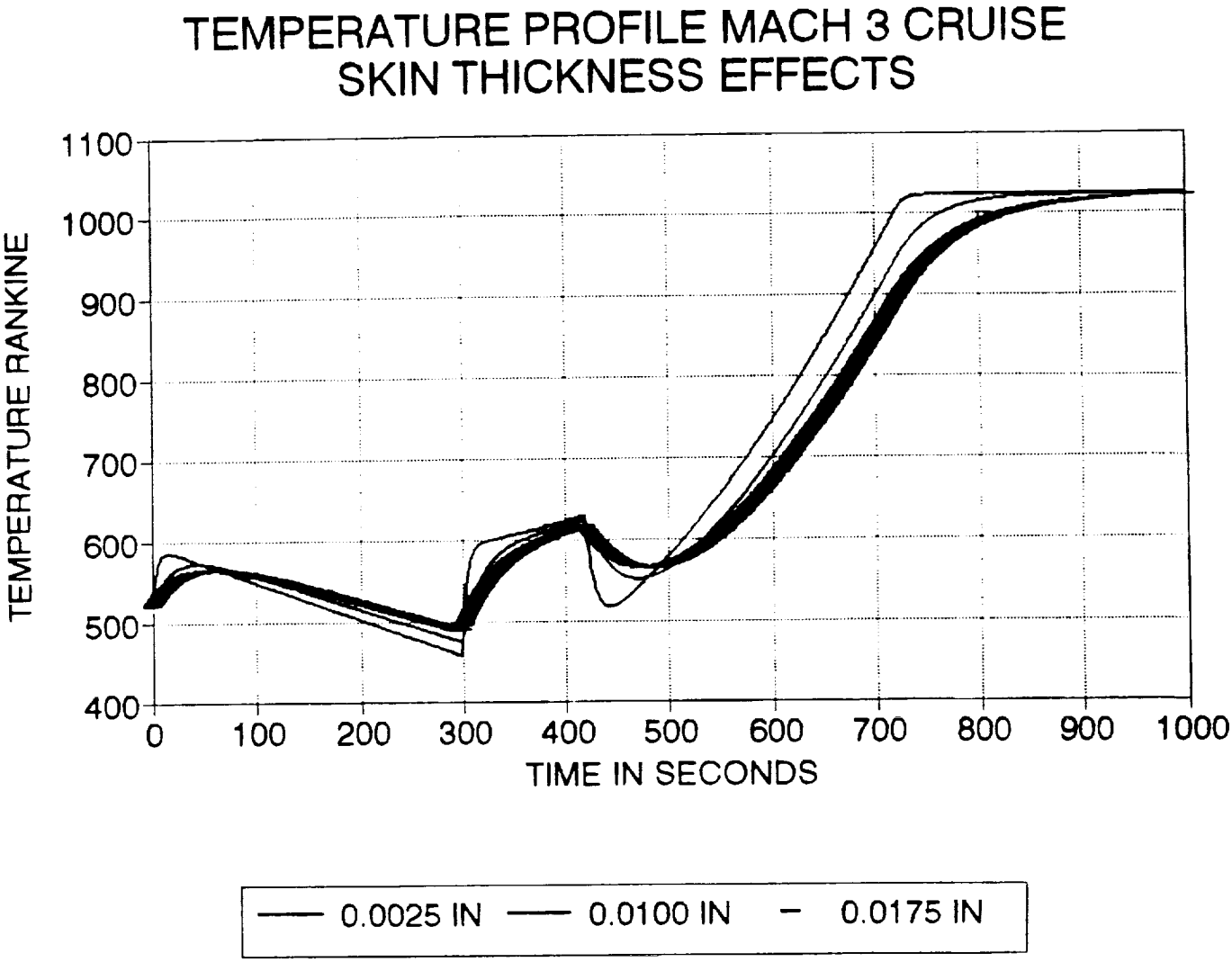

Figure 6.1: Temperature Profile (M=3.0)

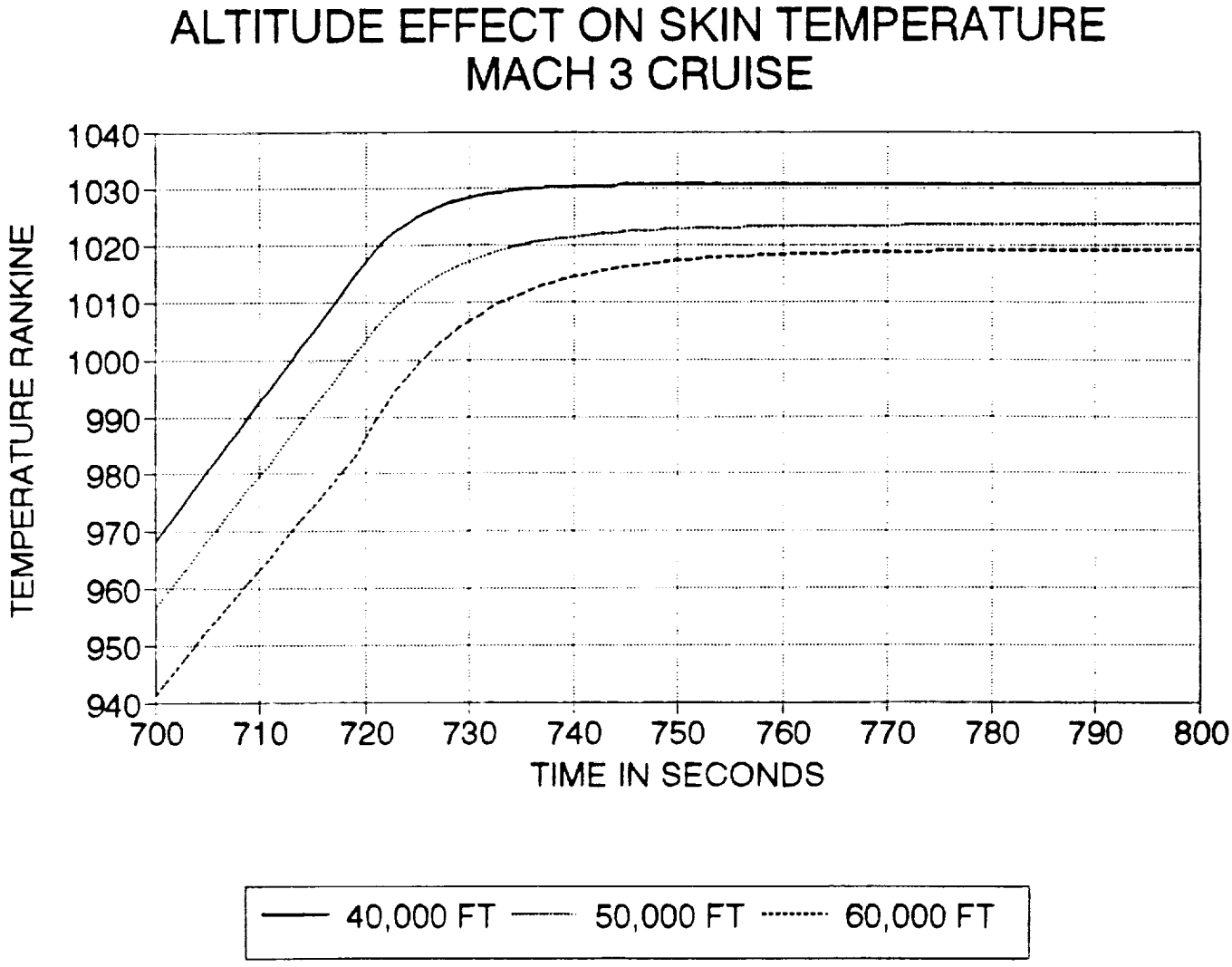

Figure 6.2: Altitude Effect on Skin Temperature (M=3.0)

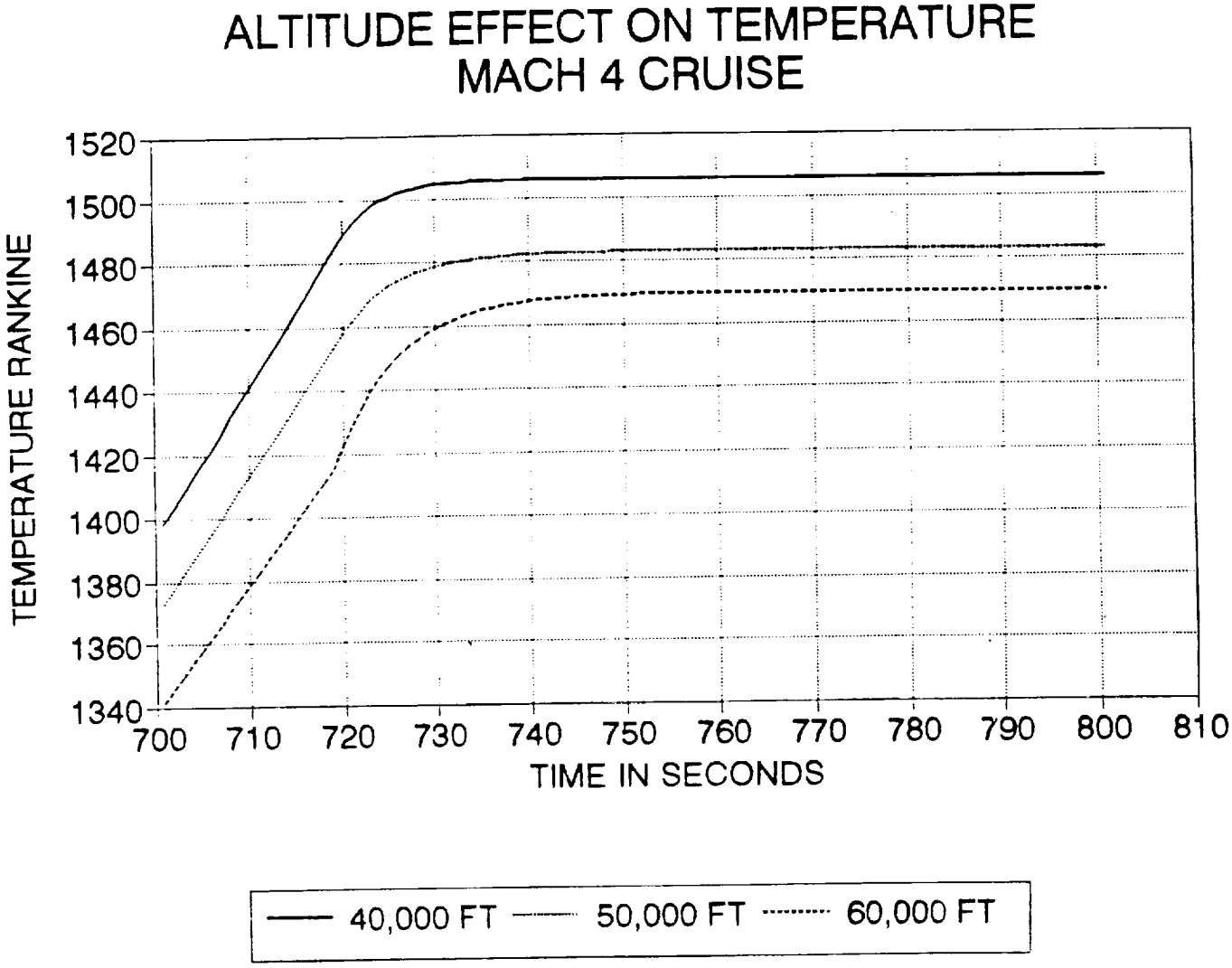

Figure 6.3: Altitude Effect on Temperature (M=4.0)

stronger with higher Mach numbers.

E. WING BOX DESIGN

The loads on the wing were determined using a 6g turn at 3.0M, 50,000 ft of altitude and a weight of 60,000 pounds. This generates a total lift of 360,000 pounds. An elliptical lift distribution was assumed.

Looking at previous interceptor designs, wings were typically thick skinned without integral stringers [Niu p 267]. However, for our design, a more conventional semi-monocoque construction was selected. This should result in weight-savings and as well as improved thermal performance [SCAR p. 608]. The design was simplified to a 4 spar design. Using MSC/MOD and MSC/PAL2 software, a finite element analysis was conducted. Figure 6.4 depicts the wing box, exaggerated deformation and a major stress plot.

F. FUSELAGE

Being a carrier based aircraft, the loads encountered during a normal life-cycle are much greater than those encountered by a land-based counterpart. The greatest loads encountered are during take-off (catapult launch) and landing (arrestment).

For catapult launch at maximum gross weight (85,000 pounds) the maximum force imparted on the aircraft was 250,000 pounds. For arrested landing the hook point load was 160,000 pounds at the maximum landing weight (42,000) and an landing speed of 142 knots (240 ft/sec).

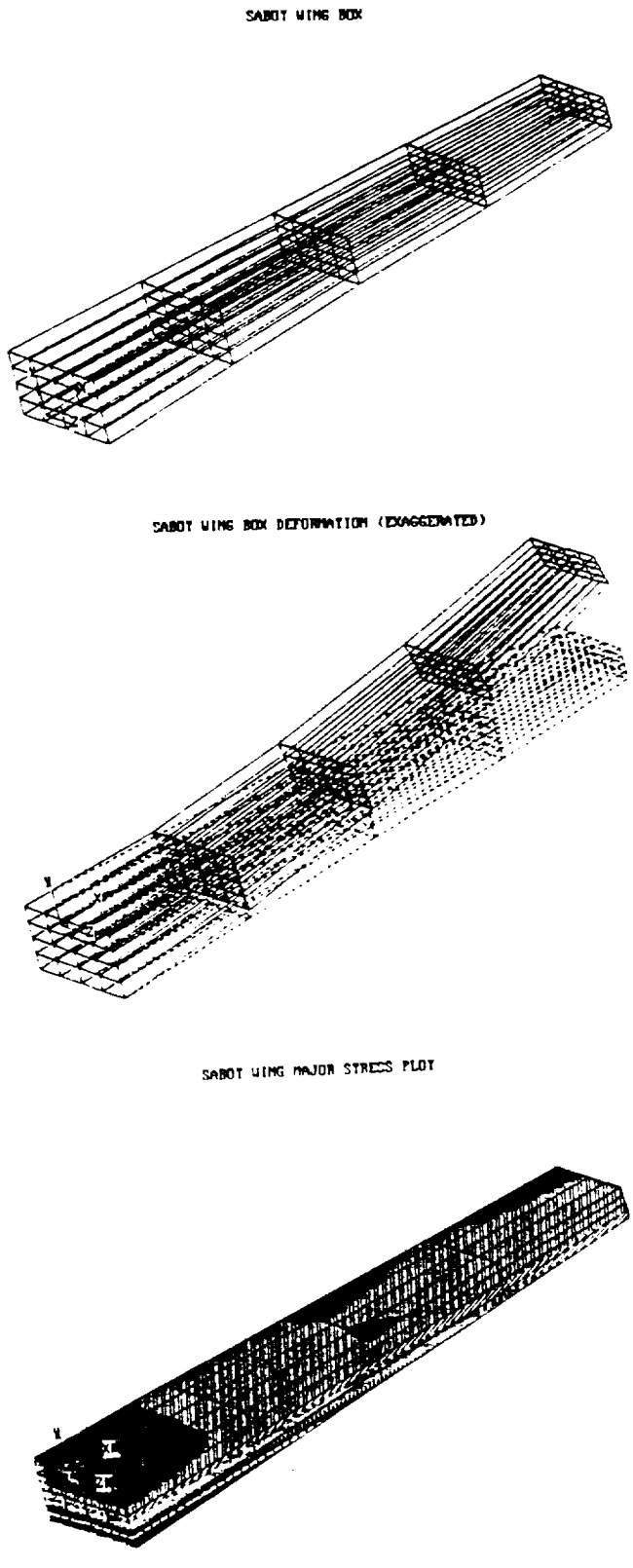

Figure 6.4: Wing Box Finite Element Anaylsis

G. LANDING GEAR

The waverider geometry necessitated the main landing gear being located fairly well aft of the center of gravity. The alternative was excessively long struts and this could lead to buckling problems [Raymer p. 370].

A vertical gear with a cross brace support was chosen for both the nose and main landing gear. A trade-off between vertical and levered gear was considered. The vertical gear was chosen for simplicity reasons and geometric constraints. The vertical gear had a tipover angle of 52 degrees and a tip back angle of 14 degrees. The nose oleo was sized at 8 inches in diameter and the main gear at 8.5 inches in diameter. Main gear oleo stroke was computed at 1.5 ft using a sink rate of 22 ft/sec.

The nose gear incorporates a carrier launch bar system and a dynamic pitch system. The dynamic pitch system is similar to that found on the F-14. Just prior to launch the nose gear oleo is compressed by the aircraft hydraulic system, when the aircraft exits the shuttle at the end of the catapult stroke the oleo extends, thereby assisting aircraft rotation.

The tires were sized with single wheels on the mainmounts and dual wheels on the nosegear in order to accommodate the launch bar mechanism. The main gear tires selected were 36 inch by 11 inch type VII with an inflation pressure of 235 psi and a maximum load of 26,000 pounds. The nose tires selected were 30 inch by 6 inch type VII, with an inflation pressure of 270 psi and a maximum load of 14,500 pounds.

VII. PERFORMANCE

A. TAKEOFF AND LANDING

1. Field Takeoff

The distance required for a standard day, sea level takeoff is 7900 ft. Figure 7.1 shows the breakdown for the ground roll, rotation, and climb out over a 50' obstacle. Rotation speed is 180 kts (301 ft/s), with an initial climb out of 7000 fpm. Due to geometric considerations, the landing gear is placed considerable aft of the CG requiring rotation to be accomplished by the nose gear. Using the method described in Nicolai to compute the takeoff characteristics produced a total drag at rotation speed that is greater then single engine thrust. Once the gear is raised, the drag drops considerably making single engine climb out possible. The failure recognition speed is, therefore, considered to be V_{TO} at 180 kts, with a critical field length of 11000 ft for standard day conditions.

2. Field Landing

The field landing was computed based on the maximum landing gross weight of 50,000 lb. The landing profile is shown in Figure 7.2. The total landing distance required is 2750 ft.

B. SPECIFIC EXCESS POWER

The excess power was computed for a range of Mach numbers and altitudes and then plotted using the Matlab contour command. The chart is for a weight of 76,000 lb on a standard day. The plot of Specific Excess Power is shown in Figure 7.3 with the design altitude and maximum q loading indicated. The maximum occurs at

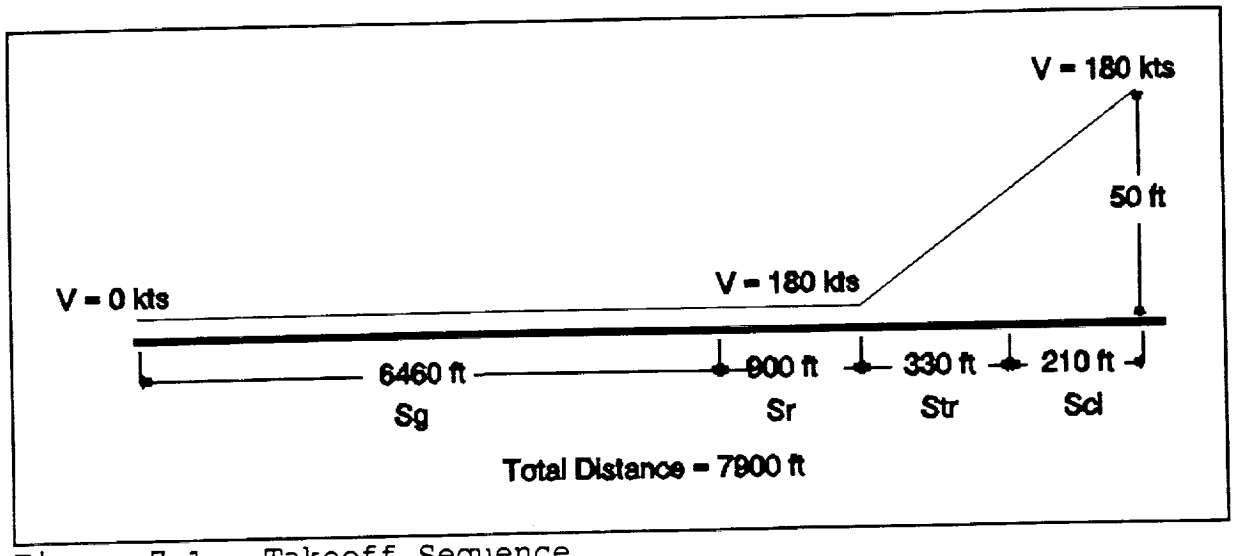

Figure 7.1: Takeoff Sequence

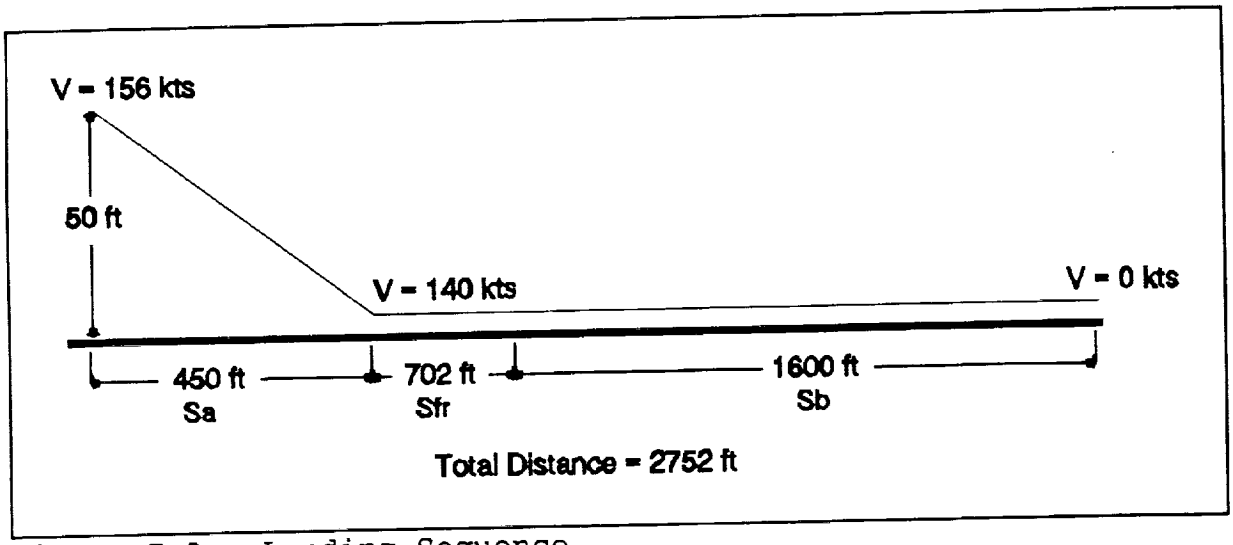

Figure 7.2: Landing Sequence

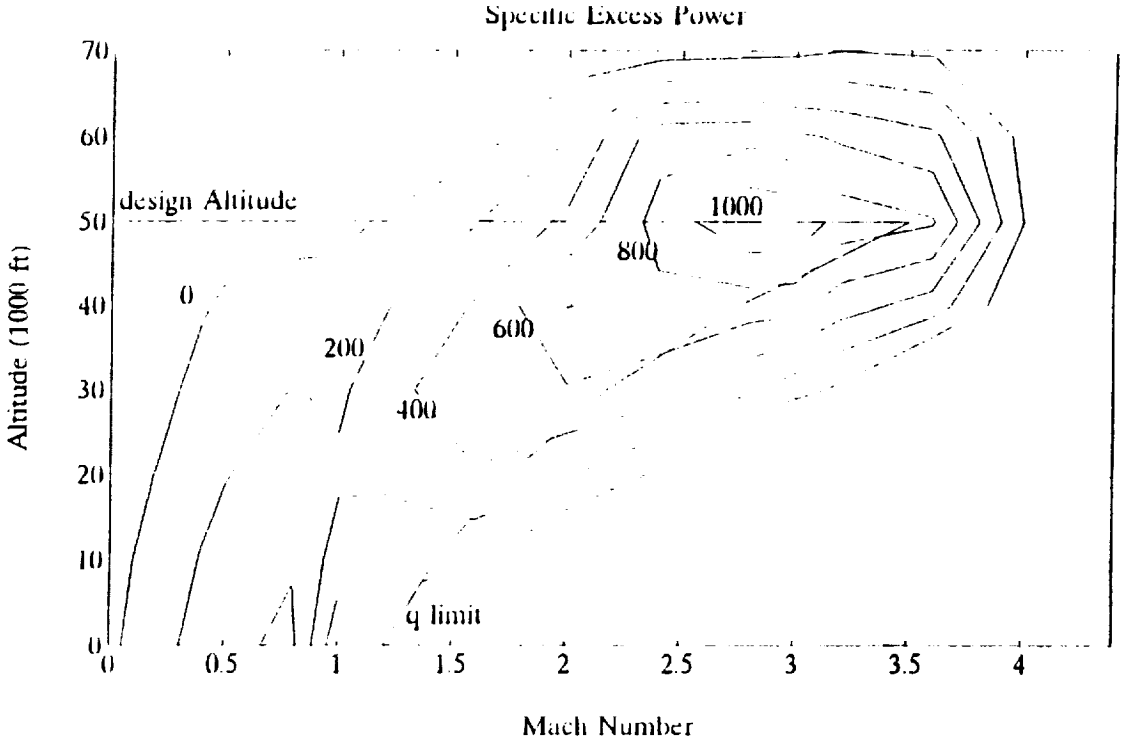

Figure 7.3: Specific Excess Power

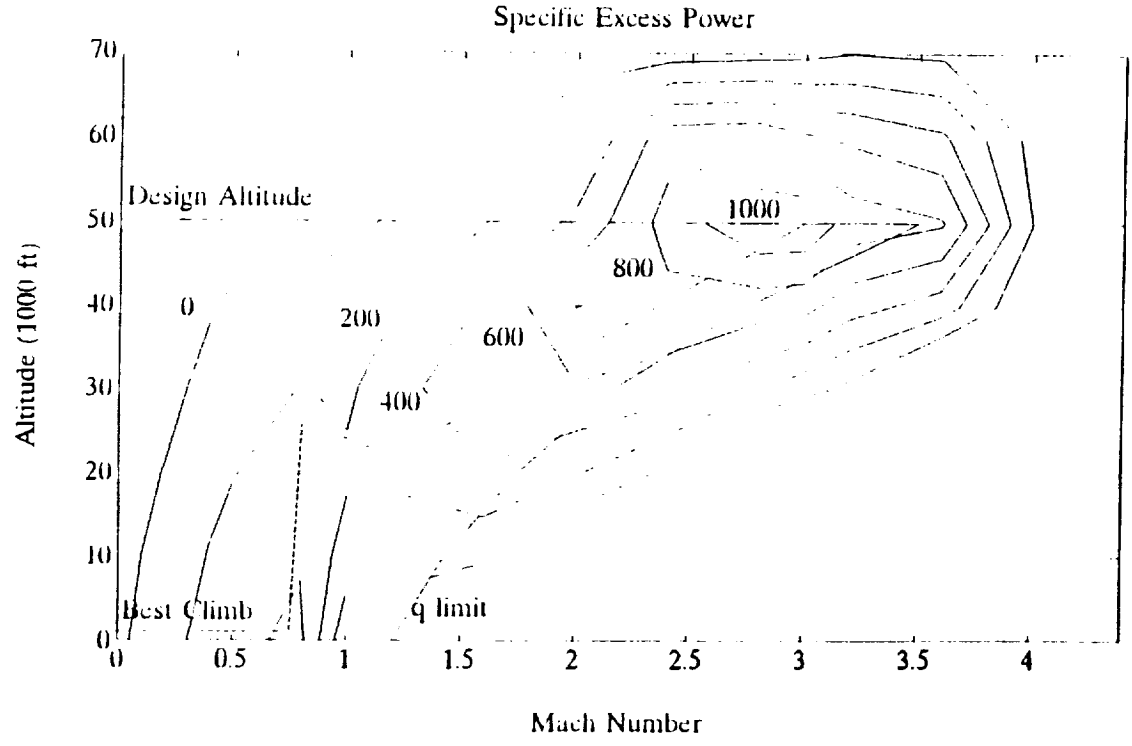

Figure 7.4: Best Climb Profile

design Mach/altitude tapering off rapidly above that. This allows a 4g sustained turn with a 2.46°/s turn rate. A 4g turn would require a 12.8 mile radius taking 73 seconds to turn 180°.

C. CLIMB

The climb profile is illustrated in Figure 8.4 with a dotted line. The best climb is obtained by accelerating to mach 0.8 on the deck, climbing to 26,000 ft, diving through mach 1 down to 22,000 ft, then maintaining an accelerated climb to mach 3 at 50,000 ft.

D. FLIGHT ENVELOPE

The flight envelope is defined by the stall speed up to Mach 0.65 at 45,000 ft, by the maximum thrust available to Mach 3.9 at 55,000 ft, by the q limit back down to Mach 1.36 at 7,700 ft, and by the maximum thrust available to Mach 0.94 at sea level. The plot in Figure 8.5 was computed for a 76,000 lb aircraft, in AB.

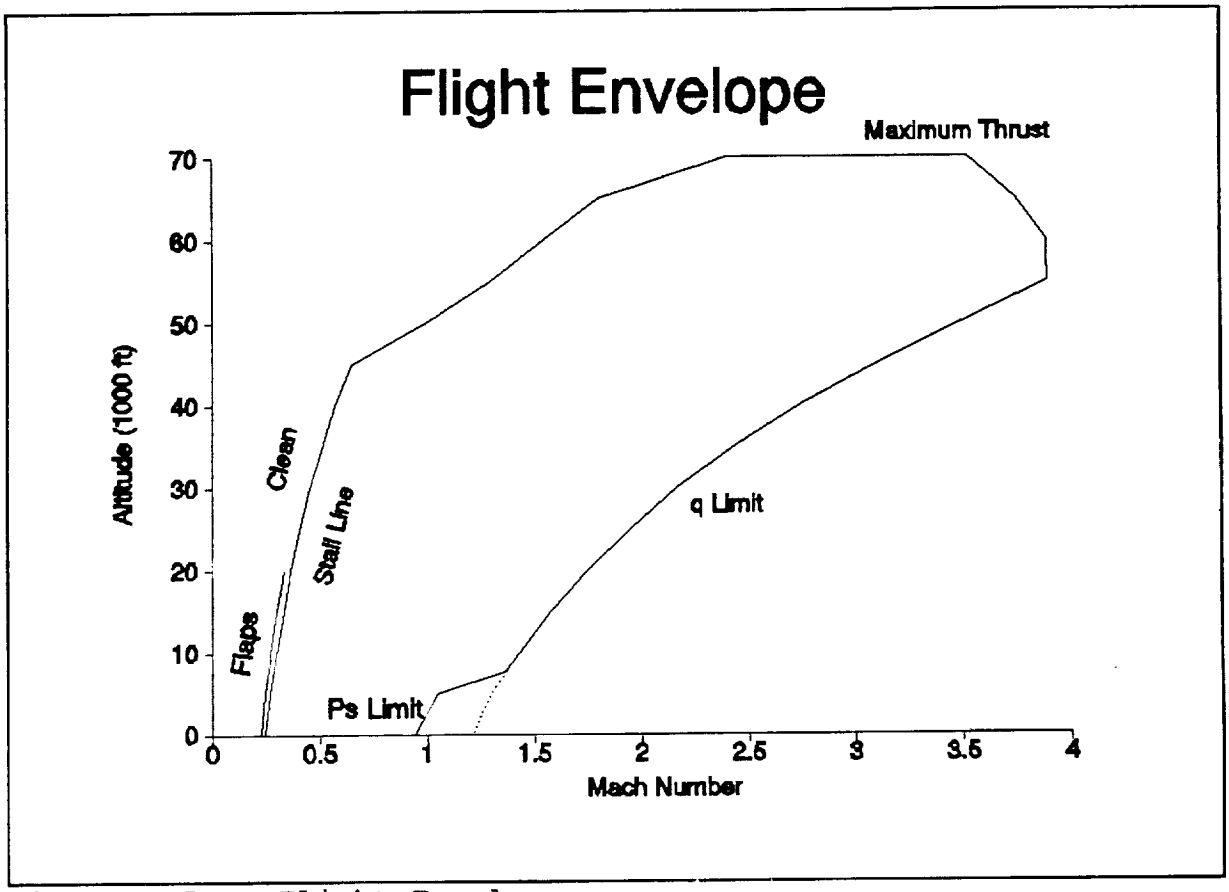

Figure 7.5: Flight Envelope

VIII. AIRCRAFT SYSTEMS

A. ELECTRICAL SYSTEM

Aircraft AC electrical power is provided by two 90-kva engine driven generators. Power is furnished to two separate buses via transfer relays working in conjunction with a runaround relay. Under normal operating conditions each generator powers a separate bus. In the event of failure of one generator, the transfer relays allow powering of flight essential equipment by the single remaining generator.

Each generator also has a protection system associated with it. If incorrect voltage, under or over frequency, or a feeder fault is detected, generator output is stopped and a GEN OFF light is illuminated in the cockpit.

DC power is furnished via a single transformer-rectifier capable of powering the entire system. Backup power is provided by two 24-volt, 31 ampere batteries with integral battery chargers. Under normal operation, the batteries receive a continuous charge from the transformer-rectifier.

Secondary power is provided by an auxiliary power unit (APU). The APU is capable of providing enough power for engine starts and can also used in flight to augment the engine bleed air to the environmental control system. A schematic of the electrical system is shown in Figure 8.1.

B. HYDRAULICS

The Sabot's hydraulic power was supplied by two separate primary systems (HYD1 and HYD2) and a third Utility system powered

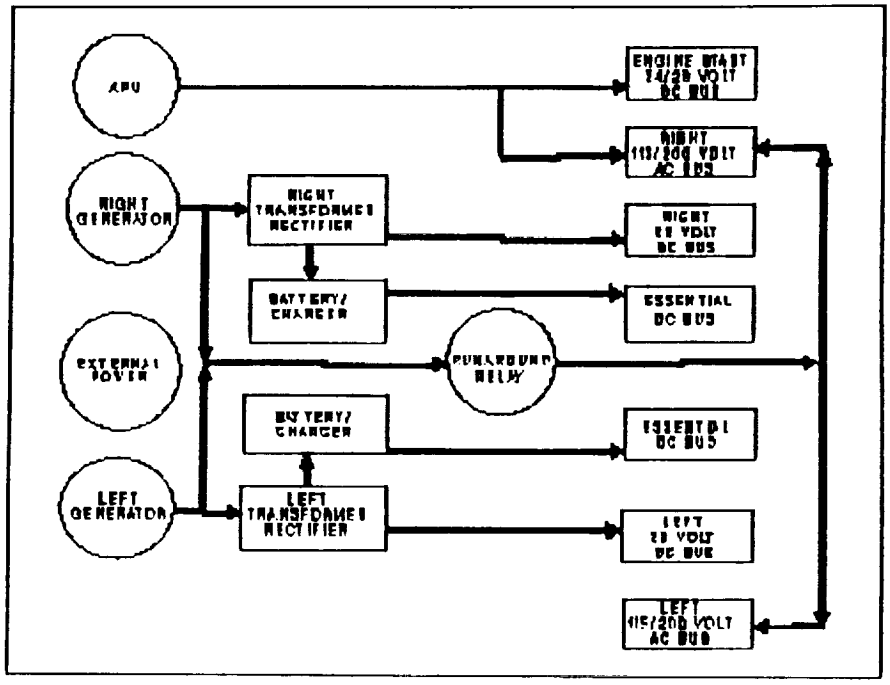

Figure 8.1: Electrical System

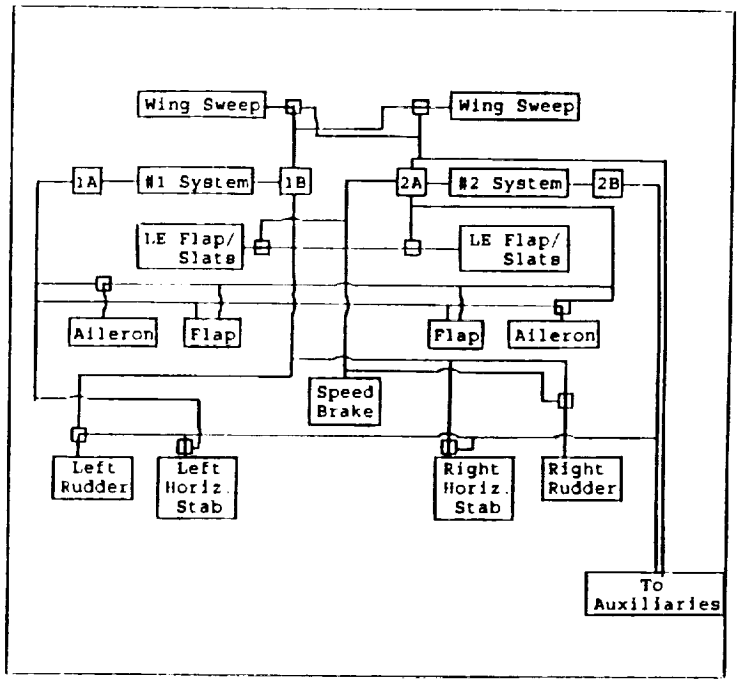

Figure 8.2: Hydraulic System

by the APU. Each primary system consists of two hydraulic circuits (Circuit A and Circuit B). The two primary hydraulic systems are identical and operate at 8000 psi. This results in a weight reduction of approximately 25 percent. HYD1 provides power to the primary flight control surface and wing sweep actuators. HYD2 provides power to the primary flight control surface and wing sweep actuators and additionally supplies power to the speed brake and non flight control actuators. The Utility hydraulic system operates at 8000 psi and powers primary flight control surface and wing sweep actuators. Figure 8.2 shows the primary hydraulic system layout. Redundancy to the flight control actuators is achieved either by simultaneously pressurizing the actuator from both systems or by supplying pressure to the actuator from one system while the other system is in a backup mode. All systems are equipped with pressure relief valves and each primary system reservoir is equipped with a reservoir level sensing system which shuts off a leaking circuit when the fluid drops below a certain level.

C. FUEL SYSTEM

The fuel system consists of four internal tanks and two wing tanks as shown in Figure 8.3. Table 8.1 presents the mass of each tank of the system. The fuel cells and interconnecting lines are self sealing which improves aircraft survivability. That is, " if a bullet passes through a self-sealing tank, the rubber will fill in the hole preventing a large fuel loss and fire hazard" (Roskam, Airplane Design Part IV). The system is ground refueled through

C.2

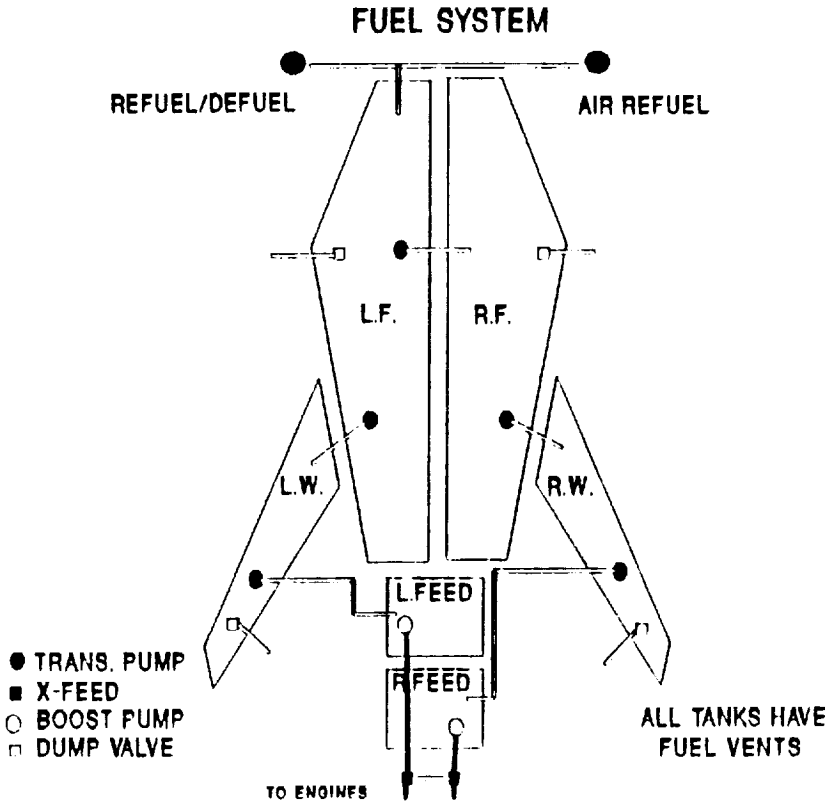

Figure 8.3: Fuel System

TANK	JP-5 (lb_m)
Left Fuselage	16500
Right Fuselage	16500
Left Wing	1100
Right Wing	1100
Left Feed	2000
Right Feed	2000
TOTAL	39200

Table 8.1: Individual Fuel Tank Capacities

single point pressure refueling and airborne refueled through a retractable aerial refueling probe.

The engines run on gravity feed in case of boost pump failure and the feed tanks are designed for inverted operation: the inner tank is equipped with flapper valves which trap fuel around the pump during inverted flight. The wing tanks, right and left fuselage tanks have fuel dump capability and transfer fuel to right and left engine feed tanks. The right and left engine feed tanks have boost pumps to drive the engines.

D. SURVIVABILITY

Survivability enhancement concepts are employed in the Sabot design to reduce the susceptibility and vulnerability of the aircraft. The Sabot is optimized for long range high speed air to air intercepts. Appropriate design features are built in to the design to improve it's combat survivability. Although all fighters eventually become bombers (F-105, F-4, F-15, F-16, F-14), the Sabot survivability design features are optimized for the high altitude environment. The primary threat to the Sabot is likely to be enemy air to air fighters and high altitude SAM's. The following susceptibility reduction features are incorporated in the Sabot design:

1). Threat Warning

- Radar and Missile Attack Warning Receivers.
- Noise jammers and Deceivers
- Airborne Self Protecting Jammer system.

2). Signature reduction

- Radar Absorbent materials, low contrast paint.

3). Expendables

- integrated chaff and flare dispensing system.

4). Threat Suppression/Tactics

- high-speed and high altitude
- thrust vectoring
- data link

The following Vulnerability Reduction features are incorporated in to the Sabot design:

1). Component Redundancy (with separation)

- dual engines
- triple hydraulic systems
- multi-channel flight control system.

2). Component location

- no fuel over intakes.

3). Passive Damage Suppression

- OBIGGS for fuel tank ullage inerting
- foam in dry bays
- self-sealing fuel tanks.

4). Active Damage Suppression

- Fire detection and extinguishing system around engines and ECS.

5). Component Shielding

- shielding around engine compressor and turbine.

6). Component Elimination

- use OBOGGS system to replace LOX hazards.

A simplified Kill Tree is drawn in Figure 8.4. This Kill Tree is for an "A" level kill (5 minute hit to out of control). The redundant engine, electrical and hydraulic systems reduce the single point kills to the pilot and catastrophic actuator failure.

A vulnerability assessment computer program, MACSAP, was run to assess the Sabot survivability and quantify the benefits derived from the incorporation of survivability enhancement features. A campaign analysis of twenty strikes, each consisting of one hundred sorties was used in this simulation. The test was first run with an aircraft not using any survivability enhancement features and resulted in a loss rate of 1.21%. Incorporation of survivability enhancement and vulnerability reduction features, resulted in a loss rate of 0.46%--an overall survivability improvement of 62%

E. COCKPIT DESIGN

Cockpit design objectives of the Sabot included sufficient room for mission accomplishment, while restricted in size and shape so as not to interfere with waverider aerodynamic properties. "Fishbowl Visibility" was desired but expected to be slightly compromised due to the non-intrusion of the canopy into the windstream. The cockpit of the Sabot is designed to conform to cockpit sizing requirements [MIL-S-188471G]--similar in design to the F/A-18 cockpit (Fig. 8.5). The F/A-18 cockpit design was chosen over the Advanced Tactical Fighter cockpit design to facilitate standardization for Naval aircraft, in respect to both

Sabot Kill Tree

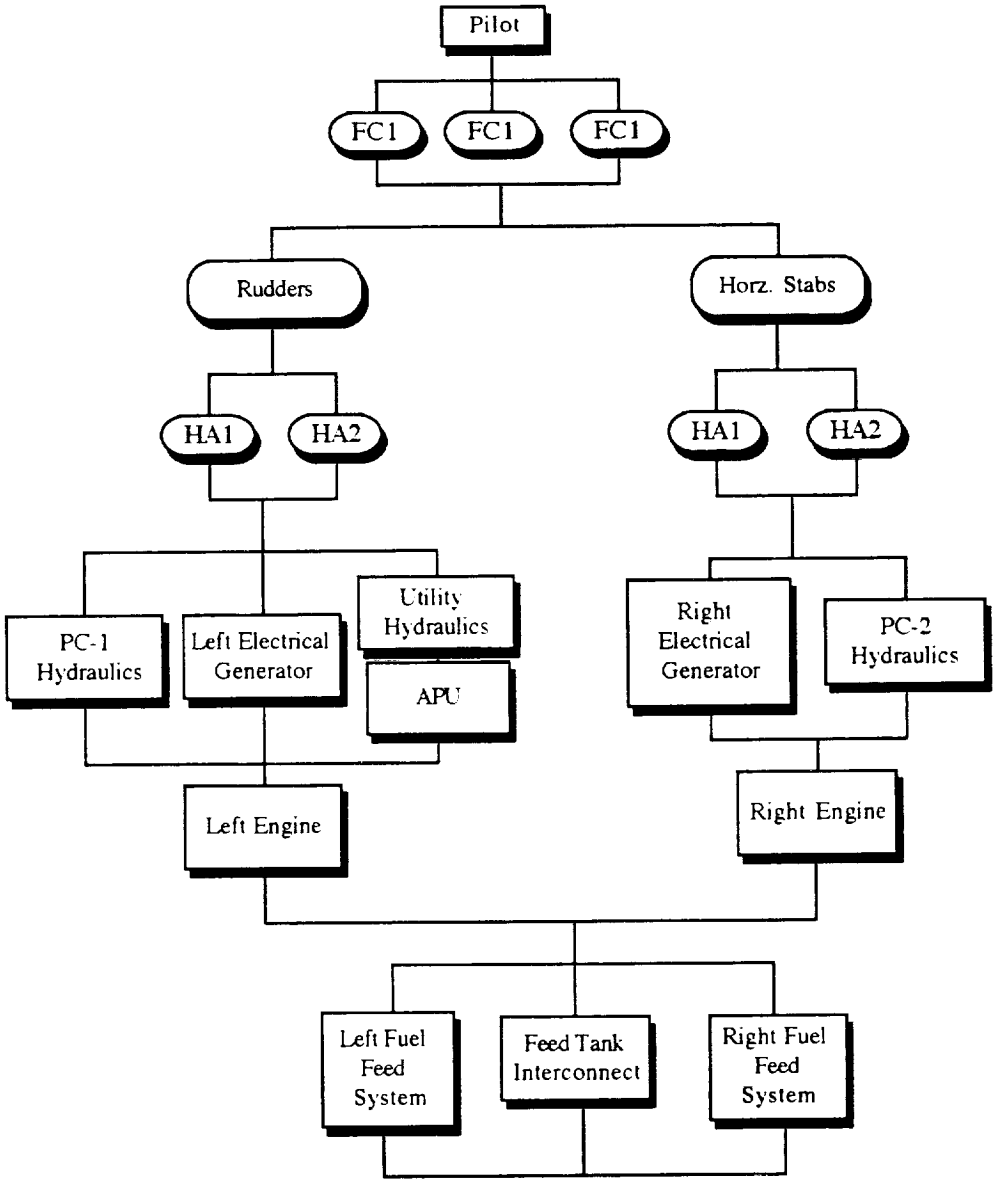

Figure 8.4: Kill Tree

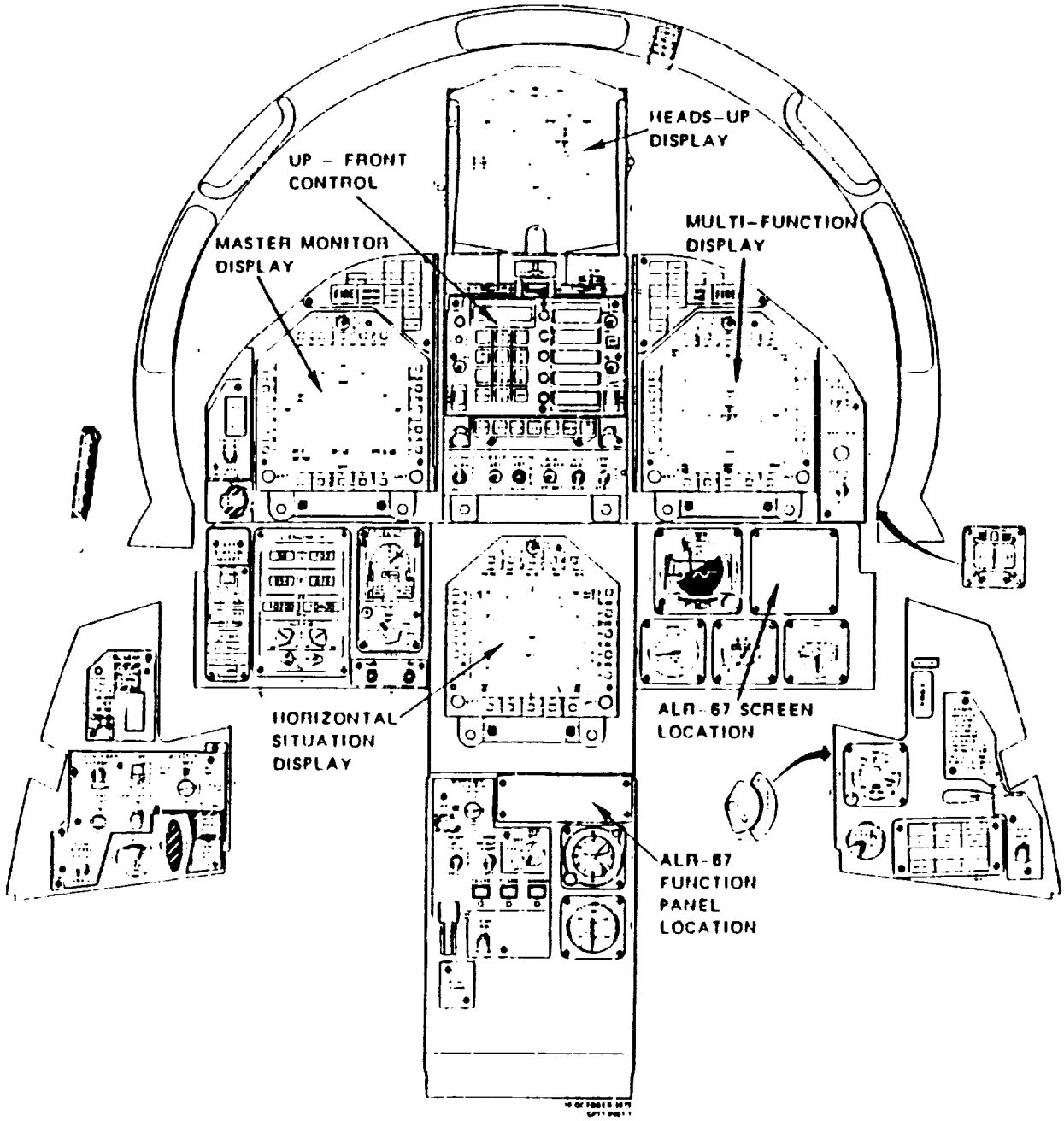

Figure 8.5: Cockpit Main Instrument Panel

component usage and center-cockpit controls.

A dual pilot cockpit was also considered, but the U.S. Navy has shown little interest in dual piloted aircraft based upon single vs. two pilot studies [Ward]. In an effort to minimize weight and cost, and based upon inconclusive test results, the Sabot was designed as a single piloted aircraft.

Also similar to the F/A-18 cockpit, the Sabot will utilize four multipurpose cathode-ray displays driven by two or more mission computers, an integrated up-front control panel, a HOTAS system, and a HUD.

1. Multi-Purpose Displays (MPD) and Integrated Up-front Control Panel.

A configuration incorporating MPD's and an Integrated Up-front Control Panel was selected to achieve the following benefits:

1). Pilot scan time reduced.

2). Reduction in the number of low-reliability electro-mechanical devices.

3). Increased reliability due to the dual-drive mission computer feature. This also includes the capability for any display format to be presented on any of the CRT displays.

2. HOTAS

The "Hands On Throttle and Stick" (HOTAS) System (Fig. 8.6 and 8.7) was selected to aid the pilot in efficiently accomplishing the mission without sacrificing attention to flight profile and situational awareness. HOTAS analysis performed according to the

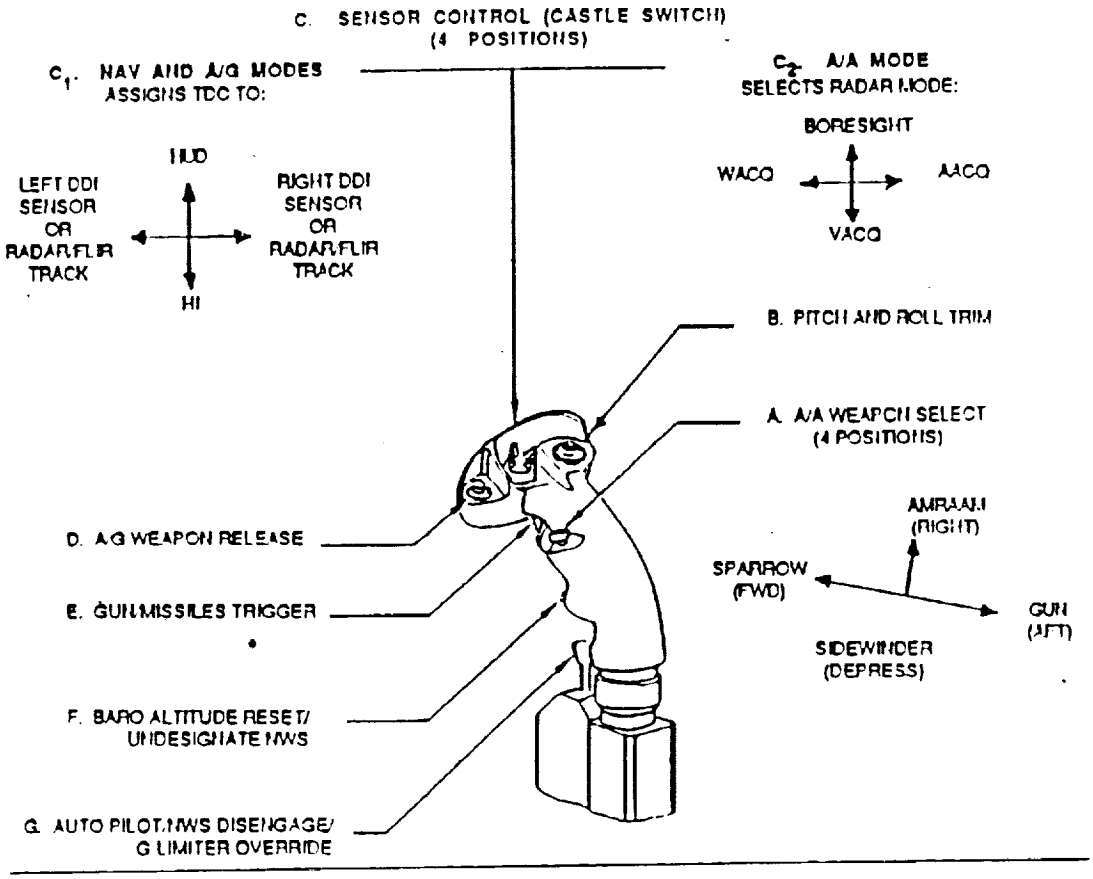

Figure 8.6: Flight Control Stick Controls

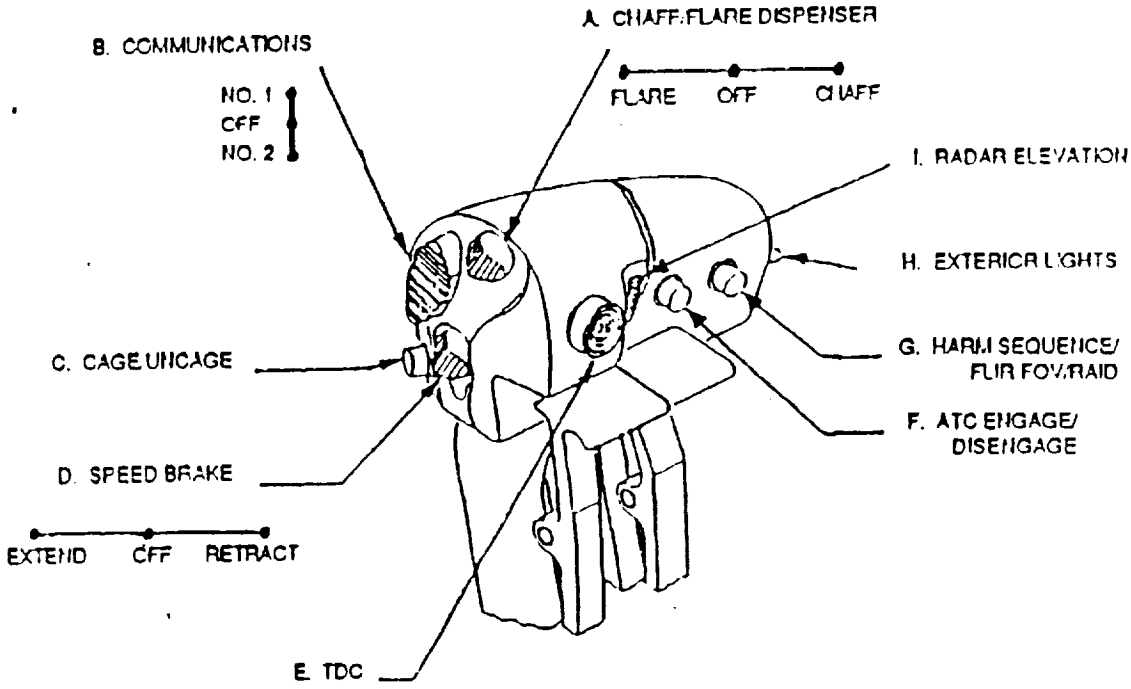

Figure 8.7: Throttle Controls

Human Factors Crew Station Evaluation Guide, identified few discrepancies with the HOTAS system. Most pilots felt that the number of HOTAS functions had reached a maximum, recommending that careful consideration be given to incorporating more functions into the HOTAS System [Frankenberger].

3. Heads Up Display (HUD).

The "Heads Up Display" (Fig. 8.8) is the primary flight instrument for intercept navigation including manual and automatic carrier landing modes. All essential flight data are projected on the HUD combiner and focused at infinity for easy assimilation by the Pilot. Several innovative components were also considered for incorporation into the Sabot cockpit:

1. F/A-18 pilots have identified a problem associated with loss of situational awareness in unusual attitudes due to confusion with current HUD symbology and the use of a substandard back-up gyro [Barnes]. In order to alleviate this problem, it has been recommended that an "Enhanced Attitude Directional Indicator" (Fig. 8.9) be incorporated into the Sabot cockpit or incorporated as standard symbology for the HUD.

2. The use of a Voice Control Interactive Device (VCID) was considered for incorporation into the Sabot (Fig. 8.10), to increase the pilots ability to exchange data. Although the system does work, test results show command recognition to be between 83-89% [Loikith]. Although it is expected that VCID devices will become operational in the future, it does not appear feasible at this time due to its poor recognition accuracy.

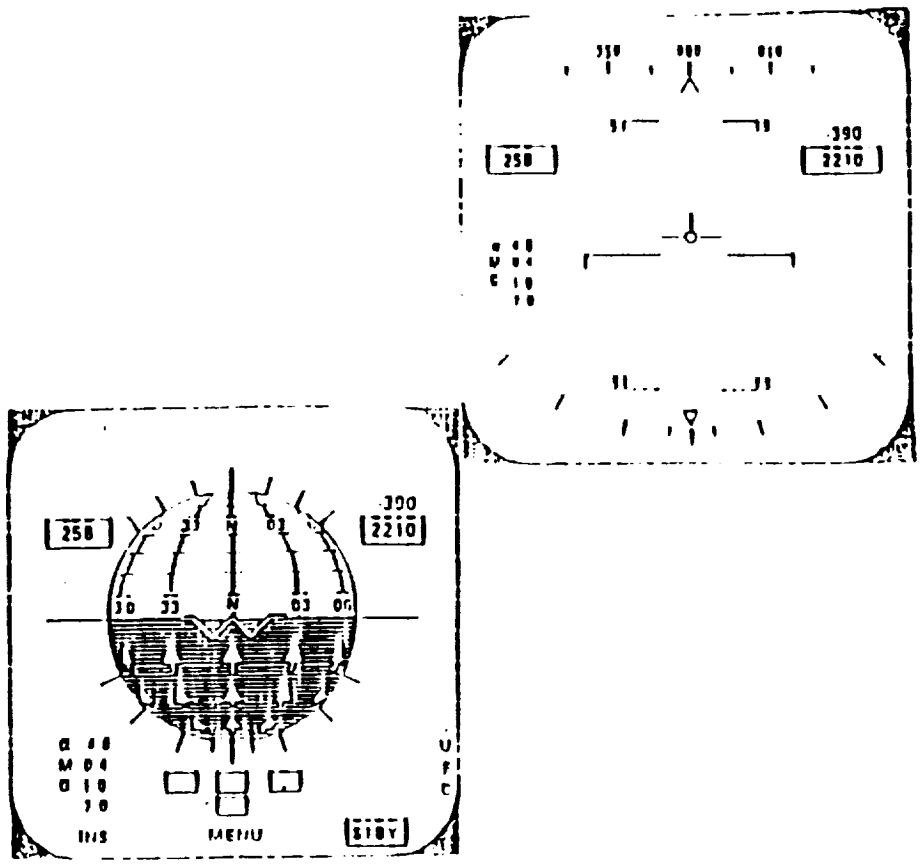

Figure 8.8: Enhanced ADI with Standard HUD

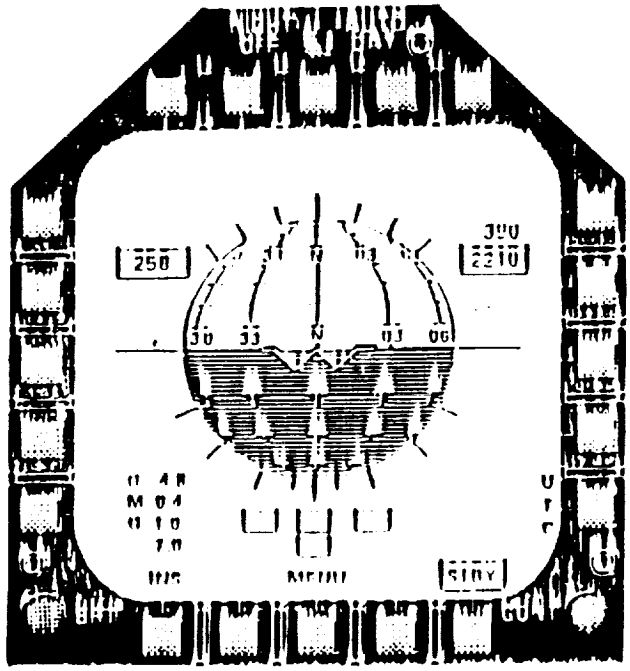

Figure 8.9: Enhanced ADI with MPD

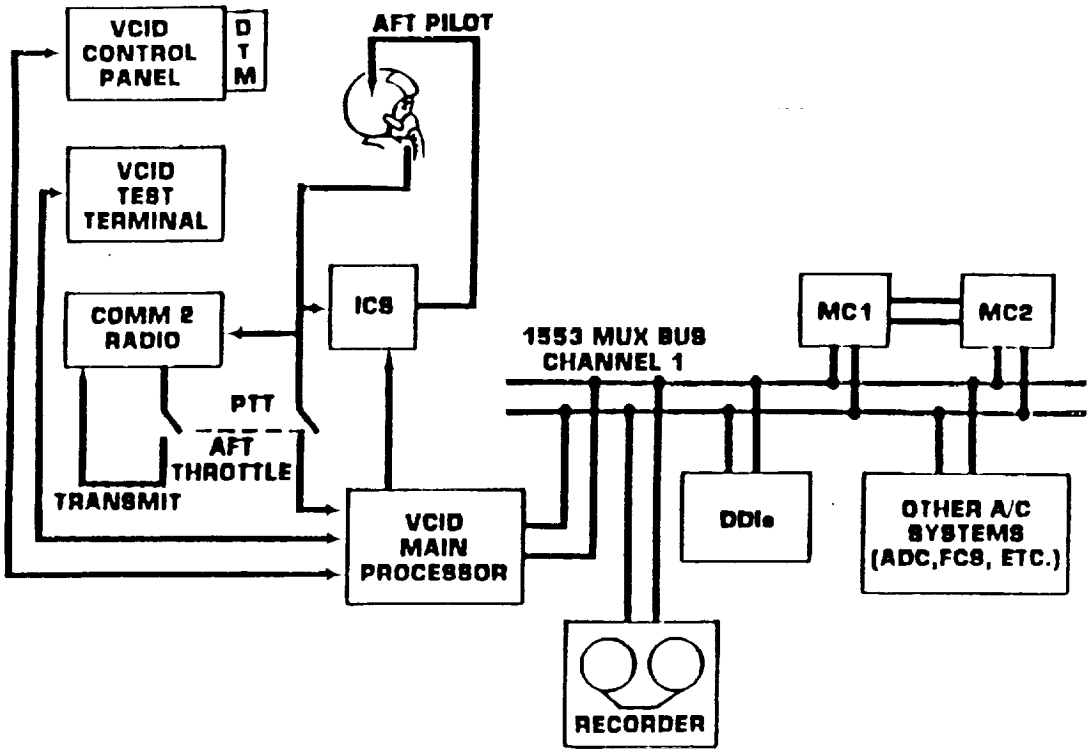

Figure 8.10: VCID Block Diagram

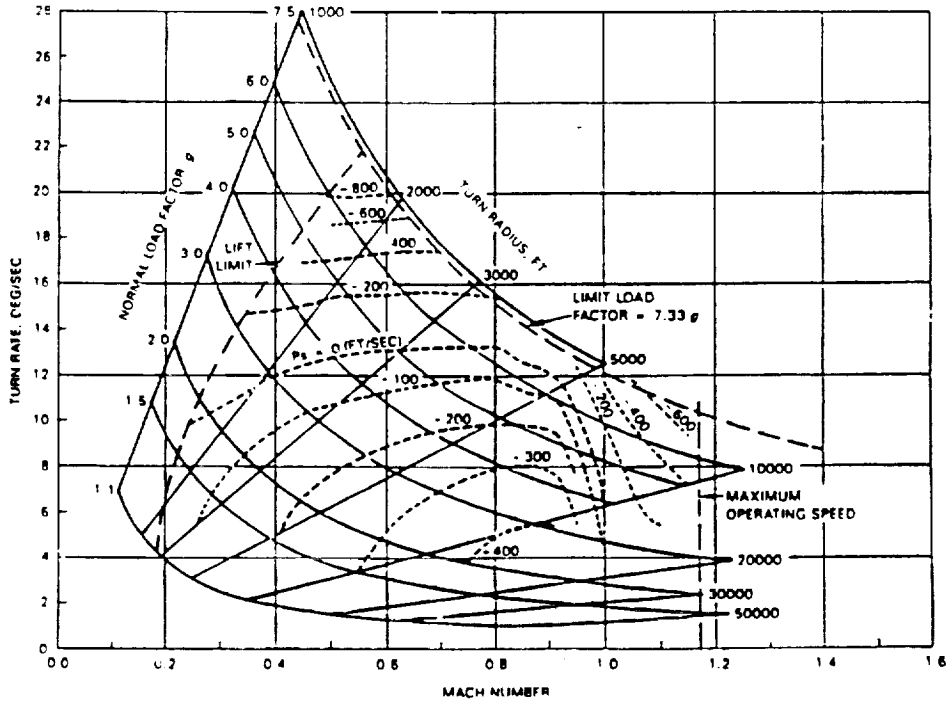

Figure 8.11: Energy-Maneuverability Display Format

3. Energy Management and Energy Maneuverability are extremely important in a tactical environment, although current aircraft performance allows pilots to achieve unusual flight profiles at the expense of energy height. To alleviate this problem, Briedenbach [Hutchins] has suggested the incorporation of an Energy-Maneuverability Envelope Display (Fig. 8.11) with an emphasis on constant g and constant turn radius lines. Due to the restriction on size and the number of displays already in use, it was decided to use a Helmet Mounted Display (HMD) to provide the pilot with Energy Management information. Of the many systems, that deemed most effective and easiest to use is the HMD format developed by Powrie (Fig. 8.12). This format consists of the use of four colored bands of light to represent aircraft energy status. The EMD unit would be mounted on the inside of the pilot's helmet visor, above his eyes but within his peripheral vision. This EMD concept was tested on an F-4J simulator and found to be compatible with ACM task loading, although no conclusive results were found.

4. Lastly, current tactics necessitate the incorporation of Night Vision Goggle (NVG) ergometrics into the Sabot cockpit design [Frankenberger].

F. MAINTAINABILITY

The Sabot is designed to be easily maintained. This is accomplished using a monitoring system akin to that used on current fleet aircraft. This system includes a central flight recorder and numerous strain gauges and sensors. This data will be downloaded post-flight by maintenance personnel into a portable computer and

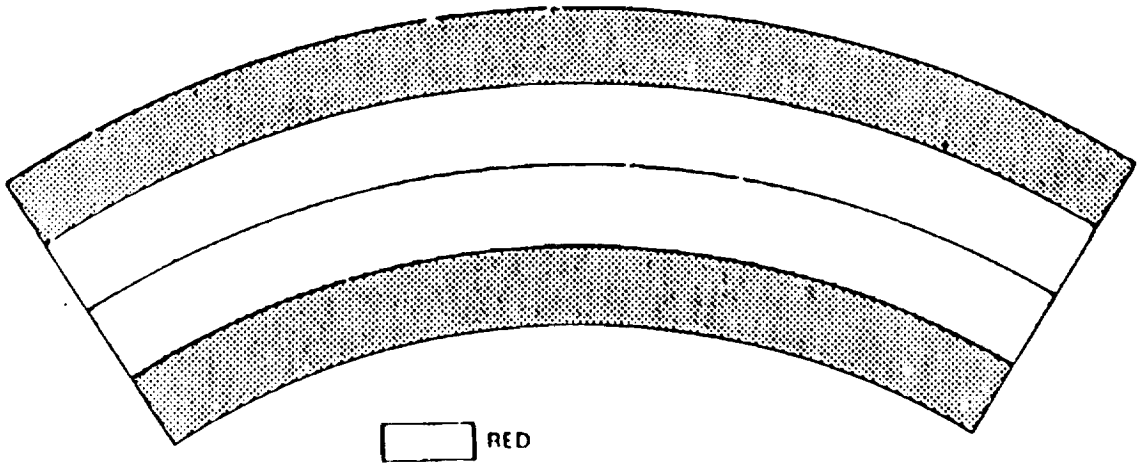

AIRCRAFT ENERGY STATUS	ENERGY STATUS CODE: UPPER GREEN	BLINK RED	STEADY RED	YELLOW	STEADY LOWER GREEN	BLINK LOWER GREEN
AIRSPEED = CORNER VELOCITY	X					
AIRSPEED = 100 KCAS		X				
AIRSPEED = 750 KCAS BELOW 30 KFT		X				
AIRSPEED = 710 KCAS AT ABOVE 30 KFT		X				
G ≤ 3 G		X				
G = POSITIVE STRUCTURAL G		X				
A = G = STRUCTURAL G			X			
B = G = A			X	X		
C = G = B				X		
D = G = C				X	X	
.05 = G = D					X	
0 = G = .05						X
-.3 = G = 0					X	

NOTE A B C AND D REPRESENT INTERMEDIATE VALUES OF g LOADING

Figure 8.12: Energy-Maneuverability Information Coding Via Use of Colored Bands of Light Mounted on Inside of Pilot's Helmet Visor

analyzed for malfunctions, impending malfunctions or other anomalies. This data will also be valuable for assessing airframe fatigue life and reliability. Maintenance of the aircraft is made simpler by drop panels and quick change mountings for the engines, and modular avionics. The hydraulic pumps and electrical generators are aircraft mounted to further ease their removal as well as engine removal.

G. SUPPORTABILITY

All maintenance and aircraft ground support use external power units, air carts, hydraulic service units, aircraft jacks, LOX (Liquid oxygen) carts, and airframe and engine stands are found with maintenance teams on-board aircraft carriers, naval air stations and air force bases.

IX. PRODUCTION FACILITIES

The success of Waverider Incorporated in the production of aircraft is due in large part to the organizational structure of the company. By using a computer aided design and manufacturing program (CADCAM) the entire production process can be monitored and controlled from the front office. CADCAM allows the engineers to produce design drawings which can be transmitted via the network to the machine casting and superplastic forming shops. This will help to ensure exact specifications are met.

The production plant is a state of the art facility completely contained in one building. This arrangement facilitates better communication and cuts down on the transportation costs, thereby reducing the overall cost of production.

The plant layout was designed to maximize productivity. The machine shops lie on one side of the building and consist of the latest in computer numerically controlled machining tools, such as single-spindle profiling machines for milling aircraft wings, laser drilling and cutting machines, vacuum chamber argon welding plants and Vacu-Blast machines for surface treatment.

To ensure high quality workmanship Waverider Incorporated maintains an aggressive inspection program which includes testing of parts using radioscopic and fluorescent techniques to locate material defects.

The assembly facilities include sub-assembly fixtures to hold aircraft parts during drilling, welding, and riveting and

jigs to hold large aircraft parts and ensure precise fitting of all connections. The jigs are designed to allow the removal of the finished product without breaking down the jig. This will allow quicker turn around between units.

X. COST/QUALITY

A. COST ESTIMATING RELATIONSHIPS

Life cycle costs (LCC) were determined using Cost Estimation Relationships (CER's) described in the AE 4273 design text [Nicolai]. A comprehensive approach was used considering total lifetime costs, from concept evaluation to retirement. Major Life Cycle Cost phases include:

- Research, development, test and evaluation - (RDT&E)
- Procurement or Acquisition
- Operations and maintenance - (O & M)

RDT&E included the costs for demonstration of airworthiness, mission capability and compliance with Mil-Specs. Military aircraft procurement costs included the production costs, as well as the costs of required ground support equipment and the cost of the initial spare parts during operational deployment. O&M covered fuel, oil, aircrew, maintenance, and various indirect costs. These major phases are further delineated in Figure 10.1.

Nicolai's Fundamentals of Aircraft Design book uses basic cost estimation relationships (CER) based on the development, test and evaluation (DT&E) and production costs for 29 aircraft built between 1945 and 1970. In addition, Nicolai's cost estimation primarily used the relationship between the AMPR(Aeronautical Manufactures Planning Report) weight, maximum speed, quantity of aircraft produced and production rate. The AMPR weight, the primary aircraft characteristic, was defined as the empty weight of the aircraft less the wheels, brakes, tires,

NICOLAI COST ESTIMATION ($ Millions)			
RDT&E			
Airframe		$970.45	
Development Support		401.78	
Flight Test Operations		44.17	
Flight Test Aircraft			
Engines & Avionics	$3.67		
Manufacturing Labor	18.33		
Material & Equipment	21.31		
Tooling	35.96		
Quality Control	2.38	81.65	
Subtotal		1498.05	
Profit (10%)		149.81	
Total RDT&E Costs			$1647.86
Production			
Engine and Avionics		$105.89	
Manufacturing and Labor		1352.11	
Material and Equipment		3450.20	
Sustaining Engineering		1015.11	
Tooling		506.71	
Quality Control		175.77	
Subtotal		6605.79	
Profit (10%)		660.58	
Total Production Costs			7726.37
TOTAL PROGRAM COST			$8914.23
Unit Cost (100 units)			**$89.14**

Figure 10.1: Life Cycle Costs

Program Unit Cost

Dev Est	22.2M
FY 82	22.7M
FY 83	22.8M

Cost Growth

FY 82-83	0.6M
TOTAL	2.8M

$in millions	<FY 81	FY 82	FY 83	FY 84	Finish	Total
Milcon/RDT&E	2104.0	202.9	114.8	11.3	20.1	2453.1
Procurement	3756.5	2420.8	2847.4	2858.5	25389	37272
Quantity Buy	105	63	84	96	1029	1377
Deliveries	23	22	60	63	1209	1377
Unit Cost FY 2000						**$54.6**

Table 10.1: F/A-18 Life Cycle Costs

engines, fluids, fuel cells, instruments, electronic equipment and other subsystems.

The CER's were developed for constant 1970 dollars, thus requiring an additional correction, based upon 5% inflation, to obtain the desired year 2000 dollars. Further assumptions were that the aircraft were produced at a rate of 1 per month, and that there wold be no costs for testing and manufacturing facilities. Due to the small program size, the development costs will be amortized over the life of the 100 aircraft buy.

Using Nicolai's methods and based upon the above assumptions, it was determined that the unit cost per Sabot would be approximately $89.14 million, FY 2000 dollars (Fig 10.1). This compares with the F/A-18 unit cost [92nd Congress Senate Hearings] of $54.6 million FY 2000 dollars (Table 10.1). Since the size of the Sabot program is considerably smaller than that of the F/A-18 and that the Sabot will be using non-standard radar due to the fuselage constraints, it is believed that the Sabot unit cost of $89.14 million is accurate.

B. QUALITY

House of quality matrices (Figure 10.2) were developed to identify major parameters in the design. These houses would need to be expanded to the production phase parameters so they could be used by management for planning and coordination. The + and - signs are indicative of positive and negative influences.

House of Quality

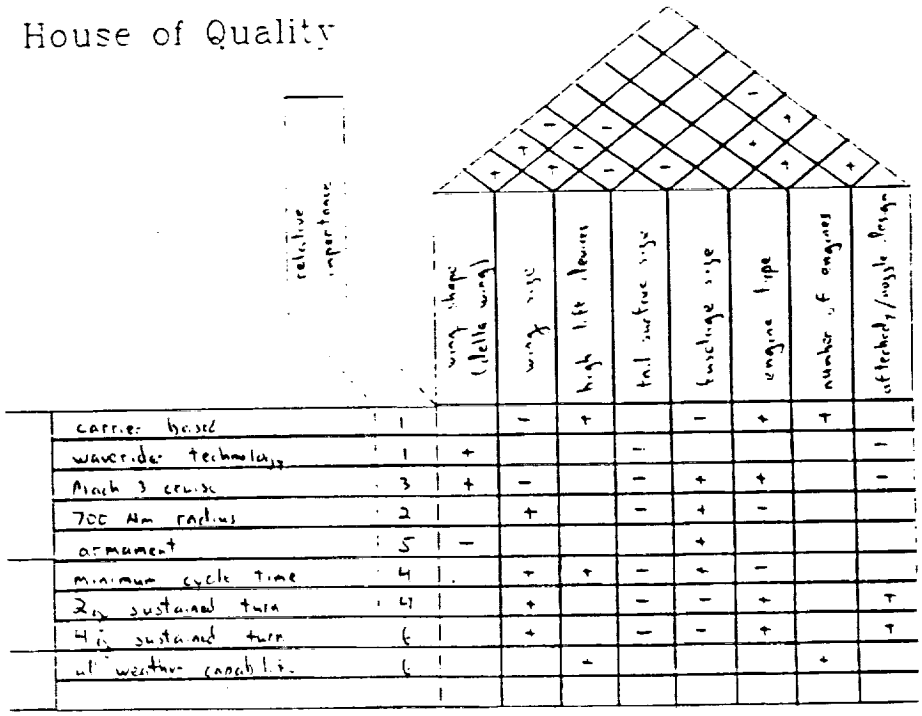

House of Quality

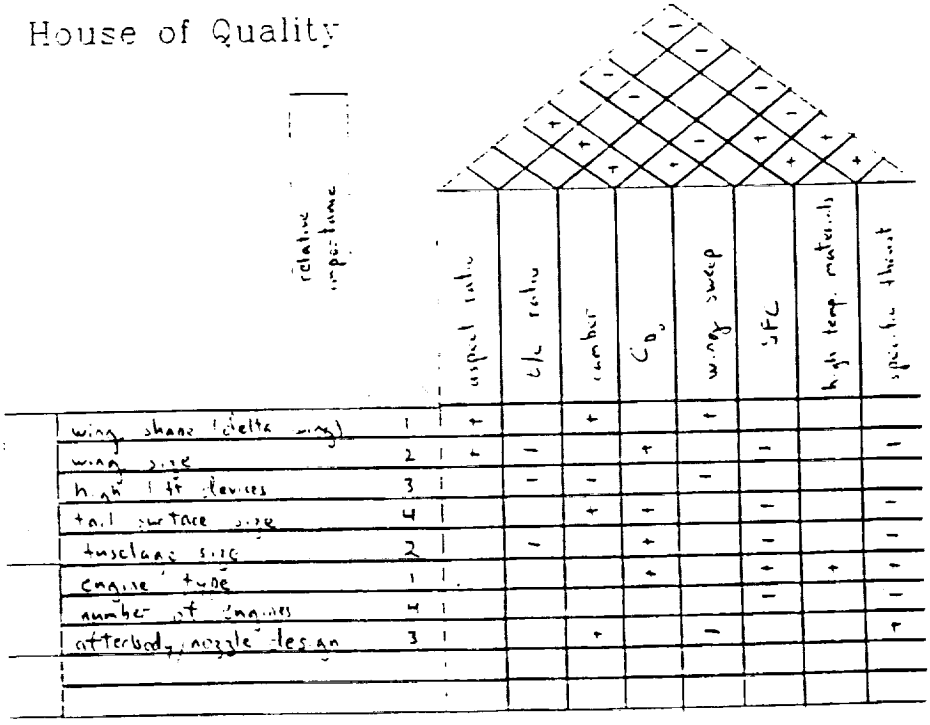

Figure 10.2: House of Quality Matrices

XI. SUMMARY

A. RFP COMPARISON

In the introductory portion of this report one of the basic design goals was to meet the requirements as set forth in the RFP. The Sabot high speed interceptor meets those requirements as evidenced by Table 11.1.

Specification	Required	Sabot
Minimum Radius	700 nm	762 nm
Dash Mach Number	<5	3
Missile Carriage (Internal/Conformal)	4	4
Cycle Time	1+00 (Min) 1+30 (Des)	1+00
Sustained Turn	2g or 4g	4g
Maximum Gross Weight	<85,000	76,036

Table 11.1: RFP Comparison

B. CONCLUSIONS

The integration of waverider technology into a viable design was not as easy as first thought. With theoretical L/D values of around 10, we believed that the waverider concept was the answer to all our range requirements. After the waverider forebody was integrated into a useful, viable vehicle the attainable L/D had dropped to an average of 4 throughout the cruise out and return legs of the mission profile.

In order to perfect the design several minor changes would have to be made. These changes were recognized very late in the

analysis. The wings may need to be place a little further aft in order to obtain more desirable stability characteristics in the supersonic flight regime. A wider fuselage half angle may be needed so that the cockpit may be placed further forward. This would result in a lower canopy height. The nose strut may need to be lengthened in order to facilitate an easier rotation on takeoff.

The major unknown in the integration of the waverider concept into a conventional aircraft was the supersonic flow field. A much more in depth analysis of the flow field is needed in order to fine tune the design. The effect of a canopy on the free stream upper surface needs to be quantified. The effects of the waverider flying at off design conditions needs to be investigated. This unknown has a direct impact on the unique problem of having too much lift out of the waverider portion of the aircraft at supersonic speeds. Also, the expansion of the flow on the after part of the aircraft needs to be quantified since it cannot be accurately determined from a two dimensional Prandtl-Meyer expansion. These areas need to be investigated prior to design refinement.

APPENDIX A

```
                    PROGRAM THERMAL
PREDICTS TEMPERATURE OF WAVERIDER IN FLIGHT (SIMPLIFIED AS A CONE)
THE FOLLOWING CAN BE VARIED FOR DIFFERENT TEMPERATURE PROFILES
MATERIAL PROPERTIES
AOA AND CONE ANGLE (IN THIS CASE 20 DEGREES)
SKIN LOCATION
FLIGHT PROFILE INCLUDING CRUISE ALTITUDE AND MACH
STANDARD ATMOSPHERE WAS ASSUMED

      REAL MINF,MLOCAL,KSTAR,MUSTAR
      DIMENSION TSKIN(3000),H(3000)
      OPEN(99,FILE='THERM1.OUT')

      SIGMA = 1.712E-9 ! stefan - boltzman constant  btu/hr ft^2 R^4

               MATERIAL PROPERTIES AND DIMENSION
        EPS = 0.4       ! EMISSIVITY - MATERIAL AND SURFACE FINISH
        RHO =  8.73      ! DENSITY - slugs/cu ft
         CP = 3049.7    ! SPECIFIC HEAT - ft lbf/slug  rankine
      THICK = 0.0025      ! THICKNESS OF THE SKIN - ft

               ANGLE OF ATTACK AND CONE ANGLE
      ALPHA = 0.1    ! RADIANS
      ANGLE = 0.35   ! RADIANS
      PCOEFF= 2*(COS(ALPHA)**2)*(SIN(ANGLE))**2   ! PRESSURE COEFFICIENT

               PROPERTIES OF AIR
      GAMMA = 1.4
          R = 1716.0      ! GAS CONSTANT - ft lbf/slug rankine
      PRAN = 0.7          ! PRANDTL NUMBER
      REC = 0.89          ! RECOVERY FACTOR

               INTIAL CONDITONS
          X = 10.0        ! DISTANCE AFT - ft
      TSKIN(0) = 520.0    ! INITIAL SKIN TEMPERATURE - degrees rankine

            DO 10 T=1,1500    ! seconds from start

               FLIGHT PROFILE (REVERSED)

               CRUISE CONDITIONS
      IF(T.LT.720)GOTO 12  ! 12 minutes from start
      MINF= 3.0           ! mach
      ALT= 50000.0         ! ft of altitude
      TINF=390.0        ! degrees rankine
      PINF=243.61       ! pounds per ft sq
      GOTO 15

               SUPERSONIC CLIMB
2     IF(T.LT.420)GOTO 13
      MINF=1.2+(T-420)/107.1                ! mach
      ALT=30000+(T-420)*33.33               ! ft of altitude
      PINF=499.34*EXP(-.00005*(ALT-35000)) ! pounds per ft sq
      TINF=390.0                            ! degrees rankine
      GOTO 15

               TRANSONIC ACCELERATION
3     IF(T.LT.300)GOTO 14
      MINF=0.9+(T-300)/400                  ! mach
      ALT=35000-(T-300)*41.67               ! ft of altitude
```

```
      TINF=394.08+0.00356*ALT                ! degrees rankine
      PINF=2112.6*(TINF/518.69)**5.27        ! pounds per ft sq
      GOTO 15

                INITIAL CLIMB TO ALTITUDE
4     MINF=0.9                               ! mach
      ALT=116.67*T                           ! ft of altitude
      TINF=518.69-0.00356*ALT                ! degrees rankine
      PINF=2112.6*(TINF/518.69)**5.27        ! pounds per ft sq


                CALCULATE LOCAL PRESSURE AND STAGNATION CONDITIONS
5     PLOCAL = PINF*(PCOEFF*(GAMMA/2)*MINF**2 + 1)
      PTLOCAL = PINF*1.89293*(MINF**7)*88.18163/(7*MINF**2-1)**2.5
                           both pounds per ft sq
      TTL = TINF*(1+0.2*MINF**2)   ! STAGNATION TEMPERATURE - rankine
      RATIO = PTLOCAL/PLOCAL

                CALCULATE LOCAL MACH, TEMPERATURE AND SPEED OF SOUND
      MLOCAL = 2.2361*SQRT(RATIO**0.28571-1)  ! mach
      TL = TTL/(1+0.2*MLOCAL**2)   ! degrees rankine
      AL = SQRT(GAMMA*R*TL)   ! local speed of sound ft/sec

                CALCULATE ADIABATIC WALL TEMPERATURE AND
                *(STAR) CONDITIONS

      TAW = TL*(1+(GAMMA-1)/2*REC*MLOCAL**2)          ! TEMPERATURE - rankine

      TSTAR = 0.28*TL + 0.5*TSKIN(T-1) + 0.22*TAW     ! TEMPERATURE - rankine

      MUSTAR = 2.27E-8*(TSTAR**1.5)/(TSTAR+198.7)     ! VISCOSITY - slugs/ft sec
               specific heat
      CPSTAR = 0.219 + (0.342E-4)*TSTAR - (0.293E-8)*TSTAR**2 ! SPECIFIC HEAT
                                                              btu/lbm rankin
      KSTAR = (1.856E-4)*SQRT(TSTAR)/(1+202/TSTAR) ! CONDUCTIVITY
                                                     ft lbf / ft sec rankine
      RHOSTAR = PLOCAL/(R*TSTAR)             ! DENSITY - slugs/ft cubed

      RENSTAR = RHOSTAR*MLOCAL*AL*X/MUSTAR  ! REYNOLDS NUMBER

      PRAN = (CPSTAR*MUSTAR/KSTAR)*32.2*778.17  ! ACTUAL PRANDTL NUMBER

      NUSTAR = 0.0292*((RENSTAR)**0.8)*PRAN**0.333333  ! NUSSELT NUMBER

      HLOCAL = NUSTAR*KSTAR/X     ! HEAT TRANSFER COEFFICIENT
                                    ft lbf /ft sq sec rankine

      H(T) = HLOCAL

                SKIN TEMPERATURE CALCULATION

SKIN TEMPERATURE AS A FUNCTION OF TIME
SUM OF THE T-1 SKIN TEMPERATURE AND CONVECTIVE HEATING
      TSKIN(T)=TSKIN(T-1)+(TAW-TSKIN(T-1))*H(T)/(RHO*CP*THICK)
MINUS THE RADIATIVE COOLING
      TSKIN(T)=TSKIN(T)-.216*SIGMA*EPS*TSKIN(T-1)**4/THICK/RHO/CP
 778.17 ft lbf/btu over 3600 secs/hr   gives .216

      WRITE(99,*)T,TSKIN(T)
0               CONTINUE
      END
```

```
                    PROGRAM STAGTEMP
 PREDICTS TEMPERATURE OF THE LEADING EDGE OF THE WAVERIDER IN FLIGHT

      REAL MINF
      DIMENSION TSKIN(3000)
      OPEN(99,FILE='stag.OUT')

      SIGMA = 4.7556e-13 ! stefan - boltzman constant  btu/sec ft^2 R^4
                MATERIAL PROPERTIES
        EPS = 0.10       ! EMISSIVITY - MATERIAL AND SURFACE FINISH
        RHO = 8.73       !  DENSITY - slugs/cu ft
         CP = 3049.7     !  SPECIFIC HEAT - ft lbf/slug  rankine
      THICK = 0.0025     ! THICKNESS OF THE SKIN - ft
      RADIUS = 0.01667   ! RADIUS OF CURVATURE OF LEADING EDGE - ft
      RINV = 1/sqrt(radius) ! USED LATER

                INITIAL CONDITIONS
      RHOSL  = 2.3769E-3   ! DENSITY OF AIR AT SEA LEVEL - slugs/cu ft   air
      GAMMA  = 1.4
      R      = 1716.0      ! GAS CONSTANT - ft lbf/slug rankine
      TSKIN(0) = 520.0     !  INITIAL SKIN TEMPERATURE - rankine

            DO 10 T=1,1500    ! seconds from start

                FLIGHT PROFILE (REVERSED)
                CRUISE CONDITIONS
      IF(T.LT.720)GOTO 12  ! 12 minutes from start
      MINF=3.0           ! mach
      ALT=50000          ! ft of altitude
      TINF=390.0         ! degrees rankine
      PINF=243.61        ! pounds per ft sq
      RHOINF = 3.6391E-4   ! slugs per cu ft
      VINF = MINF*SQRT(GAMMA*R*TINF)
      GOTO 15
                SUPERSONIC CLIMB
2     IF(T.LT.420)GOTO 13
      MINF=1.2+(T-420)/166.67                  ! mach
      ALT=30000+(T-420)*66.67                  ! ft of altitude
      PINF=499.34*EXP(-.00005*(ALT-35000))     ! pounds per ft sq
      TINF=390.0                               ! degrees rankine
      RHOINF = 7.3820E-4*EXP(-.00005*(ALT-35000))
      VINF = MINF*SQRT(GAMMA*R*TINF)
      GOTO 15
                TRANSONIC ACCELERATION
3     IF(T.LT.300)GOTO 14
      MINF=0.9+(T-300)/400                     ! mach
      ALT=35000-(T-300)*41.67                  ! ft of altitude
      TINF=394.08+0.00356*ALT                  ! degrees rankine
      PINF=2112.6*(TINF/518.69)**5.27          ! pounds per ft sq
      RHOINF = 2.3769E-3*(TINF/518.69)**4.27
      VINF = MINF*SQRT(GAMMA*R*TINF)
      GOTO 15
                INITIAL CLIMB TO ALTITUDE
4     MINF=0.9                                 ! mach
      ALT=116.67*T                             ! ft of altitude
      TINF=518.69-0.00356*ALT                  ! degrees rankine
      PINF=2112.6*(TINF/518.69)**5.27          ! pounds per ft sq
      RHOINF = 2.3769E-3*(TINF/518.69)**4.27
      VINF = MINF*SQRT(GAMMA*R*TINF)           ! ft/sec
                CALCULATE LOCAL STAGNATION CONDITIONS
```

```
5       TTL = TINF*(1+0.2*MINF**2)    ! degrees rankine
            QSTAG FROM AN EMPIRICAL FORMULA
        QSTAG = 20800*rinv*SQRT(RHOINF/RHOSL)*(VINF/26000)**3.25
        QSTAG = QSTAG*(1-TSKIN(T-1)/TTL)   !btu/ft sq sec
 TEMPERATURE CHANGE IS A FUNCTION OF STAGNATION HEATING AND
 RADIATIVE COOLING
        DELTEMP = 778.17*(QSTAG-SIGMA*EPS*TSKIN(T-1)**4)/rho/thick/cp
        TSKIN(T)=TSKIN(T-1)+ DELTEMP

        WRITE(99,*)T,TSKIN(T),DELTEMP
0               CONTINUE
        END
```

LIST OF REFERENCES

Abbot, I. H. and Von Doenhoff, A. E., Theory of Wing Sections, Dover Publications, Inc., 1959.

Allen, D. and Haisler, W., Aerospace Structural Analysis, John Wiley & Sons, 1985.

Anderson, J. D., Introduction to Flight, McGraw-Hill Publishing Company, 1989.

Ball, R. E., The Fundementals of Aircraft Combat Survivability Analysis and Design, AIAA, 1985.

Barnes, M. J., and Schwall, K. M., "Aircrew Interface with Advanced Electronic Warfare Systems", Naval Weapons Center, May 1985.

Eggers, A. J., Syvertson, C. A., "Aircraft Configurations Developing High Lift-Drag Ratios at High Supersonic Speeds", NACA, 1956.

Etkin, B., Dynamics of Flight: Stability and Control (2^{nd} ed.), John Wiley & Sons, Inc., 1982.

Federal Aviation Regulation, Parts 23 and 25.

Frankenberger, K. A., "Analysis of Night Interdiction Missions Using the Night Vision System for F/A-18, AV-8B", Naval Weapons Center, May 1987.

Frankenberger, K. A. and Battershell, S., "F/A-18 Hands on Throttle and Stick (HOTAS) Controls: A Study of Their Function and Complexity", Center for Navak Analysis, August 1988.

Herman, R., Supersonic Inlet Diffusers and Introduction to Internal Aerodynamics, Minneapolis-Honeywell Regulator Company, 1956.

Kim, B. S., Rasmussen and Jische, "Optimization of Waverider Configurations Generated from Conical Flows", Journal of Spacecraft, 1983.

Kuchemann, D., The Aerodynamic Design of Aircraft, Pergamon Press, 1978.

Loikith, G., and Hall, B., "TF/A-18 Airplane Voice Interactive System Flight Test Demonstration", Naval Air Test Center, October 1986.

Mattingly, J. D., Heiser, W. H., Daley, D. H., Aircraft Engine Design, AIAA, 1987.

McDonnel Douglas Flight Control Division, USAF Stability and

Control DATCOM, McDonnel Douglas Aircraft Corporation, 1976.

MIL-A-8861(ASL) Loading Diagram.

MIL-F-8785C, 1980.

MIL-S-188471G Cockpit Sizing.

MIL-STD-805A Towing Fittings and Provisions for Fixed Wing Aircraft.

MIL-STD-850B Aircrew Station Vision Requirements for Military Aircraft, 1970.

Nelson, R. C., Flight Stability and Automatic Control, McGraw-Hill, 1989.

Nicolai, L., Fundementals of Aircraft Design, METS Inc., 1975.

Niu, Michael C. Y., Airframe Structural Design, Conmilit Press, Limited, 1988.

Proceedings of SCAR Conference Parts 1&2, NASA, 1976.

Rasmussen, M. L., "Waverider Configurations Derived from Inclined Circular and Elliptic Cones", Journal of Spacecraft, 1980.

Raymer, D., Aircraft Design: A Conceptual Approach, AIAA, 1989.

Roskam, J., Airplane Design, Part I-VI, Roskam Aviation and Engineering Corporation, 1985.

Schindel, L. H., "Waveriders", Tactical Missile Aerodynamics, AIAA, 1986.

Sims, J. L., "Tables for Supersonic Flow Around Right Circular Cones at Zero Angle of Attack", NASA, 1964.

Syvertson, H. R., "Aerodynamic Performance and Static Stability and Control of Flat-Top Hypersonic Gliders at Mach Numbers from 0.6 to 18", NACA, 1966.

Ward, R. W., "F/A-18 Single-Seat Versus Dual-Seat Crew Evaluation", Center for Naval Analysis, July 1987.

White, F. M., Fluid Mechanics, McGraw-Hill Company 1979.

White, F. M., Heat Transfer, McGraw-Hill Company, 1984.